

WATERTOWN ARSENAL
WATERTOWN, MASS.

COPY &

1

AT1-113035

AD-A954 300

REPORT

No. WAL 671/99 - 18

BINDERS IN CEMENTED REFRACTORY ALLOYS

FINAL REPORT

CONTRACT: DA-19-020-ORD. - 10 ORDNANCE DEPARTMENT

DEPARTMENT OF THE ARMY

O. O. PROJECT NO. TM-10500 2G

DTIC FILE COPY

DTIC
DEC 14 1984
A

15 JUNE 1951

DEPARTMENT OF METALLURGY
MASSACHUSETTS INSTITUTE OF TECHNOLOGY

CAMBRIDGE, MASSACHUSETTS

This document has been approved for public release and distribution in unlimited quantities

84 10 23 218

BINDERS IN CEMENTED REFRACTORY ALLOYS

Report No. WAL 671/99-18

O.O. Project No. TM-105002G

15 June 1951

Submitted by:

J. T. Norton
J. Gurland
P. Rautala

Department of Metallurgy
Massachusetts Institute of Technology
Cambridge, Massachusetts

DTIC
ELECTE
S DEC 14 1984 D
A

This document has been approved
for public release and sale; its
distribution is unlimited.

DISTRIBUTION LIST

Technical Report WAL 671/99-18

Contract No. DA-19-020-ORD-10

Massachusetts Institute of Technology

- - -

Watertown Arsenal - ORDBE

7 copies - Attn: Laboratory

Boston Ordnance District

1 copy - Attn: A.S. McCann

Office, Chief of Ordnance

3 copies - ORDTM, Ammunition
1 copy - ORDTB, Research and Materials
1 copy - ORDTR, Artillery
1 copy - ORDTS, Small Arms
1 copy - ORDTX, AR

Ordnance Installations

1 copy - ORDBA, Frankford Arsenal, Philadelphia 37, Pa.
Attn. Pitman-Dunn Laboratory
1 copy - ORDBB, Picatinny Arsenal, Dover, N.J.
1 copy - CRDBD, Springfield Armory, Springfield, Mass.

U.S. Navy Dept. Bureaus and Installations

1 copy - Bureau of Ordnance, Attn: Re 3b
1 copy - Bureau of Ordnance, Attn: Technical Library
1 copy - Bureau of Ordnance, Attn: Naval Ordnance Laboratory
1 copy - Bureau of Aeronautics
1 copy - Bureau of Ships, Attn: Code 343
1 copy - Naval Gun Factory, Attn: Design Section

Other Agencies

1 copy - Franklin Institute, Philadelphia, Pa.
Attn: Laboratory for Research and Development.



UNANNOUNCED

FINAL TECHNICAL REPORT

Contractor: Massachusetts Institute of Technology, Cambridge, Mass.

Agency: Massachusetts Institute of Technology, Cambridge, Mass.
Under Technical Supervision of Watertown Arsenal Laboratory

Contract Number: DA-19-020-ORD-10

O.O. Project Number: TM-105002G

WAL Project Number: WAL 1.21-P

WAL Report Number: WAL 671/99-18

Priority: I C

Title of Project: Binders in Cemented Refractory Alloys

The Object of this program was

To make a detailed study of the action of the binder phase in cemented wolfram carbide alloys with the objective of explaining the several factors which control the physical and mechanical properties of the sintered parts and to provide a basis for the proper selection of the best binder materials and sintering techniques for specific situations.

Summary

The sintering behavior of wolfram carbide cobalt alloys was studied by following dilatometrically the shrinkage, or densification, which takes place during the sintering operation. It could be correlated with the wolfram-cobalt-carbon ternary system, which shows that sintering takes place in the two phase field, wolfram carbide-cobalt, and that a liquid phase is formed between 1300° and 1325°C. The liquid cobalt binder wets the solid wolfram carbide particles, which tend to surround themselves with a film of binder metal. Dilatometric and electrolytic leaching experiments proved that a strong continuous carbide skeleton is not formed during the sintering process.

A-

On the basis of the above experiments it could be shown that densification takes place by a rearrangement of the carbide particles under the influence of the surface tension forces of the binder. The resulting structure is essentially one of carbide particles embedded in a matrix of cobalt. The mechanical properties of the binder, as modified by the structure, account for the strength and brittleness of the sintered compacts. The binder, therefore not only makes possible the sintering of cemented wolfram carbide at low temperatures, but also determines the properties of sintered alloys.

A comparison of cobalt with other possible binder metals led to the conclusion that an effective binder must not lead to the presence of a third phase in the sintered products. On that basis, cobalt and nickel are suitable for use as binders for wolfram carbide, but not copper and iron.

It was found that the eta phase (W_3Co_3C) of the ternary system wolfram-cobalt-carbon is relatively resistant to oxidation at $1000^{\circ}C$. A brief study of its oxidation characteristics is included in the appendix.

Submitted by:

John J. Norton
Rehba Rautala
Joseph Gurland

ACKNOWLEDGEMENT

Special thanks are extended to Mr. William H. Campbell and Mr. Kenneth A. Carlson for their valuable assistance in the experimental work.

The authors also wish to take this opportunity to thank the various members of the staff and of the student body of the Department of Metallurgy for their friendly interest and valuable cooperation.

This work was sponsored by the Ordnance Department of the U.S. Army contracts No. W-19-020-ORD-6489 and No. DA-19-020-ORD-10, under the technical supervision of Watertown Arsenal Laboratory. The assistance of Dr. L. F. Foster, Mr. J. F. Wallace and Mr. A. M. Burghardt of that laboratory is deeply appreciated.

INDEX

	<u>Page</u>
I Introduction and Literature Survey	1
II The Wolfram-Cobalt-Carbon System	6
III Experimental Techniques	9
IV General Sintering Behavior	13
A. Sintering Runs at Constant Heating Rate	13
B. Sintering Runs at Constant Temperature	14
C. Conclusions	15
V The Wetting Properties of the Binder in Cemented WC Alloys	17
A. Theory	17
B. Wettability of Cemented Wolfram Carbide	18
C. Infiltration of Liquid Binder	21
D. Discussion of the Microstructure	23
E. Conclusions	25
VI The Physical Distribution of the Carbide Phase	26
A. Effect of Cold Pressing and Heating	26
B. Binder Solidification Phenomena	27
C. Electrolytic Leaching Experiments	29
D. Coefficient of Linear Thermal Expansion	31
E. The Relation of Strength to the Physical Distribution of the Carbide Phase	33
F. Conclusion	34
VII The Sintering Mechanism	35

	<u>Page</u>
VIII The Mechanical Properties of Cemented Wolfram Carbide Compacts	39
A. Experimental Data	39
B. Theoretical Consideration	41
IX Comparison of Cobalt with other Binder Metals	46
A. Review of the Ternary Systems	46
B. Experimental Results	48
C. Discussion of Results	53
D. Conclusions	56
X General Discussion of Results	57
XI General Conclusions	63
XII Suggestions for Further Work	64
Bibliography	66
Appendix	
I On the Metastability of the Eta Phase	71
II High Temperature Oxidation Resistance of the Eta Phase of the Wolfram-Cobalt-Carbon System	72
III A Study of the Kinetics of Isothermal Sintering	76
IV Calculation of the particle Size	78
V Temperature Dependence of the Angle of Contact of Liquid Copper on Solid Wolfram Carbide	80
VI Binder Solidification Phenomena of the Cobalt Infiltrated Compact	82
VII Calculation of Shrinkage Caused by Solution of Wolfram Carbide in Liquid Cobalt	83
VIII Cohesion of Compacts at the Sintering Temperatures	85
IX Calculation of Tesselated Stresses in Sintered Wolfram Carbide-Cobalt Compacts by the Method of Laszlo	87

I INTRODUCTION AND LITERATURE SURVEY

The purpose of this work is to determine the role of the binder phase in cemented wolfram carbide. The problem is approached by a critical evaluation of published material and by a series of experiments which will show the effect of the binder on the sintering mechanism and on the properties of cemented compacts.

Commercial cemented carbides consist of very fine particles of refractory metal carbides embedded in a matrix of a low melting metal, usually of the iron group. This leads to bodies of great hardness and high compressive strength, which are used as drawing dies, bearings and cutting tools. They represent the most extreme of a series of ferrous alloys of decreasing iron and increasing alloy content, extending from plain carbon steels (98-99 percent iron, 0.5-1 percent carbon) through high speed tool steels (60-75 percent iron, 0.5-1.5 percent carbon, 10-20 percent wolfram, 3-6 percent cobalt, 2-5 percent chromium, 0-2 percent vanadium) to cemented carbides (3-13 percent cobalt, 5.5-10 percent carbon, 60-90 percent wolfram, 0-25 percent titanium).

The first efforts (1909) to produce useable wolfram carbide products by melting and casting, failed because of the unavoidable separation of free graphite. Better success was achieved by sintering wolfram carbide powders near their melting point, (1914). However, the required temperatures were too high for industrial use and this led to the addition of metals of the iron group, first by melting the mixture (1917), then by infiltration into a pre-sintered carbide skeleton (1922), and finally by sintering of a mixture of wolfram carbide and iron group metal powders slightly above the

melting point of the latter (1922) ⁽¹⁾. The addition of small amounts of a low melting auxiliary metal lowers the sintering temperature to less than 1450°C. The latest development is the partial or total replacement of wolfram carbide by other metallic carbides, notably those of titanium and tantalum. By these means, the permissible cutting speeds for steels have been increased by a factor of more than ten since the beginning of this century.

Cemented carbides of the wolfram carbide-cobalt grade are produced by ball milling the mixed carbide and cobalt powders, pressing compacts of the desired shape, and sintering to the final density and hardness. The usual compositions vary from 3 to 25 percent cobalt. Although good sintered carbide parts are produced industrially, little is known about the phenomena that takes place during the heating and cooling cycle. The industrial heat treatment is carried out in a neutral or reducing atmosphere, within a temperature range of 1350°C to 1500°C, the sintering time varying from 1 to 2 hours. A linear shrinkage of 12 to 20 percent occurs. It has also been observed that a certain amount of grain growth takes place, the fine grains tend to disappear and the larger ones become coarsened.

The first investigators of the sintering mechanism, Hoyt ⁽²⁾, and Wyman and Kelley ⁽³⁾, showed that a liquid phase is formed at approximately 1350°C, even below the melting point of cobalt (1495°C), and that solution of wolfram carbide takes place both in the solid and in the liquid cobalt. The solubility increases with temperature; at the sintering temperature, at which the binder is liquid, it dissolves about 37 percent wolfram carbide. In a 6 percent cobalt alloy the liquid phase will then represent about

10 percent by weight or 14 percent by volume of the compact. Upon cooling, as the solubility decreases, the carbide precipitates on the existing, non-dissolved, grains which tend to take on characteristic angular shapes. At room temperature the binder is reported to contain less than 1 percent wolfram carbide⁽⁴⁾.

Whether sintering is possible at temperatures below the solidus has been the subject of considerable disagreement. Dawihl and Hinnuber⁽⁵⁾ reported that wolfram carbide-cobalt alloys can be completely sintered at a temperature as low as 1250°C, if given a sufficiently long time. Mantle⁽⁶⁾ examined the effect of the sintering temperature on the properties of cemented carbides. He concluded that 1305°C. is the lowest temperature at which sintering can be carried out. Some dilatometric studies of the sintering process were undertaken at Krupp in Germany⁽⁷⁾. The resulting curves, shrinkage versus temperature, were not evaluated in detail, but they indicate that the contraction begins between 900°C and 1000°C and attains greatest speed at barely 1400°C. The slope of the shrinkage curve increases with cobalt content. Sandford and Trent⁽⁸⁾ observed some specimens through an optical pyrometer and reported that contraction starts at approximately 1150°C, and is complete at 1320°C for cobalt contents of 6 percent and 10.5 percent. They conclude that sintering commences before a liquid phase appears, but is not completed until after it is present.

The strength, brittleness and lack of ductility of cemented wolfram carbide have been attributed to the existence of a continuous skeleton of carbide in the sintered compacts. This view is held by Dawihl and Hinnuber⁽⁵⁾, Sandford and Trent⁽⁸⁾, Kiefer⁽⁴⁾, Goetzel⁽⁹⁾, and Skaupy⁽¹⁰⁾, among others.

However, it is not universally accepted, Mantle⁽⁶⁾, for instance, mentions that a skeleton cannot account for the variation of the physical properties with composition. The only direct experimental evidence to support the skeleton theory was given by Dawihl and Hinnuber⁽⁵⁾ who showed that the strength of an acid leached sintered compact and the thermal coefficients of expansion of low cobalt alloys could be explained by the existence of a continuous skeleton, which might be formed during cooling by the deposition of wolfram carbide preferentially at the contact points of the particles, thereby increasing the area of contact. It has been suggested that adhesive forces are acting between the carbide particles, the effectiveness of which is increased by the presence of cobalt, which dissolves oxides and other impurities at the surface of the grains⁽¹¹⁾. The possibility has also been mentioned that the carbide particles have unusual plasticity in the presence of liquid cobalt, which would permit them to deform at the points of contact and thereby increase the strength of the skeleton⁽¹⁰⁾. This suggestion is based upon the observed increase of plasticity of rock salt in hot unsaturated water solutions. Whatever the mechanism by which a skeleton is formed, if it exists, it will determine, to a great extent, the physical properties of sintered carbide compacts, and the properties of the binder would not be expected to influence them appreciably. However the latter would be decisive if the structure of cemented carbides would consist of isolated carbide grains in a matrix of binder metal.

The current products and production methods of the cemented carbide industry were developed empirically. But only a full and clear understanding of the sintering mechanism and of the structure of sintered compacts will

permit the development and use of all their potential properties. The effect of the substitution of wolfram carbide and cobalt by other carbides and binder metals can then be theoretically evaluated, and new uses for cemented carbides, for instance as a high temperature material, will suggest themselves. It is hoped that the present work will contribute to such an understanding of the theory of cemented carbides. It will be shown that the binder not only influences the sintering behavior, but also the properties of sintered alloys. The role of the binder phase will be studied by a detailed consideration of the action of cobalt during sintering and its effect upon the final structure of the compacts. A sintering mechanism, accounting for the observed phenomena and structure, will be proposed. Other possible binders will be discussed and an attempt shall be made to connect the characteristic physical properties to the structure of cemented wolfram carbide.

NOTE: The nomenclature used in this report conforms to the recommendations of the Commission on Inorganic Nomenclature, International Union of Chemistry, which at its 1949 meeting, changed the name of the element Tungsten to Wolfram. Also the word "sintering", as here used, refers to the densification of cemented carbides, but does not restrict the mechanism of densification exclusively to the action of surface forces between solid particles.

II THE WOLFRAM-COBALT-CARBON SYSTEM

The ternary system has been studied by Takeda⁽¹²⁾, who suggested the existence of two systems; one stable, with the phases Co, W, W₂C, WC, and graphite; the other metastable with the phases Co, W, W₂C, W₃Co₃C and graphite. Since only two phases appear at room temperature in a normally sintered specimen: Wolfram carbide and a cobalt rich solid solution, almost all the published work concerned with the mechanism of sintering is based upon an assumed binary system wolfram carbide-cobalt. Actually the appearance of free carbon at very high temperatures makes it theoretically impossible for such a binary to exist, although a vertical section through the ternary diagram, along the wolfram carbide-cobalt line, might still show only two phases at low temperatures. Such a section is drawn as the quasi-binary, Figure 1, upper left hand corner.

Takeda introduced the metastable system mentioned above to take into account the eta phase (η), (W₃Co₃C), which occurs only under abnormal sintering conditions, and which Takeda assumed to be unstable. This phase has an undesirable effect upon the physical properties of the sintered compacts. It has been discussed by many investigators but no further evidence concerning its metastability has been published. On the contrary more and more evidence seems to indicate that eta is one of the stable phases of the Wolfram-Cobalt-Carbon system⁽⁸⁾ (Appendix I). The eta phase has a promising high temperature oxidation resistance, a study of which is discussed in Appendix II.

The ternary system is under investigation by Mr. P. Rautala and Professor J. T. Norton at the Massachusetts Institute of Technology, their

work being carried out as part of this project. On the basis of their results up to date, the isothermal sections at room temperature, and at 1400°C of Figures 2 and 3 have been proposed⁽¹³⁾. It can be seen that the two phase field cobalt-wolfram carbide is extremely narrow and that a slight change of carbon content will lead to the appearance of graphite or eta. In addition to eta, the intermediate phases: Theta (θ), and Kappa (κ) also exist.

Not enough data has yet been obtained to establish the complete ternary diagram or even the definite vertical section through the ternary along the cobalt-wolfram carbide line. But, Mr. Rautala has worked out some of the possible variations in the appearance of the vertical section, Figure 1, which might be caused by a small displacement of the corners of the three phase fields.⁽¹³⁾

An investigation of a series of alloys lying on the cobalt-wolfram carbide line by Levinger⁽¹⁴⁾, who also was connected with this project, confirmed the solubility limits of wolfram carbide in cobalt as published previously by Sandford and Trent⁽⁸⁾, Brownlee⁽¹⁵⁾, and Korolkov and Lavler⁽¹⁶⁾. He assumed a quasi-binary and found a maximum solid solubility of about 17 percent by weight of wolfram carbide in cobalt, and an eutectic composition of about 38 percent by weight. There is considerable disagreement concerning the eutectic temperature: Sandford and Trent⁽⁸⁾ report 1320°C, Wyman and Kelley⁽³⁾ 1350°C, and Sykes⁽¹⁷⁾, Takeda and Levinger found it to be near 1275°C.

From the available evidence it is not possible to decide whether the eta phase takes part in the normal sintering of wolfram carbide-cobalt compacts. It does make its appearance at room temperature, if decarburization takes place, but is not found in normal specimens however rapid the rate of cooling.

It must be noted though, that according to the vertical sections shown, the eta phase appears only at or below the so-called 'eutectic' temperature, around 1300°C. At the sintering temperature (1400°C) therefore, none of the binder is tied up as eta. The presence or absence of eta, due to small changes of composition, might account for the discrepancies of the published eutectic temperatures.

III EXPERIMENTAL TECHNIQUES

For the purpose of experimental investigation the dilatometric method was selected because it is able to supply information on the sintering process, while it happens, at any temperature or time during the heating cycle. A sintering dilatometer was therefore built, (Figure 4). It consists of a closed end 'McDanel' High Temperature Refractory porcelain tube, 18 inches long, 0.5 inches internal diameter, into which the pressed sample is inserted. The sample is a rectangular bar of the following dimensions: 1 inch x 1/4 inch x 1/4 inch. The sample stands vertically in the tube. It supports a synthetic sapphire rod which transmits its expansion or contraction to an 'Ames' micrometer gauge attached to the top of the porcelain tube. The gauge is graduated in 0.001 inch and has a range of 0.5 inch.

This assembly is inserted into a vertical tube furnace where the sample is in the constant temperature region of the furnace. Approximately 6 inches of the dilatometer tube protrudes from the furnace so that the dial gauge is essentially at room temperature. The joints, from furnace to tube, and from tube to gauge, are water cooled rubber compression seals to assure gas tightness. The temperature of the sample is measured by a platinum - platinum rhodium thermocouple, protected from the reducing atmosphere of the furnace by a porcelain tube. The thermocouple is part of the temperature control system, which consists of a variable transformer regulating the power input, a potentiometer by means of which the temperature can be measured, and an electronic temperature controller which maintains a constant temperature by activating a relay which inserts a resistance into the heating circuit. The equipment used is shown in Figure 5.

Separate gas atmospheres can be provided inside the furnace and inside the dilatometer tubing, if the experimental conditions require it. Usually, 'Forming Gas' (20 percent H₂ and 80 percent N₂) is used in both. It protects the molybdenum winding of the furnace and the sample from oxidation without being as subject to the danger of explosion as pure hydrogen would be. Oxygen and water are removed from the gas by passing it over heated copper chips and through 'Drierite' drying reagent. To prevent decarburization of the sample small graphite rings are introduced into the tube; their direct contact with the specimen is prevented by a small refractory spacer ring.

The measured temperature was checked periodically by a reference thermocouple inserted in place of the sample into the dilatometer tube. This thermocouple is standardized against the melting points of gold and silver. Although the temperature can be maintained constant within $\pm 2^{\circ}\text{C}$ over a period of days, the absolute temperature is known only to within the inherent accuracy of the thermocouple and measuring potentiometer, approximately $\pm 10^{\circ}\text{C}$.

At first, a thin, hollow porcelain tube was used as a dilatometer rod, but at high temperatures, a small amount of irreversible bending occurred. It was replaced by the synthetic sapphire rod, now in use, which stands up very well at the temperatures in question. The dilatometer system is standardized by means of a one inch long piece of metal, usually wolfram, the thermal expansion of which is known. From such a standardization run, the expansion and contraction with temperature of the porcelain and sapphire parts can be calculated, and this correction is applied to each sintering

run. The weight of the dilatometer assembly on the sample (25 grams) has no effect on the shrinkage characteristics up to a temperature as high as 1400°C. For equal times and temperatures the shrinkage is percentage wise the same in all directions whether the sample was sintered with or without the dilatometer weight resting on it.

Since the accuracy of the results is dependent upon the frequency of readings, a continuous recording system is also in use. It consists of a 'Schaevitz' linear differential transformer activated by the motion of the sapphire dilatometer rod. The transformer indicates a mechanical position electrically. The electrical impulses are fed through an amplifier-rectifier to a 'Brown' recording potentiometer, which draws a continuous record of change of length versus time at temperature. This arrangement is shown in the block diagram of Figure 6.

The sintered alloys were further examined by x-ray diffraction and metallographic methods. A "Norelco" recording x-ray spectrometer was used for the identification of phases. Microscopic examination required polishing with diamond powders. In general, the method described by Tarasov and Lundberg⁽¹⁸⁾ was followed. It consists of using a diamond hone, followed by polishing on cloth covered wheels with successively 4-8 and 0-1/2 micron diamond paste (Buehler Diamet - Hyprez polishing compound). The etchant used was alkaline potassium ferricyanide, 10 grams $K_3 [Fe(CN)_6]$ and 10 grams KOH dissolved in 100 cubic centimeters of water. Cobalt etches yellowish and the carbide gray. A two minute etching time was generally sufficient. If eta phase is present it tarnishes in a fraction of a second, offering a positive identification. The metallographic technique used exaggerates the amount of porosity

present in the sintered specimens, since it is difficult to avoid the tearing out of carbide particles, especially from incompletely sintered samples.

The samples were prepared from powders of commercial grade. The wolfram carbide used was manufactured by the Fansteel Metallurgical Corporation. It had a nominal grain size of 0.5×10^{-4} cm, its actual particle size distribution is given in Table I. Cobalt powder, 99 percent pure, was made by the Carboloy Company.

The mixtures were ball milled for 48 hours in carbide mills, loaded with wolfram carbide balls and hexane. The dilatometer specimens were pressed in a rectangular die at 16 tons per square inch. No pressing lubricant was used. Each specimen weighed about eight grams.

The following physical properties were measured on sintered specimens: density, hardness, and bend strength. Density was calculated from weight and volume, as measured. Hardness is reported as Rockwell A. Bend strength was determined on a Brinell machine, loading at the center of a 9/16 inch span. The samples were not polished, or otherwise prepared, before bend testing.

The following variables, important in their effect upon the properties of the sintered compacts, were held constant throughout this work: Preparation of powders; size, size distribution and shape of particles; milling and blending; compacting pressure; size of specimen; rate of heating and cooling; and the furnace atmosphere.

IV GENERAL SINTERING BEHAVIOR

Since any proposed mechanism of sintering of cemented carbides would have to be correlated with the sintering behavior, a general study of the changes of length occurring with time and temperature was undertaken. The sintering dilatometer, as described above, was used.

A. Sintering Runs at Constant Heating Rate

A series of samples, containing from 0 to 100 percent cobalt, were heated at a constant rate (10° per minute up to 1000°C, 5° per minute from 1000° to 1500°C). The changes of length were plotted against temperature; typical curves are shown in Figure 7. Zero, on the ordinate, corresponds to the original length of the sample at room temperature in the unsintered state. Specimens of binder contents from 1 to 15 percent have curves very similar in shape and range. The sample first expands on heating, shrinkage becomes noticeable at 800°C, becoming increasingly more rapid up to 1300-1350°C, at which temperatures most of the shrinkage is completed. On cooling, the sample shrinks linearly with temperature, except for a slight discontinuity when the binder freezes. With increasing amounts of cobalt, from 1 to 15 percent, the net amount of linear shrinkage increases from 17 to 19.3 percent. Shrinkage is incomplete with cobalt contents of less than 1 percent. A sample containing 25 percent cobalt did not support its own weight and deformed at high temperatures. The sintering of pure cobalt is completed at 950°C, and that of wolfram carbide is insignificant even at 1500°C, showing less than 1 percent linear shrinkage. Table 2 summarizes the experimental results.

B. Sintering Runs at Constant Temperature

Isothermal dilatometer curves, shrinkage versus time, were taken for various compositions, at temperatures from 1200° to 1400°C. The set of curves are reproduced in Figure 8, 9, and 10. As before, zero, as the change of length scale corresponds to the original green length of the specimen. The fact that the 1200° sample starts shrinking from 0 has no particular significance; in fact, at lower sintering temperatures, the shrinkage, at temperature, may start from a greater length than the sample's original cold dimension because of the normal thermal expansion effect. At high sintering temperatures, considerable shrinkage occurs during the heating up process, so that the sample has already sintered appreciably when the desired temperature is reached. Table 3 indicates the time required to reach the final length at various temperatures also the total holding time of each sample at temperature for a composition of 7.5 percent cobalt. After reaching the indicated dimension the sample did not shrink any further during the remaining time at temperature. Figures 11 to 14 show microstructures of cemented carbides of 7.5 percent cobalt sintered at various temperatures for similar lengths of time. At 1300°C considerable porosity is still present, which is almost completely eliminated at 1325°C. There is no further appreciable change in the character of the microstructure at 1350° and 1400°C.

As before, the amount of shrinkage increases with cobalt content. Figure 15 shows the isothermal sintering curves at 1400°C of cemented carbides with 5 - 15 percent cobalt. The maximum amount of shrinkage was attained in 3/4 hour, except for the 5 percent cobalt sample. See Appendix III for some additional considerations on the kinetics of isothermal shrinkage.

The effect of increased binder content upon the microstructure is illustrated by Figures 16 and 17, showing a 15 percent cobalt sample sintered at 1350°C for 1 1/2 and 21-3/4 hours. The carbide particles appear more angular and better defined in a greater amount of binder. These microphotographs also were used to estimate the grain growth which takes place at the sintering temperature. The average grain diameter increases by 14 percent during 20 hours at 1350°C. This was determined by measuring the length of the carbide particles along arbitrary straight lines drawn across the photographic prints. Approximately 1000 particles were measured on each sample. The average particle length along the arbitrary measuring lines corresponds to $1.8 \cdot 10^{-4}$ centimeters for the sample of Figure 16 and $2.1 \cdot 10^{-4}$ centimeters for that of Figure 17. The increase of the average grain diameter reflects a disappearance of the smallest particle present; particles of lengths of $1 \cdot 10^{-4}$ centimeters or less represent 50 percent of the total number of particles counted in the first sample, and only 20 percent in the second sample. It is to be noted that the particle length, so measured, does not correspond to the true grain diameter or to the actual particle size, both of which are considerably larger. (See calculations in Appendix IV)

C. Conclusions

1. The extremely rapid rate of shrinkage between 1300°C and 1350°C, the marked increase in the extent of shrinkage in the same temperature range is shown by the isothermal sintering curves, and the disappearance of porosity from the microstructure between 1300°C and 1325°C, all indicate the formation of an appreciable amount of liquid phase between 1300°C and 1325°C.

2. Densification does take place at temperatures when the binder is solid. The rate of shrinkage decreases with time and seems to approach a limiting value asymptotically. But to produce dense compacts in a short time, sintering above the liquids is necessary.

3. For a given temperature and time, the attainable density, expressed as percent of theoretical density, increases with the relative amount of cobalt percent. Also the rate of shrinkage increases with the amount of binder.

V THE WETTING PROPERTIES OF THE BINDER
IN CEMENTED WOLFRAM CARBIDE ALLOYS

A. Theory

The following considerations of wettability and interfacial energy are based on the excellent summary of the subject by C.S. Smith⁽¹⁹⁾. The work required to enlarge the surface of separation between two phases by a unit of area is called the interfacial surface free energy. It is often expressed as the interfacial tension γ (dynes per centimeter) which has been formally defined⁽²⁰⁾ as the partial derivative of the free energy F with respect to the area of the surface of separation A , or:

$$\frac{\partial F}{\partial A} = \gamma$$

Wetting takes place if there exists a high degree of attraction between the atoms of the liquid and those of the solid. Spreading of the liquid then results in a decrease of free energy.

In the case of a drop of liquid on a solid surface (Figure 18a), the contact angle θ depends on the interfacial tensions between the three coexisting phases: liquid, solid and gas. Calling them respectively γ_{sg} , γ_{sl} , γ_{lg} (Figure 18b), the contact angle is that needed to establish equilibrium between the tensions of the three interfaces:

$$\gamma_{sg} - \gamma_{sl} = \gamma_{lg} \cos \theta \quad \text{Equation 1}$$

Complete wetting implies a contact angle of 0° , the liquid will spread freely over the surface of the solid. If the angle has a value of 180° , absolutely no wetting takes place. By common convention, wetting is said to occur if the angle of contact is less than 90° .

If the liquid wets the solid it will penetrate into surface connected capillaries and pores because it will tend to cover all the available surface of the solid. Such a liquid would therefore be soaked up into a porous compact of solid metal. The interfacial tension of two adjacent solid grains in contact with the liquid can be represented as in Figure 19. If the liquid-solid interfacial tension is assumed to be independent of the orientation of the surfaces, then

$$\gamma_{S_1S_2} = 2 \gamma_{LS} \cos \frac{\theta}{2} \quad \text{Equation 2}$$

A liquid will therefore penetrate indefinitely along the grain boundary if the interfacial energy of the liquid solid boundary is less than half that of the grain boundary in the solid. Whether a polycrystalline mass will be disintegrated by such a liquid depends on the grain boundary energies, which in turn are a function of the crystallographic orientations of adjacent grains⁽²¹⁾. A grain boundary of low energy, a twin boundary for instance, might resist penetration, but if the grain surfaces have very different orientations they will be separated. The mechanism is one of solution. The solid will dissolve preferentially at the grain boundaries and the liquid will be carried in by capillary action until the grains are out of contact. The grains will remain separated as long as the liquid is present. If the amount of liquid is relatively small, its surface tension will hold the mass together.

B. Wettability of Cemented Wolfram Carbides

Wettability and its cause, surface energy, must play an important part in the sintering of cemented carbides. Wetting usually takes place in

alloy systems which show extensive solubilities. The very finely divided carbide particles are of almost colloidal dimensions, which by definition, would be smaller than 10^{-4} centimeters. For a particle size of 10^{-4} centimeters there would be 10^{12} particles per centimeter cube of material, with a combined surface area of six square meters⁽²²⁾. This large surface area must mean that the properties of the interface between carbide and liquid are very important, and may influence the sintering behavior of carbides.

The wettability of wolfram carbide by liquid cobalt was determined by the drop shape method, which consists of measuring the angle of contact of a liquid drop on a solid surface. The experimental work was carried out by Mr. W. D. Kingery using the equipment of the Ceramics Laboratory of the Department of Metallurgy at Massachusetts Institute of Technology. A small piece of cobalt was placed on a level wolfram carbide block and this assembly was inserted into a horizontal tube furnace. The block of carbide was prepared by sintering pure wolfram carbide powder at 2000°C for one hour to a density 80 percent that of the theoretical density of wolfram carbide. The melting of the cobalt was observed through an optical pyrometer and photographs were taken through the ends of the furnace tube. A heating rate of 15° per minute in an atmosphere of 85 millimeters of hydrogen was used for this experiment. The first evidence of melting at the interface was observed at 1375°C . The cobalt spread freely and completely soaked into the porous wolfram carbide at 1420°C . The observed contact angle was 0° . Cobalt, therefore, completely wets wolfram carbide.

A cross section of the infiltrated wolfram carbide block is shown in Figure 20. The interaction of wolfram carbide and cobalt at the surface

left a crater at the original location of the cobalt piece. The microsection shows that densification occurred as the cobalt penetrated into the metal, the highest density being attained nearest to the original supply of cobalt.

To illustrate the action of a non-reacting binder, the drop-shape experiment was repeated with copper on wolfram carbide. Carbon and wolfram are practically insoluble in liquid copper. Copper is not completely absorbed by the porous carbide block, its wetting ability is limited, at 1405°C the drop of liquid copper has an angle of contact of 20° with solid Wolfram carbide. The temperature dependence of the angle of contact is reported in Appendix V. A cross section of the carbide block (Figure 21), shows that no densification has taken place. Although most of the copper remained at the surface, some of it penetrated into the sample, congregating in lakes near the surface. The carbide grains, even near the copper rich surface, remain small, irregular, and highly fissured in contrast to the large, well-formed grains of carbide in the cobalt infiltrated sample (Figures 22 and 23). Whereas copper apparently penetrated only into surface connected pores, cobalt, by solution of grain boundaries, could reach previously closed pores, and in effect, broke up the structure, permitting it to densify.

The densification of the impregnated skeleton, also the formation of large, regular wolfram carbide grains, can be attributed directly to the action of the cobalt, namely its solution and subsequent reprecipitation of wolfram carbide during heating and cooling, and to grain growth by solution and reprecipitation at high temperatures.

C. Infiltration of the Liquid Binder

The action of cobalt and copper binders was further illustrated by an infiltration experiment during which the change of length was followed dilatometrically.

Compacts of pure wolfram carbide were prepared by sintering the powder at 2000°C from 1/2 to 1 hour to a density of 10 grams per cubic centimeter, or 67 percent of the theoretical density of wolfram carbide. The unsintered specimen had a density only 50 percent of the theoretical, therefore some densification took place during sintering. In effect, a porous skeleton of carbide was formed. These samples were placed vertically into the dilatometer furnace. About 30 percent of their weight of cobalt or copper was added, which on melting, formed a pool at the bottom of the tube, and by capillary action, was drawn into the porous skeleton.

The dilatometric behavior during infiltration with cobalt can be followed in Figure 24. The carbide skeleton expands uniformly until about 1320°C. At this temperature a noticeable contraction sets in, followed at 1450°C by a sudden expansion, and finally, a very rapid shrinkage. The initial contraction is probably caused by a reaction between the wolfram carbide body and the cobalt powder at their points of contact at the bottom of the dilatometer tube. The expansion occurs when the liquid cobalt infiltrates the compact, destroys the skeleton by attacking the grain boundaries and forces the carbide grains apart. This also causes the compact to lose its strength, it will deform under its own weight and that of the dilatometer rod, which accounts for the final observed shrinkage.

The destruction of the skeleton on infiltration was also reported recently by Kiefer⁽⁴⁾, who noticed that it can be prevented by presaturating the binder with wolfram carbide which means using a wolfram carbide-cobalt alloy as the infiltrant.

The non-existence of the skeleton, after infiltration, is also shown by the dilatometric behavior of the sample on cooling (Figure 25). At the freezing temperature of the binder a sudden expansion takes place, which is attributed to the precipitation of carbide from solution on the undissolved grains. This phenomena shall be discussed more fully in the next chapter and in Appendix VI.

A similar experiment using copper as the infiltrant, showed none of the discontinuous dimensional changes. Copper does not destroy the carbide skeleton, therefore the observed expansion and contraction curves are those of the wolfram carbide skeleton. The cooling curve of the copper infiltrated sample is shown in Figure 25. Notice that there is no discontinuity at the freezing point of copper. This sample retained its shape and did not deform even at the maximum temperature of 1400°C.

The microstructures, Figures 26 and 27, clearly illustrate the action of cobalt and copper as binders. The cobalt tends to surround each grain of carbide, copper however preserves the sintered skeleton. The angular grains indicate that considerable solution and re-deposition of carbide has taken place in presence of the cobalt binder.

The following physical properties were measured:

Pure wolfram carbide compact sintered

to 80 percent of theoretical density: Bend Strength: 40 000 psi

Hardness: 50 R_A

Copper impregnated sample: Bend Strength: 117 000 psi

Hardness: 61 R_A

Cobalt impregnated samples: Bend Strength: 206 000 psi

Hardness: 78 R_A

D. Discussion of the Microstructure

This discussion shall be based on the microstructure of Figure 28, which was found in a commercial tool material of wolfram carbide-cobalt grade. This photograph is reproduced by courtesy of the Research Laboratory of Watertown Arsenal where it was taken. Examination of a large number of specimens indicated that this structure is typical, except for the large size of the grains which makes the structure easier to see.

Extensive carbide to carbide grain boundaries exist in such a structure, but probably only where the adjacent grains are favorably oriented. The angles of the large carbide particles were measured, and it was found that about 60 percent were angles of 30°, 60° and 90°, also the contact angles between adjacent grains usually have these same values. Quite obviously certain crystallographic planes are favored and cause the carbide particles to grow along well defined habit planes. The interfacial energy between solid and liquid is therefore a function of the orientation of the surface, which is to be expected with anisotropic hexagonal crystals such as wolfram carbide. Stranski⁽²³⁾ reports that the (0001), (10 $\bar{1}$ 0) and (10 $\bar{1}$ 1)

faces most often form the surfaces of hexagonal crystals when growing from a solution under equilibrium conditions. These planes would cause the observed crystal shapes, namely triangular prisms, with angles of 30° , 60° and 90° . Since the polished surface cuts the crystals at random not all angles will show up with their true values. But the true angle will constitute a majority of the measured values. The angular relationships between coherent grains suggests that the crystallographic orientations, of these grains are related, by being of the same or of twinned orientations. Such relations have been observed with other crystals and are brought about by either coalescence of existing grains or growth of one grain on another. Experiments with non-metallic salts have shown that, if a great number of small crystals are agitated together in a liquid, some of them will cohere to each other. It is found that all the coherent crystals show either a parallel or twin orientation across their common interface⁽²⁴⁾. It has also been demonstrated, with sodium chloride crystals, that precipitation on a seed crystal from a supersaturated solution, will result not only in the growth of that crystal but also in the formation of new crystals, attached to the seed, and having a twin orientation with it⁽²⁵⁾. Unfortunately the grains are so small that orientation measurements on individual grains by x-rays are not possible.

It has been suggested⁽²⁶⁾ that grain growth alone is not enough to explain the increase of grain size, but that coalescence of similarly oriented grains takes place. This would account for the small areas of cobalt, inside the carbide grains which are observed in Figure 28.

Larger areas of cobalt, called "lakes" are frequently encountered in the microstructure of cemented carbides. Mantle⁽⁶⁾ shows microphotographic evidence that these lakes disappear if the sintering temperature is raised from 1300°C to 1325°C. The origin of these lakes has not been adequately explained, but their disappearance can be attributed to the formation of the liquid binder phase, the wetting characteristics of which will force it to distribute itself more evenly throughout the compact.

E. Conclusions

On the basis of the preceding experiments and considerations it can

- be concluded that:
1. Liquid cobalt wets solid wolfram carbide.
 2. Liquid cobalt tends to surround each carbide grain and will attack an existing carbide skeleton.
 3. The characteristic angular shapes of the wolfram carbide particles are brought about by solution and reprecipitation in and from the cobalt matrix.

VI THE PHYSICAL DISTRIBUTION OF THE CARBIDE PHASE

The problem of the existence of a skeleton of wolfram carbide in sintered compacts was investigated by the series of experiments described below. The experimental data shall be used to deduce the structure and distribution of the carbide phase while heating the pressed compact to the sintering temperature, at the sintering temperature and at room temperature, after sintering.

A. Effect of Cold Pressing and Heating

A compact of pure wolfram carbide powder, containing no binder, has a certain amount of cohesion after being cold pressed. This cohesion is attributed to metallic junctions between adjacent carbide grains, similar to the phenomena of "cold" or "pressure" welding observed with other metals. Such a bond between two powder particles could theoretically attain the strength of a grain boundary in a polycrystalline metal if the plasticity is sufficient to produce a large contact area⁽²⁰⁾. However, in the case of wolfram carbide powder the cohesion is quite weak, the pressed compacts can be easily broken up between the fingers. The force of adhesion is not sufficient to cause appreciable contraction by plastic flow at room temperature and therefore, the area of contact between the irregular particles is very small. In addition, many of the existing joints are probably broken by the elastic recovery when the load is removed.

In the presence of a ductile binder metal, the cohesion is increased by the large contact area between binder and carbide. In addition, a weak skeleton of carbide may exist, which would be expected, however, to be

destroyed on heating by: a) the solution of wolfram carbide in the binder especially at the carbide to carbide grain boundaries, b) the thermal stresses caused by the expansion of cobalt, which has a larger coefficient of thermal expansion than wolfram carbide.

Table 4 shows the measured expansion of pressed compacts of various binder contents. The expansion increases with the binder content, therefore a continuous skeleton of carbide does not exist during the heating up period.

B. Binder Solidification Phenomena

The dimensional changes occurring on cooling were observed by means of the sintering dilatometer. Four compacts with 5, 7.5, 10 and 12.5 percent cobalt were sintered at 1450°C and cooled at a controlled rate of 10°C per minute. In Figure 29 the shrinkage on cooling is plotted against temperature. The curves are discontinuous between 1350°C and 1320°C, there being a sudden contraction for the 7.5, 10 and 12.5 percent cobalt samples, and an expansion for the 5 percent cobalt sample. The corresponding plot for pure wolfram carbide, sintered at 2000°C with no binder, and cooled through the same range, shows a continuous shrinkage along the normal thermal contraction curve.

The discontinuous changes of length vary with the composition gradually from a contraction at high cobalt content to an expansion at low cobalt content. (Table 5)

These phenomena can be understood by considering the physical changes which take place at the freezing temperature of the binder:

1. Precipitation of wolfram carbide from the liquid solution on the undissolved carbide particles. Each particle will increase in diameter and if we assume that each grain is separated from its neighbors by a thin

film of liquid binder, the length of the specimen will increase as the growing particles tend to push each other apart.

2. Shrinkage of the volume of the binder as it changes from the liquid to the solid state. This will result in a decrease of specimen length.

The two phenomena are opposite in their effects upon the length of a sintered wolfram carbide cobalt sample. But at very low binder contents most of the binder is concentrated in the pores of the carbide compacts. Only that thin layer, required to satisfy the low wolfram carbide cobalt interfacial energy, will surround each carbide grain and will separate two adjacent particles. Therefore, the contraction of the binder during freezing cannot alter the dimensions of the specimen since the carbide grains cannot approach each other any closer. However, the precipitation of wolfram carbide from the binder, which takes place on all surfaces of the undissolved carbide grains, will force the growing grains apart, and the specimen will expand.

A discontinuous behavior on cooling might be caused by the effect of the latent heat of freezing of the binder on a carbide skeleton. But this explanation must be rejected since this phenomena was not observed on cooling the copper infiltrated compact, referred to in the previous chapter (Figure 25). This sample consisted essentially of a skeleton of wolfram carbide in a matrix of copper and showed no discontinuity at the freezing temperature of copper. Copper and cobalt have the following latent heats of fusion: 3.11 and 3.7 kilogram calories per mole.

With a high percentage of cobalt, the structure becomes more and more that of isolated carbide grains in a matrix of cobalt. The contraction

of the binder will bring the carbide particles closer together, without causing them to come into contact with each other, and the specimen as a whole will shrink. Since the grains are more uniformly distributed in the binder, they are equally surrounded by cobalt in all directions, and their growth, due to precipitation from solution, will not alter the length of the compact. The solidification contraction of the binder accounts for the observed shrinkage of 10 and 12.5 percent cobalt alloys if a linear freezing shrinkage for cobalt of 1 percent is assumed. This assumption is based on the corresponding freezing shrinkages for copper and iron of 1.4 and 0.7 percent respectively. With high cobalt contents the linear distribution of carbide and binder becomes equal to the volume percent of each constituent. The possible change of density, as wolfram carbide diffuses from liquid to solid, has been neglected in this discussion.

From this experiment it is concluded that:

1. The cobalt binder freezes over a range of temperatures: 1350°-1320°C.
2. The dilatometric changes at the freezing temperature of the binder indicate that a continuous skeleton of wolfram carbide does not exist at that temperature.

C. Electrolytic Leaching Experiments

Experimental evidence to prove the existence of a strong and continuous skeleton in cemented carbides was presented by Dawihl and Hinnuber⁽⁵⁾, who leached out the binder with boiling hydrochloric acid and found that the remaining skeleton still had appreciable strength. They concluded that the carbide particles grow together during sintering and form a skeleton in samples with up to 10 percent cobalt. Sandford and Trent⁽⁸⁾, however,

refer to an experiment by which the binder was reacted with zinc to form a zinc cobalt alloy which could then be leached out. In this case the compact disintegrated into a powder.

For the purpose of establishing the existence of a continuous skeleton, electrolytic leaching methods were applied to sintered compacts of various binder contents. The leaching method used was based on the work of Cohen and co-workers^(27, 28) on the electrolytic isolation of carbides from annealed steels. The cell of Figure 30 was used. If the sample is made the anode in such a cell, using 1 =10 hydrochloric acid as the electrolyte, the ferrous binder is attacked, but the rate of solution of wolfram carbide is negligible. A current density of 0.2 amperes per square inch was applied. Results are reported in Table 6 and shown in Figure 31.

The loose carbide particles remained on the samples as a powdery layer, which could easily be removed by washing with water. The sample of 100 percent wolfram carbide was used as a control to demonstrate that wolfram carbide itself is not significantly affected by the leaching operation. It showed, after 56 hours of leaching, a weight loss of 0.3 percent. This loss is attributed to the presence of very fine carbide particles in this sample sintered to only 64 percent of its theoretical density.

The solubility of wolfram carbide in the electrolyte must be even less in the samples sintered with a binder, where considerable grain growth occurs during sintering and where the smallest particles are most easily dissolved in the binder. An attempt was made to account for all the constituents by a weight balance. However only 80 percent of the theoretical amount of cobalt present was extracted from a fully disintegrated sample.

The remainder must remain trapped among the coherent carbide particles which broke away.

This experiment indicates that no strong, continuous skeleton exists at room temperature with binder contents of 7.5 percent cobalt and higher. The conflicting results of Dawihl and Hinnuber must be attributed to an insufficient leaching action of boiling hydrochloric acid.

D. Coefficient of Linear Thermal Expansion

The thermal coefficients of expansion of sintered wolfram carbide alloys, with 0 to 25 percent cobalt, were measured with the sintering dilatometer. The results are reported in Table 7.

Figure 32 compares the measured coefficients with those calculated for a mechanical mixture assuming the law of mixtures to hold, using $5.4 \cdot 10^{-6}$ and $16.2 \cdot 10^{-6}$ inch/inch $^{\circ}\text{C}$.⁽²⁹⁾ as the coefficients of thermal expansion of pure wolfram carbide and pure cobalt. This value for pure wolfram carbide was experimentally determined on a compact of wolfram carbide sintered at 2000°C without binder. It represents an average value of coefficients in all possible crystallographic directions, since wolfram carbide, of hexagonal structure, shows considerable anisotropy. Becker⁽³⁰⁾ reports values of $5.2 \cdot 10^{-6}$ and $7.3 \cdot 10^{-6}$ inch/inch $^{\circ}\text{C}$ for the thermal coefficient of expansion (20° - 1930°C) in the orthohexagonal [100] and [001] directions.

The data plotted in Figure 32 show that, at low binder contents, the measured coefficient of thermal expansion (20 - 800°C) is less, and with high cobalt contents it is higher than that to be expected from the law of mixtures. This reflects the existence of a continuous matrix of cobalt when

the compact contains a great amount of binder and the well dispersed particles of carbide have proportionally little effect on the expansion. Correspondingly, the low coefficients with low binder contents could indicate the existence of a continuous wolfram carbide skeleton. This was the interpretation of Dawihl and Hinuber⁽⁵⁾, who had measured the thermal expansion of cemented wolfram carbide, and had noticed a similar depression of the coefficient at low cobalt contents. However, this phenomena would also be expected to occur without a skeleton. The coefficients of thermal expansion of a mixture do not necessarily obey the law of mixtures, especially at the extreme ends of the composition range. The coefficients are not only a function of the coefficients of expansion and the proportion by volume of the components, but also of their relative moduli of elasticity. This was shown to be true in the case of lead-antimony and beryllium-aluminum alloys⁽³¹⁾. The value of Young's modulus for wolfram carbide is about three times as high as that of cobalt^(29, 32). Its effect in the mixture will be to depress its coefficient of expansion below the average value when the composition is such that the carbide restrains the free expansion of the binder, namely at the high carbide end of the composition range. Accurate calculations would have to take into account the effect of distribution, size and shape of the carbide particles, but a qualitative estimation of the coefficients of expansion gave values of 5.70 and $5.85 \cdot 10^{-6}$ inch/inch - °C for alloys of 5 and 7.5 percent cobalt, which agrees well with the measured values of 5.6 and $5.9 \cdot 10^{-6}$ inch/inch - °C. However the agreement ceases with greater amounts of cobalt, the thermal expansion of the binder becomes predominant and the expansion of the alloy becomes less and less affected by the dispersed carbide phase.

Consequently, the observed deviations of the coefficients of thermal expansion from the law of mixtures do not prove the existence of a continuous skeleton, since they can also be explained on the basis of a discontinuous carbide phase.

E. The Relation of Strength to the Physical Distribution of the Carbide Phase.

The variation of strength with composition and temperature depends on the distribution of the carbide phase. If a continuous skeleton would exist, the strength would be expected to decrease with increasing cobalt content, and it would not be expected to be strongly affected by increased temperatures, at least up to the melting point of the binder. The strength data published in the literature, indicates, however, that the strength increases with increasing cobalt content up to 20 - 25 percent by weight, and only then decreases^(8, 33), it also shows a rapid decrease of strength with temperature.

As part of the present work, the bend strength was measured for samples of 1 to 25 percent cobalt which were sintered at 1400°C. The results are plotted in Figure 33 and show that a maximum of strength occurs between 15 and 25 percent cobalt.

The available data, regarding the strength of sintered carbides at high temperatures, is limited. Data quoted Goetzel⁽³²⁾, and reproduced here in Table 8, indicates a decrease of strength with increasing temperatures, especially marked around 900°C. At high temperatures, rapid oxidation occurs, and the strength cannot be measured further.

These data support the theory that the strength of sintered compacts depends, not on a carbide skeleton, but rather on the matrix of binder and its reaction to the structure. Indications are that a wolfram carbide

skeleton would not be of comparable strength, even if it were to exist. The copper infiltrated wolfram carbide skeleton, referred to in Chapter V, showed a strength of only 117 000 psi, compared to a similarly cobalt infiltrated sample, in which the skeleton was destroyed, and which had a strength of 200 000 psi. The highest value found in the literature for the transverse rupture strength of pure wolfram carbide, prepared by sintering, was 70 000 - 85 000 psi⁽³⁴⁾.

F. Conclusion

The experiments which have been presented here prove that a continuous skeleton of wolfram carbide does not exist at high or low temperatures in sintered wolfram carbide-cobalt compacts.

VII THE SINTERING MECHANISM

Pores in a powder compact are undesirable, not only do they reduce the cross section of metal for a given dimension, but they also act as "stress raisers" and thereby lower the effective strength. Sintering at elevated temperatures permits the pores to be eliminated through the influence of the surface tension forces.

Densification of a homogeneous metal powder compact occurs in two stages:

1. Formation of a skeleton, the particles weld together at their points of contact.
2. The area of contact is increased by diffusion, or plastic or viscous flow of metal.

However the densification of wolfram carbide-cobalt compacts is brought about by a different mechanism, which does not involve the sintering forces of the carbide particles, but relies on the surface tension of the binder as the driving force. In a compact of low binder content the carbide aggregate determines the dimensions of the piece. For a given composition, the density is related to the size, number and packing arrangement of the carbide particles, which are free to move relative to each other, and will be forced by the surface tension of the binder into positions of closest packing. The stresses introduced by the surface tension have been calculated by Shaler⁽²⁰⁾, in his work on the sintering of copper: assuming a surface tension of 1200 dynes per centimeter, they range from 35 to 35 000 psi with pores of radii from 10^{-3} to 10^{-6} centimeters. The stresses are transmitted by the binder, either solid or liquid, and force the carbide particles to move in the direction of the pore exerting the greatest stress.

As shown by capillarity phenomena, liquids may sustain very high tensile stresses under suitable conditions, namely as very thin films⁽³⁵⁾. In addition to the rearrangement of the packing of carbide particles, two more phenomena contribute to the shrinkage:

1. That directly caused by the solution, which makes the particles smaller and permits their geometrical centers to approach each other, without altering their relative positions.

2. Grain growth will also result in shrinkage, since the decrease of diameter of small grains is greater than the increase of diameter of large grains, for equal volumes of carbide dissolved and reprecipitated.

The three stages of the heat treatment: Heating, sintering at temperature, and cooling shall now be considered. After pressing, the compact consists of an aggregate of wolfram carbide, the interstices of which are partially filled by cobalt metal. On heating the sample at first expands, but as soon as the sintering forces are large enough to overcome the thermal expansion, a measurable shrinkage sets in. This occurs at about 800°C, which coincides with the effective sintering temperature of pure cobalt. As the temperature increases further, shrinkage becomes more and more rapid: The increased solubility of wolfram carbide in cobalt increases the mobility of the carbide particles, also the plasticity of the binder increases. Between 1300° and 1325°C the binder reaches the eutectic composition and it becomes liquid. This is associated with a jump of the solubility of wolfram carbide in cobalt and with the formation of a liquid film which surrounds all carbide particles, both of which factors markedly increase the rate of shrinkage. The liquid

film reduces the resistance to particle motion. Such an effect has been studied in the case of the packing and slipping of sand under load,⁽³⁶⁾ where it was found that a very small amount of liquid contributes to a closer packing of sand grains by facilitating their sliding over and by each other.

At the sintering temperature the binder is liquid. The compact continues to shrink, although at a decreasing rate. (See Appendix III for a study of the kinetics of isothermal shrinkage). The shrinkage due to solution of wolfram carbide in cobalt will cease as soon as the binder is saturated. The total contribution of this effect can be approximately calculated; for a sample of 10 percent cobalt, assuming uniform particle size of $3 \cdot 10^{-4}$ centimeters, a closed packed arrangement of particles, and a solubility of wolfram carbide in cobalt of 40 percent, the solution shrinkage amounts to 2 percent, compared to a total linear shrinkage of about 18 percent at 1400°C. (Method of calculation in Appendix VII)

The major part of the densification must, therefore, be attributed to a rearrangement of particles towards a denser packing and to grain growth. As the porosity decreases the rearrangement will reach a limit because the particles will abut against each other. Probably only the grain growth mechanism will permit densification as long as any porosity is present. It occurs because an aggregate of finely divided particles is in a state of higher free energy than a single crystal of the same metal, therefore the grains of favorable surface orientation will continue to grow at the expense of other grains by transfer of material through the saturated liquid.

The cohesion of the compact at the sintering temperature is also attributed to the surface tension of the liquid binder, and is discussed in

Appendix VIII. This cohesion is limited, specimens of odd shapes and great height have to be supported to prevent deformation.

On cooling, the solubility decreases and wolfram carbide will precipitate on the undissolved particles, which will continue to be separated by a film of liquid. At the freezing temperature of the binder a large amount of precipitation occurs which results in the discontinuous dilatometric change observed with small amounts of binder. The structure at room temperature is that of carbide particles embedded in a cobalt matrix. Only those carbide particles which have related surface orientations adhere to each other, all other particles tend to be separated by a film of binder.

The double role of the binder phase during the sintering of cemented wolfram carbide may be summarized as follows: It supplies the driving force towards densification, namely its surface tension, and it increases the mobility of the carbide particles, allowing them to achieve a closer packing. The effectiveness of cobalt as a binder of cemented wolfram carbide is based upon the following characteristics:

- a. It provides a liquid phase at relatively low temperatures.
- b. Wolfram carbide is soluble in the binder.
- c. The binder wets the carbide particles.

VIII THE MECHANICAL PROPERTIES OF CEMENTED WOLFRAM CARBIDE COMPACTS

A. Experimental Data

Sintered wolfram carbide-cobalt compacts are characterized by high hardness, high rupture strength, high compressive strength (up to 900 000 psi), a modulus of elasticity higher than that of any other known material (79 000 000 psi), but they possess little or no ductility. The hardness and the strength are the mechanical properties usually determined as a check on the quality of industrial products. The variation of these with composition is shown in Table 9 and the strength is plotted in Figure 33. The strength of the 20 percent cobalt alloy was not measured experimentally but was taken from equivalent data in the literature, and is included here to illustrate the fact that the strength reaches a maximum at about 20 percent cobalt, as had been found by other investigators^(8, 33). The strength is measured by a transverse rupture or bend test. The modulus of rupture as calculated from the bend strength represents the highest tensional stress in the section of the test specimen. The hardness is normally determined on the "A" scale of a Rockwell hardness tester, using a diamond penetrator with a 60 kilogram load. This scale was established as an arbitrary standard by the manufacturers of cemented carbides. Since the hardness of heterogeneous alloys is determined principally by the hardness of the constituent grains, it decreases as the cobalt content increases.

The effects of sintering temperatures and times on the strength of sintered compacts are summarized in Tables 10 and 11 for 7.5 percent and

15 percent cobalt alloys. The experimental work was carried out at the Watertown Arsenal Laboratory. It shows that a certain minimum time at temperature is required to attain maximum strength, but that further holding does not improve the properties. The 1300°C sintering treatment of 24 hours produced material of greater strength than sintering at high temperatures for shorter times. The overall strength of the 15 percent cobalt alloy series is below that of commercial products of a similar composition. Comparable densities were not attained during the sintering treatment. However, the data is useful as an indication of the effect of time and temperature.

Attempts to increase the strength of alloys of various compositions by a thermal cycling treatment, through a temperature range around the freezing temperature of the binder, were not successful.

A metallographic study of fine cracks found in fractured specimens, Figures 34 and 35, shows that failure takes place principally through the binder, however it may go through the carbide grains if they are large and are so situated that they lie across the fracture path. The fracture strength of binder and carbide grains are, therefore, not very different from each other. Figure 34 shows a fracture through a sample of normal particle size. The specimen of Figure 35, showing abnormally large grains, was used as a support in a sintering furnace where it underwent the sintering cycle a countless number of times. The failures were produced by fracturing the samples with a hammer. The cracks shown are adjacent to the area of complete fracture.

B. Theoretical Considerations

In this section an attempt shall be made to account for the high strength and brittleness of sintered wolfram carbide cobalt alloys by considering: 1) The residual stresses present at room temperature; 2) The internal stress conditions set up by an external tensile load. Both effects lead toward an increase of the yield stress, a reduction of ductility and to brittle fracture, if the fracture strength is lower than the increased yield strength of the metal.

1. Residual Stresses

In any composite alloy, which is cooled from a high temperature, considerable residual stresses are present at room temperature if the constituents have different coefficients of thermal expansion and different elastic properties. If the constituents are finely dispersed the stresses exist in microscopic regions, and have been named "tesselated" stresses by Laszlo⁽³⁷⁾ who developed a stress analysis technique to evaluate them. Metallographic evidence of such microstructural stresses was presented for certain alloys by Boas and Honeycombe⁽³⁸⁾, and Nielsen and Hibbard⁽³⁹⁾ showed, by an x-ray study, that they exist in aluminum-silicon alloys.

Stresses of high magnitude have been found to exist in the binder of sintered wolfram carbide-cobalt alloys by means of magnetic measurements. The coercive force is a measure of the internal stresses in ferro-magnetic metals, it is especially sensitive to small scale stress systems and is less affected by homogeneous residual stress⁽⁴⁰⁾. The extremely high coercive force of sintered alloys, increasing with decreasing cobalt content, and

reaching a value of 350 oersteds with as little as 0.5 percent cobalt, was attributed by Ritzau⁽⁴¹⁾ to the presence of high stresses in the binder, the nature of which must be similar to those discussed above. The coercive force of pure cobalt is only 9 oersteds.⁽²⁹⁾ The increase of the coercive force with decreasing binder content indicates that the phenomena is not due to solution of wolfram carbide in cobalt.

High internal stresses may also be the cause of the observed line broadening of cobalt lines in an x-ray diffraction pattern of sintered carbide compacts. The cobalt lines practically disappear when the cobalt content becomes less than 15 percent by weight. However other effects may contribute to the diffuse nature of the cobalt lines, namely: Particle size, possible solution gradient of wolfram carbide in cobalt, and possible partial transformation of cobalt. The cobalt transformation may be responsible also for a portion of the internal stresses since the transformation, on cooling, from a face centered cubic to a hexagonal close packed structure is accompanied by a volume shrinkage of 0.3 percent. In addition, evidence has been found in high cobalt alloys that the transformation does not go to completion^(14, 8) and, that therefore, microstresses would be expected in the binder from this source also. However more work is required to clear up the structure of the binder and evaluate the stresses by x-ray means.

It is possible to estimate the magnitude of stresses of thermal origin by the formulas derived by Laszlo. Two cases have to be distinguished, according to the distribution of the constituents:

a. The binder fills the cavities of a carbide structure, the grains of which are wedged rigidly against each other. Since the coefficient of thermal expansion of cobalt is about three times that of wolfram carbide, the binder will be subject to tensile stresses of a complex nature. For a compact cooled from 1300°C to a room temperature, the calculated tensile stresses at, and normal to, the wolfram carbide-cobalt interface, reach a magnitude of 250 000 psi (calculated in Appendix IX).

b. More or less isolated carbide particles are embedded in a cobalt rich matrix. On cooling the matrix contracts against the particles, setting up compressive stresses on both sides of the interface, in the carbide and in the binder⁽³⁹⁾. The radial compressive stresses, at, and normal to, the wolfram carbide-cobalt interface have a calculated magnitude of 100 000 psi (Appendix IX)

Both types of distribution of the constituents are present in a sintered wolfram carbide-cobalt compact. The binder therefore is subject to tensile and compressive stresses in adjacent regions. The actual magnitudes of the stresses are limited by the flow stress of the binder. Since the metal here is present as a thin film subject to complex stresses its flow stress must be appreciably higher than that corresponding to uniaxial stress conditions. The residual stresses will influence the mechanical properties of sintered alloys. They will increase the effective yield stress⁽⁴²⁾, especially if compressive and tensile stresses alternate in small neighboring areas⁽⁴³⁾ as is the case in sintered wolfram carbide cobalt compacts.

2. Complex Internal Stresses Set Up by an Externally Applied Load

In a compact of the usual compositions an externally applied tensile force will set up triaxial tensile stresses in the binder. Since plastic deformation is closely related to the maximum shear stress, and since triaxial stresses lead to shear stresses of minimum value, plastic flow is inhibited, the ductility is reduced, and the yield stress is apparently increased. These stresses are a result of constraint exerted on the binder by the carbide particles which are not free to move, and which prevent a lateral contraction of the binder in microscopic regions of the structure. The stress system is similar to that found, on a microscopic scale, in notched tensile bars and soldered or brazed joints.

In a notched bar, the metal at the notch carries the tensile load and tries to contract laterally. The contraction is prevented by the resistance of the unloaded mass in the shoulder above the notch. Therefore triaxial stresses are set up at the notch, which increase the yield stress and make it possible for brittle fracture to occur if the cleavage strength is sufficiently low.

Similarly, triaxial stresses are set up in a soldered or brazed joint under tension. The thin layer of soft metal between two bulks of much harder material is prevented from contracting laterally. Thereby the yield strength of the joining metal is raised and fracture takes place usually not through the joint, but at the boundary layer between the two metals, or even through the parent metal. With tin solders, the strength of the joint has been found to be 5.5 times as high as that of unworked tin⁽⁴⁴⁾. A similar increase of strength is recognized in copper brazing of steel.

On a microscopic scale, the stress condition in cemented carbides must be similar to those in soldered or brazed joints, and a similar variation of strength with composition is encountered. With tin solder, joining copper, brass and steel, a maximum of strength occurs with a joint 0.004 inches thick. The strength decreases radically with thinner joints and decreases, more gradually, with thicker joints⁽⁴⁵⁾. The strength of cemented carbides also shows a maximum which may be attributed to the change of strength with the thickness of the cementing layer between carbide particles.

The optimum amount of binder is that required to completely envelop the carbide particles present. With lesser amounts the carbide aggregate is not fully "cemented", the binder phase is not completely continuous, increased porosity is present and the structure is weakened. With greater amounts of binder the stresses in the binder become more uniaxial in nature, and the yield stress is decreased.

Therefore, even without the assumption of residual stresses, the mechanical properties can be accounted for by triaxial stresses set up by an external load. The residual stresses, in addition, raise the effective yield stress and contribute to the strength and brittleness.

IX COMPARISON OF COBALT WITH OTHER BINDER METALS

A number of attempts have been made to substitute other binders for cobalt in cemented wolfram carbide alloys, especially in Germany where the supply of cobalt was limited during the war. Takeda⁽¹²⁾, on the basis of his study of the ternary systems wolfram-nickel-carbon and wolfram-iron-carbon, concluded that nickel and iron would not be as suitable as cobalt as binders for wolfram carbide, because the binder phase would be brittle at room temperature. He attributed great importance to the varying stability of the eta phase and showed that it would be retained at room temperature in the case of an iron binder. In the case of nickel, the binder would be brittle because not all the dissolved wolfram carbide is reprecipitated on cooling. Nevertheless, iron and nickel indicated the best results of all the metals tried for binder use, although the sintered compacts only have 40 to 60 percent of the breaking strength of cobalt alloys⁽⁴⁶⁾. Additions of copper, silver, lead, zinc, tin, brass or bronze to compacts of wolfram carbide did not lead to satisfactory products⁽⁴⁷⁾.

This part of the report is concerned with a comparison of cobalt, nickel, iron and copper as binders for cemented wolfram carbide, with the purpose of isolating and identifying the qualities which make a good binder. The effect of the wetting characteristics, solubility of wolfram carbide, phases present during the after sintering shall be discussed.

A. Review of the Ternary Systems

1. Wolfram - Iron - Carbon

Takeda⁽⁴⁸⁾ found that the phases Fe_3W_3C (eta) and Fe_3C (cementite)

occur in all reactions involving the iron rich corner of the ternary diagram. He assumed that these phases are metastable, and that there exists in this ternary two sets of equilibria, the stable iron-carbon-wolfram carbide and the metastable iron-cementite- $\text{Fe}_3\text{W}_2\text{C}$. In that case the relation between eta and wolfram carbide would be similar to that between Fe_3C and graphite in the Fe-C system. On annealing at high temperatures eta would decompose into the stable phases wolfram carbide and austenite (Fe).

However there has not been published any further evidence regarding the metastability of these phases. For all practical purposes they may be considered to be stable phases of the wolfram-iron-carbon system as far as wolfram carbide-iron alloys are concerned, since they appear in all sintered compacts independently of the rate of cooling. The decomposition of eta, reported by Takeda, as proof of its metastability, can be attributed to carburization of the specimen at high temperature (See Appendix I). Figure 36 shows schematically the phase relations of the ternary system. Figure 37 shows a vertical section of the wolfram-iron-carbon ternary diagram with compositions on the iron-wolfram carbide line. It is to be noted that at 1400°C the binder would consist of liquid and eta, the saturated liquid containing about 48 percent wolfram carbide in solution.

2. Wolfram - Nickel - Carbon

Nickel has the same type of ternary diagram with wolfram and carbon as cobalt (Figure 2). It is basically different from that of the wolfram-iron-carbon ternary, in that no stable nickel-carbon or cobalt-carbon compacts

are formed. Therefore, the possibility of two-phase areas nickel-wolfram carbide and cobalt-wolfram carbide exists and these fields are actually observed. With nickel, as with cobalt, slight changes of composition will bring about the appearance of eta, (W_3Ni_3C), or graphite. The possible vertical sections nickel-wolfram carbide are similar in appearance to those shown in Figure 1 for cobalt-wolfram carbide. Takeda has found, though, that the ternary eutectic temperatures of the wolfram-nickel-carbon system are approximately $50^\circ C$ higher than those of the wolfram-cobalt-carbon system. He also attributed to the nickel binder a greater solubility for wolfram carbide at room temperature, so that the amount of binder is increased after sintering.

3. Wolfram - Copper - Carbon

Wolfram carbide is insoluble in solid or liquid copper since the solubility of carbon in copper is less than 0.0005 percent at $1400^\circ C$ ⁽⁴⁹⁾, and there is no solubility of wolfram in liquid copper⁽⁵⁰⁾. At all temperatures, only two phases, wolfram carbide and copper coexist in the sintered specimens.

B. Experimental Results

All samples were prepared by ball milling compositions of 92.5 percent wolfram carbide and 7.5 percent copper, iron, or nickel, for five hours, using benzene as dispersant. Compacts were pressed from these mixtures at 32 000 psi. Corresponding data for cobalt binder are usually included for comparison.

1. Sintering Runs at Constant Heating Rates

The general effect of different binders was compared by heating the

specimens at constant rate and plotting the change of length versus temperature (Figure 38). The extent of shrinkage and the shrinkage rate increase in the order copper, nickel, iron and cobalt.

2. Sintering Runs at Constant Temperature

Figure 39 shows the isothermal changes of length at 1400°C for specimens with different binder metals. The sintering curves of copper, nickel and iron binders have the same shape as that of a cobalt binder, although the amount of contraction, after one hour at 1400°C is appreciably less for copper, and somewhat less for nickel and iron than for cobalt. After 2 1/2 hours sintering at 1400°C the following densities were attained: Copper binder - 74 percent; Iron binder - 86 percent; Nickel binder - 38 percent; Cobalt binder, 96 percent, of the calculated theoretical densities for these compositions.

A series of isothermal sintering curves of 7.5 percent iron binder are shown in Figure 40. The marked jump in the extent of shrinkage between 1250°C and 1300°C is associated with the appearance of a considerable amount of liquid phase in this temperature range.

To demonstrate the dependence of the attained densities on the amount of binder present, a sample containing 15 percent nickel was sintered at 1400°C for 2 1/2 hours. It attained 93 percent of its theoretical density.

3. Measurement of the Wetting Properties

The wettability of solid wolfram carbide by nickel and iron was measured by the same methods already discussed for cobalt and copper (see Chapter V). The results for all four metals are summarized as follows:

Wolfram carbide-copper: Copper was observed to melt at 1085°C forming a drop with a contact angle of 62°. As the temperature was increased, a portion of the copper soaked into the porous carbide, and the contact angle decreased to 20° at 1405°C. (See Appendix V).

Wolfram carbide-nickel: Interfacial melting occurred at 1400°C. The liquid metal freely spread and completely soaked into the carbide block. The contact angle is 0°.

Wolfram carbide-cobalt: Interfacial melting, spreading and complete absorption took place at 1375°C. The contact angle is 0°.

Wolfram carbide-iron: Interfacial melting, spreading and complete absorption took place at 1450°C. Contact angle equals 0°.

Typical microstructures of the infiltrated wolfram carbide blocks are shown in Figures 41 to 44. Although the binder metal itself cannot be seen, its effects are illustrated by the increased grain size, regularity of grains and disappearance of grain cracks and fissures, with nickel, iron and cobalt binder. The effect of cobalt as contrasted to that of copper has been shown in Figures 22 and 23. The binders, therefore, must be present as extremely thin films, which make possible the solution and subsequent reprecipitation of wolfram carbide. The following phases were identified throughout the cross sections of the samples:

Wolfram carbide and cobalt, in the cobalt infiltrated specimen

Wolfram carbide, and eta, in the nickel infiltrated specimen

Wolfram carbide, Fe₃C, eta and iron, in the iron infiltrated specimen

Wolfram carbide and copper, in the copper infiltrated specimen.

The eta phase was identified by rapid darkening with an alkaline ferricyanate etch. Fe_3C was etched electrolytically in sodium picrate. These phases could also be identified by x-ray diffraction. A structure only found in the nickel infiltrated sample is shown in Figure 45. Three phases are present: Wolfram carbide, eta and nickel. The large dendritic structure, yellow in color, has been identified as resulting from an eta and nickel eutectic.

4. Binder Freezing Phenomena

The changes of length during cooling of wolfram carbide compacts sintered with copper, nickel and iron binders are plotted in Figure 46. An expansion is observed with iron, discontinuous contractions occur with nickel and copper binders. A 15 percent nickel alloy was used because a 7.5 percent nickel sample only contracted very slightly and the temperature range could not be clearly determined. These phenomena can be interpreted similarly to those observed with cobalt binders. An expansion occurs with the iron binder because the amount of liquid phase, present at the freezing temperature, is small. In the case of 7.5 percent nickel sufficient liquid binder is present to overcome the expansion effect, and with 15 percent nickel the freezing contraction of the binder is clearly dominant. The very small contraction of the wolfram carbide-copper compact near the freezing temperature of copper, indicates that only a small amount of liquid copper was present between adjacent carbide grains. From these experiments it may be concluded that:

- a. No continuous carbide skeleton is formed with these binders.
- b. On cooling, the liquid phase disappears at $1225^{\circ}C$ in wolfram carbide-iron cemented alloys; at $1350^{\circ}C$ in wolfram carbide-nickel

alloys; and at 1075°C for wolfram carbide-copper alloys.

5. The Microstructure of Sintered Compacts

Compacts of wolfram carbide and 7.5 percent binder metal were sintered at 1400°C for 2 1/2 hours. The resulting microstructures are presented in Figures 47 to 50. The structures are similar, showing carbide grains surrounded by binder metal, but the grain size, grain regularity and density attained with different binders increases in the order; copper, iron, nickel, cobalt.

The following phases were found in the sintered specimens:

Cobalt binder: Wolfram carbide and cobalt

Nickel binder: Wolfram carbide and nickel

Copper binder: Wolfram carbide and copper

Iron binder: Wolfram carbide, eta and Fe₃C

The phases present in the sintered wolfram carbide-iron compacts were determined by x-ray diffraction. Strong lines of wolfram carbide and weak lines of Fe₃C and eta were recorded. No iron could be detected. In Figure 51, the eta phase is brought out by lightly etching with an alkaline solution of K₃Fe(CN)₆, which colors it a bright yellow in a fraction of a second. It is present in the form of blotches inside large pores. The remainder of the structure is not attacked. On prolonged etching the eta phase shows up less distinctly.

The structure of a sample containing 15 percent nickel, sintered one hour at 1500°C, is shown in Figure 52. Except for less porosity, and more binder area, the microstructure is very similar to that of Figure 48.

6. Physical Properties

The physical properties measured on compacts sintered with various binders are reported in Table 12.

7. Summary of Experimental Results

See Table 13

C. Discussion of the Effectiveness of Various Binders

The experimental data indicate that the mechanism of sintering of cemented wolfram carbide with the binders copper, iron and nickel is fundamentally the same as that with a cobalt binder, although the extent of densification varies. The following requirements were derived for a binder in such a system:

- a. Existence of a liquid phase at the sintering temperature
- b. Extended solubility of wolfram carbide in the binder
- c. The binder must wet the solid carbide.

But the binder phase affects not only the extent of densification of cemented compacts, it also contributes directly to the strength of the sintered pieces. How the various binders affect the densification and the strength shall be discussed as follows:

Copper, as a binder, satisfies only the first requirements. Its solubility for wolfram carbide is nil, its wetting ability is limited, therefore it cannot contribute effectively to the densification when added in small amounts. Such sintered compacts will be porous and weak.

Iron satisfies all three requirements for a good binder. However, at the sintering temperature, the amount of liquid is limited, since some of the binder has combined with wolfram carbide to form eta. Therefore less

densification takes place than with a cobalt binder. Also, in the wolfram carbide-cobalt system the binder rejects most of the dissolved wolfram carbide on cooling, in the wolfram carbide-iron system, however, the binder transforms essentially to Fe_3C and ϵ . This results in the presence of a greater amount of binder at room temperature, and the compact is brittle, because of the presence of the brittle phases Fe_3C and ϵ . Iron as a binder, therefore, leads to a compact of high porosity and greater brittleness.

Nickel, also is not as effective a binder as cobalt, although it satisfies the listed requirements for a good binder and moreover shares with cobalt the same type of diagram with wolfram and carbon. A striking difference is found in the microstructure: The nickel cemented carbide particles have obviously not undergone the solution and reprecipitation process which leads to grain growth in the wolfram carbide-cobalt system. According to Takeda⁽¹²⁾ nickel retains a good portion of the carbide in solution at room temperature, so that less precipitation and less grain growth takes place on cooling. The amount of binder phase would thereby be increased from 7.5 percent to about 10 percent weight after sintering. But the smaller amount of densification, also the presence of a great number of very small particles, indicates that, at the sintering temperature, the amount of wolfram carbide transferred through the liquid phase is less than with a corresponding amount of cobalt binder. That means that there exists either a smaller solubility of wolfram carbide in the nickel binder or that the amount of liquid present is less.

Takeda⁽¹²⁾ found very similar solubilities at $1400^{\circ}C$ in the wolfram carbide-cobalt and wolfram carbide-nickel systems. The amount of liquid

phase should therefore be about the same if only the two phases, wolfram carbide and liquid, exists. However, it is possible that the eta phase takes part in the sintering reaction of wolfram carbide-nickel alloys. Then, the amount of liquid would be limited since some of it is tied up as eta. This would satisfactorily explain the lack of grain growth and the slower densification. On cooling, eta would react to form wolfram carbide and nickel solid solution, and therefore would not be present at room temperature. This view is supported by the following considerations:

a. Takeda found that the wolfram-carbide-nickel system comprises the composition range where both eta and wolfram carbide can coexist with the liquid at the sintering temperature.

b. The ternary eutectic temperatures of the wolfram-nickel-carbon system are appreciably higher than those of the wolfram-cobalt-carbon system. This increases the probability of eta being present at the sintering temperature (See Figure 1).

c. The eta phase was found in the nickel infiltrated carbide skeleton which was cooled rapidly from the sintering temperature (Figure 41). However it could never be seen in normally sintered samples, even after very fast rates of cooling when the sintered specimen was cooled in a blast of helium after being heated by induction. Of course, the above discussion does not include eta normally found at the surface of samples sintered in a reducing atmosphere.

A full study of the wolfram-nickel-carbon system is necessary before more definite conclusions concerning the sintering reactions of wolfram carbide-nickel alloys are possible. The lower strength of nickel cemented

wolfram carbide compacts can be attributed not only to the brittleness of the carbide containing binder but also to the presence of many pores due to a lack of complete densification. However, the experimental data indicate that, with a higher binder content and a higher sintering temperature, the attainable densities and strength of wolfram carbide-nickel compacts improve and it is conceivable that a suitable combination of sintering time and temperature might be found which would make the performance of nickel equal that of cobalt.

D. Conclusions

It has been shown that copper, iron and nickel are not as effective as cobalt for use as binders for cemented wolfram carbides. At the normal sintering temperature, with small amounts of binder, an insufficient volume of liquid is formed to permit the attainment of full densities within reasonable times. The strength of the sintered compacts is further reduced by the brittleness of the binder phase at room temperature. As a result of this comparison an additional requirement for binders of cemented carbides can be stated as follows:

To assure full densification and optimum properties, the ternary system of the binder with wolfram and carbon must be such that only two phases coexist in the compacts, at the sintering temperature and at room temperature.

X GENERAL DISCUSSION OF RESULTS

It has been shown that densification of cemented wolfram carbide-cobalt alloys takes place by a rearrangement of the carbide particles under the influence of the surface tension of the binder. The resulting structure of the sintered compacts is essentially one of carbide grains embedded in a matrix of the binder metal. The ability of the binder to bring about densification is a result of the solubility of wolfram carbide in the binder and of the wetting ability of the latter. The solution effect only indirectly assists the sintering process by breaking up existing carbide to carbide bridges, causing grain growth by solution and reprecipitation, and, by eliminating surface and shape irregularities decreasing the resistance to movement. The wetting property of the binder, however, is essential to the process since it forces the liquid to surround all particles and thereby allows the surface tension stresses to act upon them. Densification cannot take place with a non-wetting binder, but it can occur with a binder of no appreciable solubility for wolfram carbide.

With a given amount of binder, full density can only be reached if the packing arrangement of the carbide grains is such that the binder fills the interstices of the structure. Spherical particles, of selected sizes, have been packed in such a manner as to reduce voids to less than 4 percent by volume⁽⁵¹⁾. However, by careful selection of the particle size distribution, it should be possible to approach the theoretical density to any desired degree. It is therefore quite reasonable to expect that a compact of good density can be produced with as little as one percent by weight of binder, which corresponds to about 2 percent by volume.

The only alternative to the densification mechanism proposed here would be a mechanism by which the carbide particles would sinter to each other, by diffusion or flow of wolfram carbide through the effect of its own surface tension. In this case the binder would only have an auxiliary role, such as cleaning the surface of the particles by dissolving oxide films and other impurities.

The effectiveness of such sintering forces increases with temperature, and therefore, sintering would be expected to take place at the highest temperature reached, namely the sintering temperature. But the evidence presented here indicates that welding of the particles does not take place while the binder is liquid, therefore this mechanism does not contribute to densification at high-temperatures. Also, if a skeleton does not exist at high temperatures, precipitation, on cooling, will take place uniformly on all surfaces and will not change the structure of the compact.

The stresses, produced on cooling by the different thermal contraction of the constituents, might bring about an increase in the number of points of contact between adjacent grains. But these are formed at low temperatures, and similarly to the weak skeleton formed by cold pressing, are not expected to contribute either to the strength or to any other property of the sintered compact. This effect may be responsible for the point contacts between particles, which are observed in the microphotographs of the structure. That these do not, however, form a strong skeleton was shown by the experimental work under discussion.

The prevalent hypothesis, found in the literature, that the mechanical properties of sintered wolfram carbide compacts can be attributed to a

continuous carbide skeleton, tacitly assumes that the binder phase, by comparison, is weak and ductile and does not contribute to the strength. But even if a skeleton were to exist, it would contribute to the existence of stresses in the binder, the nature of which has been discussed in this thesis, which effectively would raise the strength of the binder and might make it the determining factor. There is no evidence that a carbide skeleton would actually be strong. On the contrary, the nature of a skeleton would cause it to be brittle because of the stress concentration produced by the many notches in its structure. Also, it has been shown by microphotographs, that the large wolfram carbide grains are not necessarily stronger than the binder phase under complex stresses. In addition, the formation of a continuous skeleton would be undesirable during the sintering of cemented wolfram carbide-cobalt alloys. It would restrict the mobility of the carbide particles, and prevent densification at the temperatures used.

It has been shown in this thesis that the mechanical properties of sintered compacts can be attributed to the binder. Although the calculated bend strength represents the tensile stress at the outer fiber of the test specimen, it is considerably higher than the strength measured in simple tension. A ratio of two between the bend strength and tensile strength is commonly observed for brittle materials such as cast iron, and tool steels⁽⁵²⁾, also for cemented carbides⁽⁵³⁾. A bend strength of sintered compacts of approximately 300 000 psi corresponds therefore, to a tensile strength of about 150 000 psi. Since cobalt, as a pure metal, has a tensile strength of 40 000 psi⁽⁵⁴⁾, an increase of strength by a

factor of approximately four has to be accounted for. The residual stresses would be expected to raise the strength by a factor of 2, if it is assumed that their effect is similar in nature and magnitude to that of cold work. The alloy content of the binder at room temperature also raises its strength. The solubilities of wolfram and carbon in cobalt are small, and the strength, thereby, is probably not increased by more than a factor of two. The strength of the binder must therefore be attributed, to a major extent, to the effect of the triaxial stress conditions produced by an external load. As has been mentioned, this effect increases the strength of joining metals about 5 times. In cemented carbides it similarly raises the yield strength so that the brittle strength, which is measured, probably approaches the true fracture strength of the binder.

The sintering mechanism of cemented wolfram carbide is the same as that encountered in other powder metallurgical products sintered in presence of a liquid phase, such as copper-silver, wolfram-copper-nickel, wolfram-cobalt and molybdenum-nickel alloys⁽⁵⁵⁾. They all show the characteristic structure of grains of a refractory phase surrounded by a matrix of a lower melting phase, which was liquid at the sintering temperature. A similar microstructure is found in cobalt cemented titanium carbide compacts, but here, large areas of contact between adjacent titanium carbide grains are visible⁽⁵⁶⁾, suggesting the possibility that a strong skeleton is formed. Of all the systems mentioned, only cemented wolfram carbide shows the characteristic angular carbide grains, the refractory particles in the other systems are round, indicating that the effect of the crystallographic orientation on the surface energy is negligible.

Considering the substitution of other binders for cobalt in cemented wolfram carbide compacts, it has been shown that, of those considered, only nickel comes nearest to satisfy the theoretical requirements of an effective binder, but the properties attained with nickel are inferior to those attained with cobalt. Nickel, however, warrants further investigation. With suitable variations of sintering times and temperatures, to permit the attainment of theoretical densities with low binder contents, the properties might be appreciably improved. A substitution of other binders, of higher melting point than cobalt, may lead to compacts of greater strength at high temperature. The high temperature strength of course, disappears at the melting temperature of the binder phase. For wolfram carbide-cobalt sintered alloys this was found to be between 1300°C and 1325°C, which agrees with the findings of Sandford and Trent⁽⁸⁾ (1320°C) but not with those of Wyman and Kelley⁽³⁾ (1350°C), or Sykes⁽¹⁷⁾, Takeda⁽¹²⁾, and Levinger⁽¹⁴⁾ (1275°C). It is interesting to note that the low temperatures were found with cobalt rich alloys, the composition of which is the same as that of the binder phase at high temperatures, whereas the higher temperatures were measured on sintered compacts of the usual, low-cobalt, composition. This disagreement of results can be attributed either to the effect of the difference of structure, or to a chemical effect such as the transitory existence of the eta phase near the melting temperature as a result of the diffusion of wolfram and carbon into the binder.

Of all the variables, which were held constant during this work, the sintering atmosphere is probably one of the most important in its effect on the properties of sintered compacts. If it is either carburizing or

decarburizing it will lead to the formation of a third phase: Eta or graphite, both of which weaken and embrittle the products. The two phase field, wolfram carbide-cobalt, is very narrow and it requires a truly neutral atmosphere, or one in perfect equilibrium with the alloy, to keep the composition constant. The work on the high temperature oxidation resistance of the eta phase (Appendix II) supports the contention that eta is a stable phase of the ternary system wolfram-cobalt-carbon.

The particle size of the carbide, a variable which also was held constant, is expected to influence the strength of the sintered compacts. The strength is a function of the thickness of the cementing layer between particles. For a given composition the layer becomes thinner as the particle size decreases, since the surface area increases inversely proportional to the radius of the grains. The stresses in the binder, and therefore the strength of the compact, increase until the amount of binder present is insufficient to cover all the available surface and achieve full density.

XI GENERAL CONCLUSIONS

1. Densification of cemented wolfram carbide-cobalt alloys takes place by a rearrangement of the carbide particles, which achieve a denser packing, under the influence of the surface tension forces of the binder.

2. The resulting structure is one of carbide particles embedded in a cobalt rich matrix. A continuous wolfram carbide skeleton is not formed during the sintering treatment.

3. This structure accounts for the characteristic mechanical properties of cemented compacts. Their strength and brittleness can be attributed to the binder, the yield strength of which is increased by the presence of residual stresses of thermal origin, and by a complex internal state of stress set up by external loads.

4. The following are the essential characteristics required of an effective binder for cemented wolfram carbide compacts:

- a. It must supply a liquid phase at relatively low temperatures.
- b. Wolfram carbide must be soluble in the binder.
- c. The liquid binder must wet the solid carbide particles.
- d. The ternary system wolfram-carbon-binder must be such that no third phase appears, in addition to wolfram-carbide and the binder rich phase, either at the sintering temperature or at room temperature.

5. Of the four binders investigated cobalt and nickel satisfy the theoretical requirements, although for reasons not fully understood, cobalt is more effective than nickel. Copper and iron are not suitable for use as binders of wolfram-carbide to produce strong sintered compacts.

XIII SUGGESTIONS FOR FURTHER WORK

It is realized that this work is mainly qualitative and that almost every phase of it can be subject to further fruitful study. The problem touches on many fields and some of its constituent parts will probably be solved by fundamental research in other branches of science. For instance, the study of the rate of shrinkage is related to the problem of sintering in general, and to that in presence of a liquid phase, in particular; the role of the binder phase here is the same as that of similar acting binders in ceramics; the effect of the stresses in the binder cannot be analyzed before more is known of the effect of residual and triaxial stresses on the properties of metals in general. It is hoped that the result of such studies will be applied to the problem of cemented carbides and will further clarify their sintering mechanism and their structure.

The following suggestions for further work are thought to lead to results of immediate usefulness:

- a. A study of the effect of all possible variables on the properties of cemented compacts. The following variables ought to be included: The nature of the raw materials; grinding and mixing; particle size distribution; compacting pressures; composition; sintering atmospheres; temperatures and times; rate of heating and cooling; etc.
- b. A study of nickel as a binder of wolfram carbide.
- c. Consideration of other binders with the purpose of attaining an improvement of specific properties such as ductility, high temperature strength, etc.

d. A study of the oxidation of cemented carbides at high temperatures, with special emphasis on the effect of the eta phase.

e. A study of the sintering mechanism of other cemented carbides with various binders.

f. A study of the structure, grain size etc. of the binder phase by x-ray means, for instance.

BIBLIOGRAPHY

1. R. Kieffer and W. Hotop, Pulvermetallurgie und Sinternokstoffe, Springer - Verlag, Berlin, (1943), 273.
2. S. L. Hoyt, Hard Metal Carbides and Cemented Tungsten Carbides, Trans. A.I.M.E. 89, (1936), 9.
3. L. L. Wyman and F. C. Kelley, Cemented Tungsten Carbide, A Study of the Action of the Cementing Material, Trans. A.I.M.E. 93, (1931), 208.
4. R. Kieffer, Cemented Carbides, Seminar on Sintering, Sylvania Electric Corporation, Bayside, N.Y. (1949), (To be published)
5. W. Dawihl and J. Hinnuber, Ueber den Aufbau der Hartmetalllegierungen, Kolloid Zeitschrift, 103 - 104, (1943), 233.
6. E. C. Mantle, The Sintering of Tungsten Carbide with a Cobalt Binder, Metal Treatment 14, (1947), 141.
7. The German Hard Metal Industry; B.I.O.S. Final Report 1385, H.M. Stationery Office, London (1947), 294.
8. E. J. Sandford and E. M. Trent, The Physical Metallurgy of Sintered Carbides, Iron and Steel Inst., Symposium on Powder Metallurgy, Special Report No. 38, (1947), 84.
9. C. G. Goetzl, Treatise on Powder Metallurgy, Vol. II, Interscience Publishers, New York, (1950), 110.
10. F. Skaupy, Dispersoid - Chemische und Verwandte Gesichtspunkte bei Sinterhartmetallen Kolloid Zeitschrift, 98, (1942), 92.
11. W. Dawihl, as quoted in: Tungsten Carbide Research in Germany; B.I.O.S. Final Report No. 925, H. M. Stationery Office, London, (1947), 17.
12. S. Takada, A Metallographic Study of the Action of the Cementing Material for Cemented Tungsten Carbide; Science Reports of Tohoku Imperial University, Hondu Anniversary Volume (1936), 864.
13. J. T. Norton, P. Rautala and J. Gurland, Role of the Binder Phase in Cemented Refractory Alloys, Report No. WAL 671/88-20, U. S. Army Ordnance Department, (1950)

14. B. Levinger, The Constitution of Cobalt-rich Co-WC alloys, Master's Thesis (1950), Department of Metallurgy, Massachusetts Institute of Technology.
15. C. D. Brownlee
Report No. 9545, March 1947, Research Department, Metropolitan Vickers Electrical Company, Ltd: Manchester, England
16. A. M. Korolkov and A. M. Lavler, The Phase Diagram of the WC-Co System Metallurgy 2 (1934), 53 (In Russian)
17. W. P. Sykes, Discussion to Reference (3)
Trans. A.I.M.E. 93 (1931), 227.
18. L. P. Tarasov and C. O. Lundberg, Rapid Polish with the Diamond Hand Hone Metal Progress 55, (1949), 183.
19. C. S. Smith, Grains, Phases, and Interfaces - An Interpretation of Microstructure
Trans. A.I.M.E. 175, (1948), 15.
20. A. J. Shaler, The Kinetics of the Sinter Process, Sc.D. Thesis, (1947) Department of Metallurgy, Massachusetts Institute of Technology
21. C. G. Dunn and F. Lionetti, The Effect of Orientation Difference on Grain Boundary Energies
Trans. A.E.M.E. 185, (1949), 125.
22. G. Ritzau, Konstruktion von Legierungen als Metallkeramisches Problem. Archiv F. Metallkunde 1, (1946-1947), 305.
23. I. N. Strauski, Forms of Equilibrium of Crystals, Discussion of the Faraday Society, 5, Crystal Growth, (1949), 13.
24. G. Friedel, Sur un Novean Type de Macles, Bull. Soc. Franc. Mineral. 56, (1933), 262.
25. G. Deicha, Macles et Desiquilibre Cristallogenetique, Experintia, 4, (1949), 67.
26. E. J. Sandford, Discussion to Reference (6)
Metal Treatment 14, (1947), 239.
27. D. J. Blickwede and M. Cohan, The Isolation of Carbides from High Speed Steels.
Trans. A.I.M.E. 185, (1949) 578.

28. R. W. Belluffi, M. Cohen, and B. L. Averbach,
The Tempering of Chromium Steels.
Trans. A.S.M. (1950), to be published.
29. W. C. Ellis and E. S. Greiner; Cobalt,
Metals Handbook, 1948 edition, A.S.M., Cleveland, 1136
30. K. Becker, Die Kristallstruktur und der Lineare Wärme Ausdehnungskoeffizient
der Wolfram Carbide,
Z. F. Physik, 51, (1928), 489.
31. P. S. Turner, Thermal Expansion Stresses in Reinforced Plastics
Inst. of Research, National Bureau of Standards, 37, (1946), 241.
32. C. G. Goetzal, Treatise on Powder Metallurgy,
Vol. II, Interscience Publishers, New York, (1950), 125.
33. E. W. Engle, Cemented Carbides
Powder Metallurgy; J. Wulff, Editor
A.S.M. Cleveland, (1942), 436
34. C. G. Goetzal, Treatise on Powder Metallurgy, Vol. II
Interscience Publisher, New York, (1950), 81
35. A. Nadia, Plasticity
McGraw Hill, New York, (1931), 13.
36. E. N. da C. Andrade and J. W. Fox; the Mechanism of Dilatancy
Proc. Physical Society, 62B, (1949), 483.
37. F. Laszlo, Tesselated Stresses, Part I, No. 1.
J. Iron and Steel Inst., 147, (1943), 173.
38. W. Boas and R.W.K. Honeycombe, The Anisotropy of Thermal Expansion,
As a Cause of Deformation in Metals and Alloys.
Proc. Royal Society, 188, (1947), 427.
39. J. P. Nielsen and W. R. Hibbard Jr., X-Ray Study of Thermally Induced
Stresses in Microconstituents of Aluminum-Silicon Alloys.
J. Applied Physics, 21, (1950), 853.
40. R. King, The Investigation of Internal Stresses by Physical Methods
Other than X-Ray Methods.
Symposium on Internal Stresses and Alloys, The Institute of Metals
London, (1948), 13.
41. C. Ritzan, Beitrag zur Magnetischen Analyse von Hartmetallen
Stahl u. Eisen, 60, (1940), 891.

42. Sub-committee on Relief of Residual Stress, Relief of Residual Stress, Metals Handbook, 1948 edition. A.S.M. Cleveland, 237
43. F. Seitz, The Physics of Metals
McGraw Hill, New York, (1943), 95
44. E. Orowan, J. F. Nye and W. J. Cairns, Notch Brittleness and Ductile Fracture in Metals.
Theoretical Research Report No. 16/45, Ministry of Supply (London) (1944)
Also: The Fracture Strength of Solids, Reports on Progress in Physics, The Physical Society, XII, (1948-1949), 185.
45. S. J. Nightingale, Tin Soldiers.
British Non Ferrous Metals Research Association (London), (1932), 45.
46. O. Meyer and E. Eilander, Die Sinterung von Hartmetallegerungen
Arch. f. d. Eisenhuttensesen 11. (1937-1938), 545.
47. J. T. Norton and R. B. Russell, Translation of Selected Reports on the Role of the Binder Phase in Cemented Refractory Alloys issued by the Osram Gesellschaft, Berlin. WAL Report No. 671/88-4 (1948), Boston Ordnance District. OSRAM Report 65/690 (1941) HEC. 11285.
48. S. Takeda, On the Carbides in Tungsten Steels
Tech.Report of Tohoku Imperial University,
9 (1931), 483, 627, and 10, (1931), 42.
49. Metals Handbook, 1948 edition
A.S.M. Cleveland, 1181.
50. M. Hansen, Der Aufbau der Zweistofflegierungen,
J. Springer, Berlin, (1936) 652
51. H. E. White and S. F. Walton, Particle Packing and Particle Shape.
Journal of Am. Ceramic Society, 20, (1937), 155.
52. T. H. Gray, Bend Tests for Hard and Brittle Materials
Metals Handbook, 1948 edition
A.S.M. Cleveland, 125
53. C. J. Smithells, Metals Reference Book
Interscience Publishers, New York, (1950), 581.
54. Loc. cit. 577.
55. F. V. Lenel, Sintering in the Presence of a Liquid Phase.
Metals Technology, A.I.M.E. 15, (June 1948) T P 2415

56. J. C. Redmond and E. N. Smith, Cemented Titanium Carbide. Trans. A.I.M.E. 185, (1949), 987.
57. L. J. Hull and D. L. Schwartz, Cemented Sintered Carbides, Metals Handbook, 1948 edition A.S.M. Cleveland, 61
58. F. V. Lenel, Sintering with a Liquid Phase Symposium on the Physics of Powder Metallurgy, Sylvania Electric Products, Inc. (1949) as summarized in Metal Powder Report 4, No. 4 (1949).
59. W. Badger and W. McCabe, Elements of Chemical Engineering, McGraw Hill, New York, (1936), 451
60. J. S. McFarlane and D. Tabor, Adhesion of Solids and the Effect of Surface Films. Proc. Royal Society A 202, (1950), 224
61. C. J. Smithells, Metal's Reference Book Interscience, New York, (1949) 416

APPENDIX I

ON THE METASTABILITY OF THE ETA PHASE

Takeda's conclusion concerning the metastability of W_3Co_3C seems to have been based upon his study of the iron-wolfram-carbon system⁽⁴⁸⁾, where he observed that wolfram carbide is formed in high carbon alloys by the decomposition of the eta phase on annealing. The microstructure, Figure 53, which he uses to illustrate his theory, shows large crystals of eta, the peripheries of which have changed to wolfram carbide. If this were a process of transformation, proceeding by nucleation and growth, one would expect areas of the second phase distributed throughout the polycrystalline eta. As shown, the microstructure suggests a process of diffusion, probably one of carburization during the annealing treatment, which caused the eta to wolfram carbide transformation.

APPENDIX II

HIGH TEMPERATURE OXIDATION RESISTANCE OF THE ETA PHASE OF THE WOLFRAM-
COBALT-CARBON SYSTEM

Introduction

Cemented carbides are subject to corrosive attack by both acids and certain alkalies. In the case of acids the binder is affected and corrosion proceeds intergranularly. The carbide constituent is attacked by many of the alkalies⁽⁵⁷⁾. Sintered wolfram carbide-cobalt alloys oxidize easily above 700°C in air. It is generally agreed that titanium carbide base cemented carbides have the most promising oxidation resistance. For instance, an 80 percent titanium carbide, 20 percent nickel compact was reported to increase its dimension by only 0.002 - 0.003 inch after 18 hours in air at 1000°C⁽⁵⁶⁾.

During the present work it was observed that the eta phase (η, W_3Co_3C), sometimes formed on the surface of sintered wolfram carbide-cobalt compacts, was relatively resistant to attack by concentrated hydrochloric acid and also to oxidation at higher temperatures. The presence of eta phase indicates that the composition of the compact does not lie within the two phase area wolfram carbide-cobalt, but that the sample is deficient in carbon, bringing the composition within the ternary three phase region: WC-W₃Co₃C-Co. The eta phase may be formed from an initial powder mixture of W₃Co₃C composition or by decarburization of a wolfram carbide-cobalt alloy. The results of an investigation of the high temperature oxidation resistance of eta are reported here.

Experimental Results

a. Oxidation Resistance of Eta Surface Layer

Powder specimens of 90 percent wolfram carbide and 10 percent cobalt were sintered in vacuum at 1400°C, for 1 hour, which treatment produced the normal structure of sintered compacts: Carbide particles embedded in a cobalt rich binder. They were then subjected to decarburization in an atmosphere of pure hydrogen at 1450°C for 1, 5 or 24 hours. It could be shown by x-ray diffraction and by visual evidence that a layer of eta was formed at the surface of the decarburized samples, which had a brilliant silvery appearance.

Oxidation tests were carried out in a tube furnace open at both ends. The experimental results are summarized in Table 14, and illustrated in Figures 54 and 55. Figure 54 shows, from left to right: A sintered sample, wolfram carbide-cobalt, normally treated and exposed to air at 1000°C for 1 hour; a specimen illustrating the appearance of eta phase on the surface; and two samples showing the appearance of the oxidized eta phase layer after respectively 24 and 96 hours in air at 1000°C. Whereas the eta phase on the last two samples was produced by decarburization in hydrogen for 5 and 22 hours at 1450°C, only 1 hour of decarburization was used for the samples of Figure 55. Their appearance after exposure to air at 100°C for 11 1/2 and 24 hours is shown in this figure. The resistance to oxidation increases with the time of decarburization and is therefore related to the thickness of the layer of eta phase. The increase of dimension is commonly used as a measure of the progress of oxidation⁽⁵⁶⁾, however it is not a

completely satisfactory criterion in cases where the deterioration is localized, as it is here where it starts at the edges of rectangular specimens. Nevertheless it gives more reliable information than the change of weight method, since the products of oxidation frequently flake off and are not included in the weight.

b. Oxidation Resistance of Samples of Eta Composition.

Samples were prepared of a chemical composition corresponding to eta (W_3Co_3C) namely 23.9 weight percent cobalt, 26.4 weight percent wolfram carbide, and 49.6 weight percent wolfram. The powder mixture was ball milled and sintered in vacuum, one hour at 1500°C. Only eta was present in these samples, no other phase was shown by x-ray diffraction. The compacts had a hardness of 85 RA, a bend strength of 90 000 psi.

Table 15 lists the results of oxidation tests at 1000°C.

c. The Products of Oxidation

Immediately after exposure to air at high temperatures the bright, shiny appearance of eta phase changes to dark grey-silver color. On further oxidation an inner layer, blue in color, shows up when the outer layer breaks and curls up at the edges. With a sintered wolfram carbide-cobalt sample, protected by an eta layer at the surface, deterioration continues at the edges. But if the sample is of eta phase throughout, the silver layer peels off, exposing the blue layer, which in turn changes to the grey-silver color, as oxidation proceeds.

The microphotographs of Figure 56 shows a cross section through the surface layers formed as a result of oxidation of a sintered wolfram carbide-cobalt compact protected by a layer of eta phase (Sample No. 4). In addition

to the normal wolfram carbide-cobalt core and the eta phase, two additional layers are visible: One blue in color adjacent to the eta phase, and the outside layer, silver-grey in color. The remainder of the picture is occupied by the bakelite mounting compound. The blue layer could not be identified, it is not one of the common oxides of cobalt. The dark silver-grey layer seems to be a composite alloy, one of its components being the delta phase (wolfram cobalt) of the wolfram-cobalt binary system, as was shown by x-ray diffraction.

Conclusions

The eta phase has a considerably greater resistance to oxidation at high temperatures than the normally sintered wolfram carbide-cobalt compacts. The rates of oxidation are comparable to titanium carbide base sintered compacts; however, localized deterioration takes place at the edges of rectangular specimens. The resistance to oxidation is attributed to the formation of protective layers on the surface.

Although the practical importance of these particular compositions is probably limited by the restricted availability of the constituents, the above results illustrate a new type of oxidation resistant material, which combines the properties of cemented wolfram carbide with an oxidation resistant surface.

APPENDIX III

A STUDY OF THE KINETICS OF ISOTHERMAL SINTERING

The rate and extent of shrinkage increase with the amount of cobalt and with the temperature (See Figures 8 - 10). A limiting value, beyond which no further shrinkage was observed on holding at temperature, was reached at 1300°C and higher, but was not attained at lower temperatures within the sintering times used. The low temperature curves seem to tend asymptotically towards a vanishing sintering rate.

Line⁽⁵⁸⁾, studying the sintering of Fe-Cu alloys above the melting point of copper, found that a linear relation holds between the logarithm of time and density modulus. The rate of sintering of cemented carbides seems to follow a similar relation; the maximum rate of sintering occurs at the beginning, followed by a steady decrease with time. This would correspond to a rate equation of the type:

$$\frac{dy}{dt} = \frac{k}{t} \quad \text{Equation 1}$$

where y is the shrinkage at time t , expressed as percent of original length, and k is a constant. The relation applies only up to the maximum amount of shrinkage obtainable for any one composition. If the experimental points fall on a straight line on a plot of shrinkage versus the logarithm of time, it can be concluded that the sintering mechanism follows the relation of equation 1. The data for wolfram carbide-cobalt compacts of 7.5 and 15 percent cobalt were so plotted in Figures 57 and 58. The plots do show straight lines of different slopes at low and high temperatures, which suggests

that densification takes place in two stages; one at the beginning of shrinkage up to 12-14 percent and therefore only measurable at low temperatures, the second coming into play toward the latter part of the shrinkage, attainable at high temperatures only. Only the sintering curve at 1300°C shows both stages. The slope of the lines is constant with temperature and composition for at least the first stage.

An attempt was made to correlate the observed data with actual physical mechanisms which might control the rate of sintering. But no such simple correlation was found. The possible mechanisms which would have to be taken into consideration are quite numerous, for instance: a) The rate of solution of wolfram carbide in the binder. b) The rate of creep of the binder. c) The rate of grain growth of the carbide particles. d) The rate of elimination of the pores from the compact etc. Some of the phenomena, even in simple systems, are not yet sufficiently understood to furnish quantitative data. Another factor to be considered is the effect of the sintering atmosphere, which, by carburization or decarburization, might change the dimension of the sample. The furnace atmosphere here used 20 percent H₂, 80 percent N₂ in contact with graphite, produced no noticeable effects at temperatures below 1450°C. At this higher temperature however, decarburization slowly took place as shown by the presence of eta on the surface of the specimen. The problem of finding a truly neutral atmosphere is not simple since the equilibrium composition would change with temperature, if a mixture of hydrogen and a carburizing gas is used. The problem of studying the kinetics of the sintering of cemented carbides is therefore extremely complex.

APPENDIX IV

CALCULATION OF TRUE PARTICLE SIZE

The grain growth of Chapter IV section B, was derived from a measurement of the length of grains along arbitrary straight lines across the microsections. The measured lengths of a great number of particles were then averaged and compared. The true particle size may be estimated from such an average by the following calculations:

Let the average grain size represent a uniform grain size, and assume that the measuring line randomly intercepts the circular grains on the plane of polish; then the average length of the intersecting lines represents the mean value of a series of chords, parallel to the diameter. The length of the chord (2y) varies with its distance from the center of the circle (x), the two are related by:

$$y = \sqrt{r^2 - x^2} \quad \text{Equation 1}$$

where r is the radius of the circle. The relation between the radius of the circle and the average value of a number of random intersections is then:

$$y = \frac{\int_0^r \sqrt{r^2 - x^2} \, dx}{r} = 1/4 \pi r = 0.785 r \quad \text{Equation 2}$$

The same relation holds between the average grain diameter, measured on the plane of polish, and the true particle diameter, if it is assumed that the plane of polish randomly intersects the particles.

Therefore, the measured average particle length (l) along a randomly intersecting line is related to the average particle diameter (d) by:

$$l = 0.785^2 d \qquad \text{Equation 3}$$

According to the above calculation and assumptions, the true average particle diameter of the sample of figure 16 is $2.9 \cdot 10^{-4}$ centimeters, and that of figure 17 is $3.4 \cdot 10^{-4}$ centimeters.

APPENDIX V

TEMPERATURE DEPENDENCE OF THE ANGLE OF CONTACT OF LIQUID COPPER
ON SOLID WOLFRAM CARBIDE

The temperature of melting and the angle of contact of copper on a block of wolfram carbide were observed for the purpose of determining the wettability of wolfram carbide by liquid copper. Melting of the copper occurred at 1085°C. The following contact angles were observed at the indicated temperatures:

<u>Temperature</u>	<u>Angle of Contact</u>
1115°C.	62° (Approximately)
1230°C.	46°
1330°C.	38°
1405°C.	20°

The measurement of the angles of contact was done on the photographic negatives of the wolfram carbide-copper profiles, prints of which are shown in Figure 59.

From equation 1 (Chapter V) it can be seen that $\cos \theta$ is a function of $\frac{\gamma_{sg} - \gamma_{sl}}{\gamma_{lg}}$. The angle of contact becomes 0 if $\gamma_{sa} - \gamma_{sl} = \gamma_{lg}$. By extrapolation (Figure 60), this occurs at a temperature of about 1550°C, where complete wetting would therefore be expected. With phases completely insoluble in each other a large change in relative surface energies with temperatures have not been observed⁽¹⁹⁾. However, the interfacial energies are extremely sensitive to minute changes of composition, and

the observed decrease of interfacial energy between wolfram carbide and copper can be attributed to the increase of solubility of carbon in copper, which, from 1200°C to 1500°C, increases from 0.0001 percent to 0.0006 percent (49).

APPENDIX VI

BINDER SOLIDIFICATION PHENOMENA OF THE COBALT INFILTRATED COMPACT

It might be surprising that an expansion occurs on cooling the infiltrated sample, and not a contraction, as might be expected from a high cobalt alloy. (See Binder Solidification Phenomena, Chapter V). It can be explained by similar considerations as were used to explain the expansion of low cobalt alloys. The binder is mainly concentrated in the pores of the skeleton, only a relatively small proportion is present in the place of the former grain boundaries. The contraction of the binder on freezing will not change the length of the specimen, but the growing grains, which push each other apart, will cause an expansion. In a normally sintered cobalt-wolfram carbide alloy, of similarly high cobalt content, the number of disconnected particles is much greater, their distribution is more uniform, so that the pores, present in the carbide skeleton, do not exist.

APPENDIX VII

CALCULATION OF SHRINKAGE CAUSED BY SOLUTION OF WOLFRAM CARBIDE
IN LIQUID COBALT

The weight loss of a batch of crystals by solution can be calculated⁽⁵⁹⁾ from the equation:

$$W_t = \int_0^{W_s} \left(1 - \frac{\Delta D}{D_s}\right)^3 dW_s \quad \text{Equation 1}$$

where W_t = final weight of batch of particles

W_s = initial weight of batch of particles

D_s = initial diameter of particles

ΔD = change of diameter of particles during solution.

Knowing the initial particle size distribution and the initial and final weights of the batch, the resulting particle size distribution can be calculated by graphical integration, since the particle size distribution provides a relation between D_s and W_s .

For the purpose of this calculation, however, it was assumed that a uniform particle size exists. Then equation 1 becomes:

$$W_t = \left(1 - \frac{\Delta D}{D_s}\right)^3 W_s \quad \text{Equation 2}$$

For a sample of 10 percent cobalt, a particle size of $3 \cdot 10^{-4}$ centimeters, a closed packed arrangement of particles, and a solubility of 40 percent wolfram carbide in cobalt, the equation can be solved for $\Delta D = 2$ percent approximately. The solution only gives the order of magnitude of the expected shrinkage and therefore the assumption of uniform particle size is justified, since a strict application of Equation 1 would have to consider

the effect of particle size, surface curvature, etc. on the rate of solution. Also, the effect of wolfram carbide solution on the density of the liquid has been disregarded here.

APPENDIX VIII

COHESION OF COMPACTS AT THE SINTERING TEMPERATURE

The cohesion of the compacts at high temperatures is due to the surface tension of the liquid binder. Marked adhesion occurs between surfaces wetted by an interposed liquid. This phenomena accounts for the adhesion between Johannsen flats and similar gauges which are strongly held together by the surface tension of an intermediate oil film. The force of adhesion between glass plates, wetted by a film of paraffin oil, was found to be, by experiment and by calculation, approximately 5 kg/cm² or 70 psi. With an incomplete film of liquid the surface tension forces are sufficient to cause a buckling of thick glass plates⁽⁶⁰⁾.

The force of adhesion can be calculated for the case of a small spherical particle separated by a thin film of liquid from a larger particle, the radius of which is assumed to be infinitely great. It is given by the relation⁽⁶⁰⁾:

$$Z = 4\pi R \gamma \cos \theta$$

where Z = adhesion (dynes)

R = radius of small particle (centimeters)

γ = surface tension of liquid (dynes/centimeters)

θ = angle of contact between liquid and solid

thus adhesion is independent of the thickness of the liquid film and is directly proportional to R. The equation applies strictly only if the thickness of the liquid film is very small and the angle is also small.

In the case of a wolfram carbide-cobalt compact, the angle of contact of liquid and solid is 0° , and film thicknesses of 10^{-4} centimeters or less are frequently observed. Assuming a surface tension of 1000 dynes/centimeter based on a value of 1120 dynes/centimeter for the surface tension of copper in hydrogen at 1140°C (61), a particle of radius of 10^{-4} centimeters, the force of adhesion is:

$$Z = 4 \pi (1 \cdot 10^{-4}) \cdot 1000 = 1.3 \text{ dynes}$$

or approximately 10^{-3} grams. Since such a small particle would weigh only about 10^{-10} grams, the adhesive force is sufficient to support it against the pull of gravity.

APPENDIX IX

CALCULATION OF TESSELATED STRESSES IN SINTERED WOLFRAM CARBIDE-COBALT
COMPACTS BY THE METHOD OF LASZLO⁽³⁷⁾

A composite alloy, where one component is embedded at random in the other, can be treated, for the purpose of calculation, as a compound sphere or cylinder of the same composition.

Case (a) was calculated for a 5 percent cobalt alloy, by assuming that the cobalt constitutes the inside core and the carbide the outside shell of a compound cylinder. The stresses of this cylinder are:

$$\gamma = \frac{\beta_2 + \beta_3}{\beta_1 \beta_3 - 2 \beta_2} (a_o - a_i) \cdot t$$

$$\beta_1 = \frac{m_i - 1}{m_i \cdot E_i} \left(\frac{1}{m_o \cdot E_o} + \frac{1 + \nu_i}{\nu_o \cdot E_o} \right)$$

$$\beta_2 = \frac{1}{m_i \cdot E_i} + \frac{\nu_i}{\nu_o \cdot m_o \cdot E_o}$$

$$\beta_3 = \frac{1}{E_i} + \frac{\nu_i}{\nu_o \cdot E_o}$$

where:

γ = radial stress at the surface of contact of inner and outer component

$a_o a_i$ = linear coefficients of thermal expansion of outer and inner material,

$$a_{Co} \approx 16 \cdot 10^{-6} \text{ in/in}\cdot\text{C}$$

$$a_{NC} \approx 5 \cdot 10^{-6} \text{ in/in}\cdot\text{C}$$

t = decrease of temperature (negative)

m = reciprocal of Poissons' ratio:

Assumed to be 3 for both metals

E = Young's modulus of elasticity

$$E_{Co} = 30 \cdot 10^6 \text{ psi}$$

$$E_{WC} = 102 \cdot 10^6 \text{ psi (32)}$$

V_i, V_o = volume fraction of inner and outer components of compound cylinder.

$$V_{Co} = 0.1,$$

$$V_{WC} = 0.9$$

For case (b) it was assumed that the system can be represented by a compound sphere, the carbide forming the core, the cobalt the outside shell.

The following equation applies:

$$\gamma = \frac{1}{\frac{m_o - 1}{2 m_o E_o} \cdot \frac{1 + 2 V_i + 1}{V_o} + \frac{m_i - 2}{m_o E_o} + \frac{m_i - 2}{m_i E_i}} (a_o - a_i) t$$

For a cobalt content of 15 percent, for which this stress was calculated,

$$V_{Co} = 0.26, V_{WC} = 0.74.$$

LIST OF ILLUSTRATIONS AND TABLES

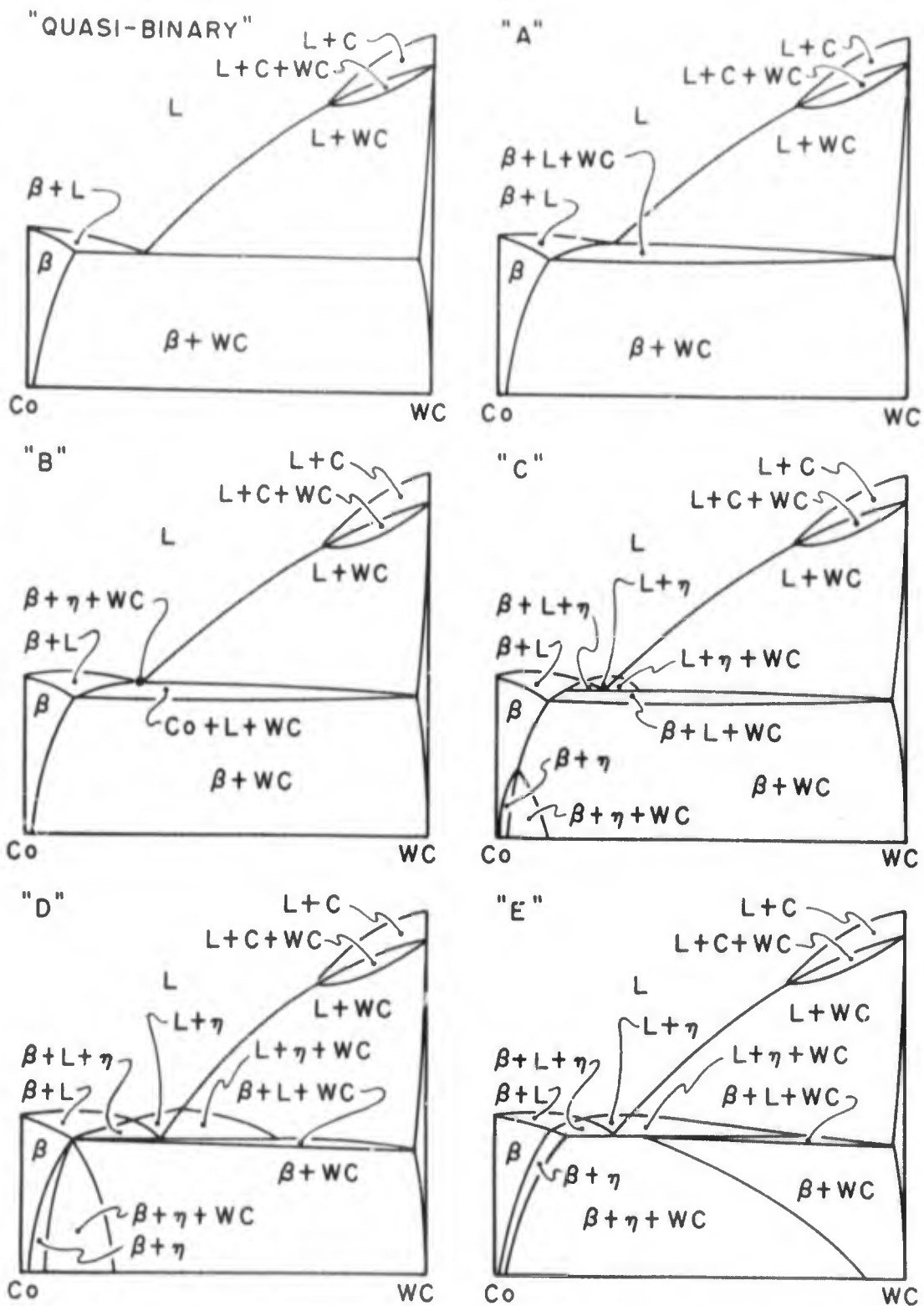
<u>Tables</u>	<u>Figures</u>	<u>Page</u>
	1 Possible Vertical Sections Cobalt-Wolfram carbide in Wolfram-Cobalt-Carbon Diagram	1
	2 Isothermal Section at Room Temperature Wolfram-Cobalt-Carbon Diagram	2
	3 Isothermal Section at 1400°C Wolfram-Cobalt-Carbon Diagram	3
	4 Sintering Dilatometer	4
	5 Sintering Dilatometer and Auxiliary Equipment	5
	6 Components of Continuous Dilatometer Recorder	6
1	Particle Size Distribution of Wolfram Carbide	7
	7 Sintering Curves - Constant Rate of Heating	8
2	Sintering Runs at Constant Heating Rate	9
3	Isothermal Shrinkage	9
	8 Effect of Time and Temperature on Shrinkage 7.5 percent Cobalt	10
	9 Effect of Time and Temperature on Shrinkage 12.5 percent Cobalt	11
	10 Effect of Time and Temperature on Shrinkage 15 percent Cobalt	12
	11 Microphotograph: Sintered Wolfram Carbide-Cobalt Alloy. 7.5 percent Cobalt, 3 hours at 1300°C	13
	12 Microphotograph: Sintered Wolfram Carbide-Cobalt Alloy. 7.5 percent Cobalt, 2 hours at 1325°C	13
	13 Microphotograph: Sintered Wolfram Carbide-Cobalt Alloy. 7.5 percent Cobalt, 3 hours at 1350°C	14
	14 Microphotograph: Sintered Wolfram Carbide-Cobalt Alloy. 7.5 percent Cobalt 2 hours at 1400°C	14

<u>Tables</u>	<u>Figures</u>	<u>Page</u>
	15 Isothermal Sintering Curves at 1400°C	15
	16 Microstructure, Sintered Wolfram Carbide-Cobalt Alloys, 15 percent Cobalt 1 1/2 hours at 1350°C	16
	17 Microstructure, Sintered Wolfram Carbide-Cobalt Alloys, 15 percent Cobalt 21-3/4 hours at 1350°C	16
	18 Interfacial Tensions at the Interfaces of Solid Liquid and Gas	17
	19 Interfacial Tensions of Liquid in Contact with a Solid Grain Boundary	17
	20 Cross Section through Cobalt Infiltrated Block	18
	21 Cross Section Through Copper Infiltrated Block	18
	22 Microstructure of Cobalt Infiltrated Wolfram Carbide Block	19
	23 Microstructure of Copper Infiltrated Wolfram Carbide Block	19
	24 Infiltration with Cobalt-Dilatometric Curve	20
	25 Dilatometric Cooling Curve of Infiltrated Wolfram Carbide Compacts	21
	26 Microstructure of Cobalt Infiltrated Wolfram Carbide Compact	22
	27 Microstructure of Copper Infiltrated Wolfram Carbide Compact	22
	28 Microstructure of sintered Wolfram Carbide-Cobalt Alloy. 12 percent Cobalt	23
4	Thermal Expansion of Pressed Wolfram Carbide Cobalt Compacts, unsintered	24
	29 Discontinuous Change of Length on Cooling of Sintered Wolfram Carbide-Cobalt Alloys	25
5	Dimensional Changes at the Freezing Temperature of the Binder	26
	30 Electrolytic Leaching Cell	27

<u>Tables</u>	<u>Figures</u>	<u>Page</u>
	31 Sintered Compacts after Electrolytic Leaching Experiments	28
6	Results of Electrolytic Leaching Experiments	29
7	Thermal Coefficients of Expansion	29
	32 Coefficients of Linear Thermal Expansion of Cemented Wolfram Carbide-Cobalt Alloys	30
	33 Effect of Composition on Transverse Rupture Strength	31
8	Strength of Cemented Wolfram Carbide	32
9	Strength and Hardness of Wolfram Carbide-Cobalt Alloys Sintered at 1400°C	33
10	Effect of Time and Temperature on the Strength of Wolfram Carbide-Cobalt Alloys. 7.5 percent Cobalt	33
11	Effect of Time and Temperature on the Strength of Wolfram Carbide-Cobalt Alloys. 15 percent Cobalt	34
	34 Crack in Sintered Wolfram Carbide-Cobalt Alloy	35
	35 Crack in Sintered Wolfram Carbide-Cobalt Alloy	35
	36 Iron-Carbon-Wolfram Ternary System	36
	37 Vertical Section Iron-Wolfram Carbide	37
	38 Shrinkage Curves - Constant Rate of Heating Various Binders	38
	39 Isothermal Shrinkage Curves - Various Binders	39
	40 Sintering Curve at Constant Temperature 7.5 percent Iron	40
	41 Microstructure of Copper Infiltrated Wolfram Carbide Block	41
	42 Microstructure of Nickel Infiltrated Wolfram Carbide Block	41

<u>Tables</u>	<u>Figures</u>	<u>Page</u>
	43 Microstructure of Iron Infiltrated Wolfram Carbide Block	41
	44 Microstructure of Cobalt Infiltrated Wolfram Carbide Block	41
	45 Microstructure of Eta Phase - Nickel Infiltrated Wolfram Carbide Block	42
	46 Discontinuous Change of Length of Compacts with Various Binders	43
	47 Cemented Wolfram Carbide - Iron Binder 7.5 percent Iron	44
	48 Cemented Wolfram Carbide - Nickel Binder 7.5 percent Nickel	44
	49 Cemented Wolfram Carbide - Copper Binder 7.5 percent Copper	45
	50 Cemented Wolfram Carbide - Cobalt Binder 7.5 percent Cobalt	45
	51 Eta Phase in Wolfram Carbide-Iron Alloy	46
	52 Cemented Wolfram Carbide - Nickel Binder 15 percent Nickel	46
12	Physical Properties of Cemented Wolfram Carbide - Various Binders	47
13	Summary of Experimental Results	48
	53 Eta Phase, as shown by Takeda	49
14	Results of Oxidation of Sintered Wolfram Carbide-Cobalt Compacts Protected by Eta Phase	50
	54 Photograph of Samples 1, 2, 3, and 4	51
	55 Photograph of Samples 5 and 6	51
15	Results of Oxidation of Sample of Eta Phase Composition	52
	56 Microphotograph of Oxidized Eta Phase	53

<u>Tables</u>	<u>Figures</u>	<u>Page</u>
	57 Sintering Curves, Shrinkage vs log. time 7.5 percent Cobalt	54
	58 Sintering Curves, Shrinkage vs log. time 15 percent Cobalt	55
	59 Profiles of Drop of Liquid Copper on Solid Wolfram Carbide	56
	60 Variation with Temperature of the Angle of Contact of Liquid Copper on Solid Wolfram Carbide	57



POSSIBLE VERTICAL SECTIONS Co-WC IN Co-W-C DIAGRAM.
 "QUASI-BINARY" SECTION IS THEORETICALLY INCORRECT.

FIGURE 1

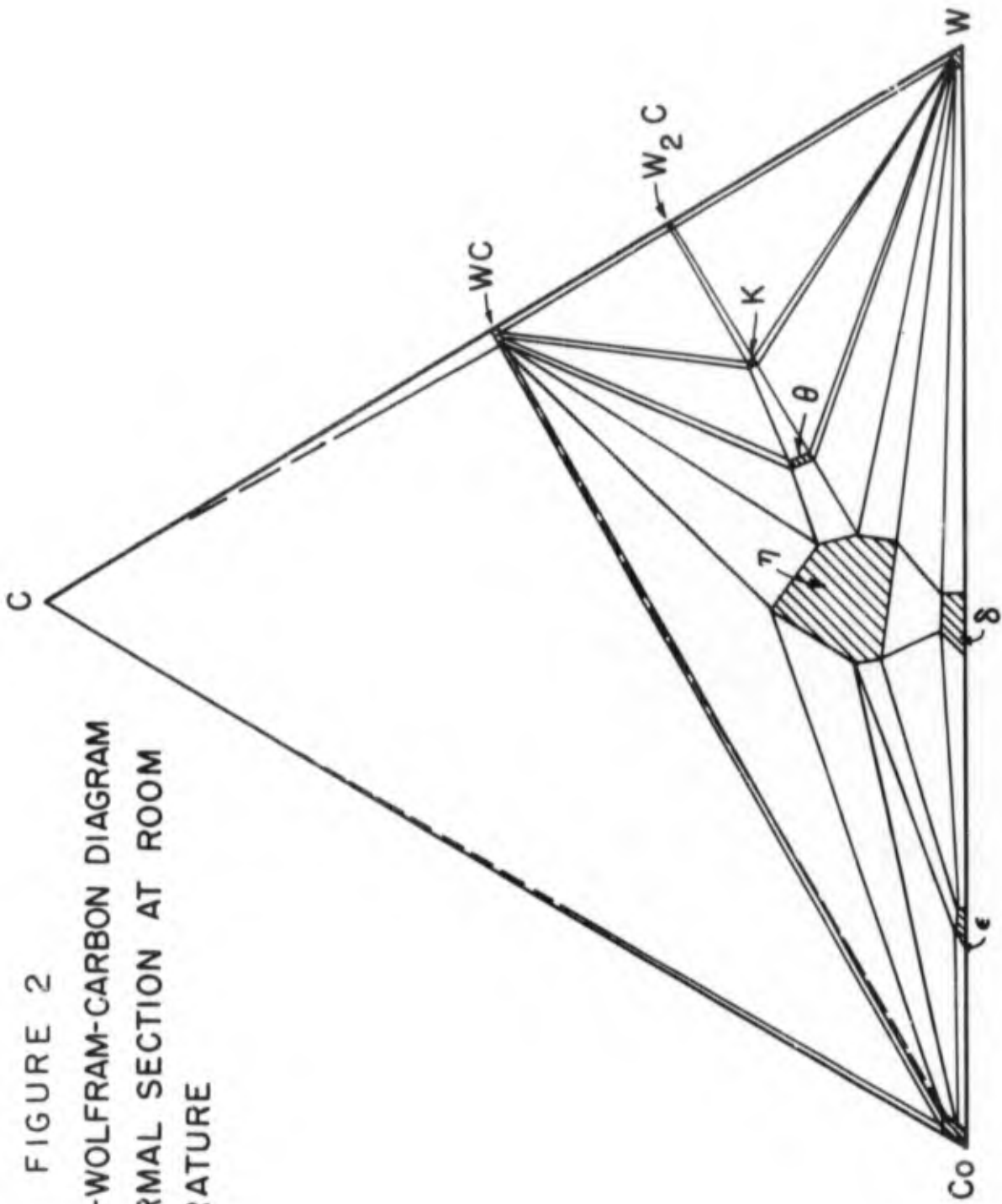


FIGURE 2
 COBALT - WOLFRAM-CARBON DIAGRAM
 ISOTHERMAL SECTION AT ROOM
 TEMPERATURE

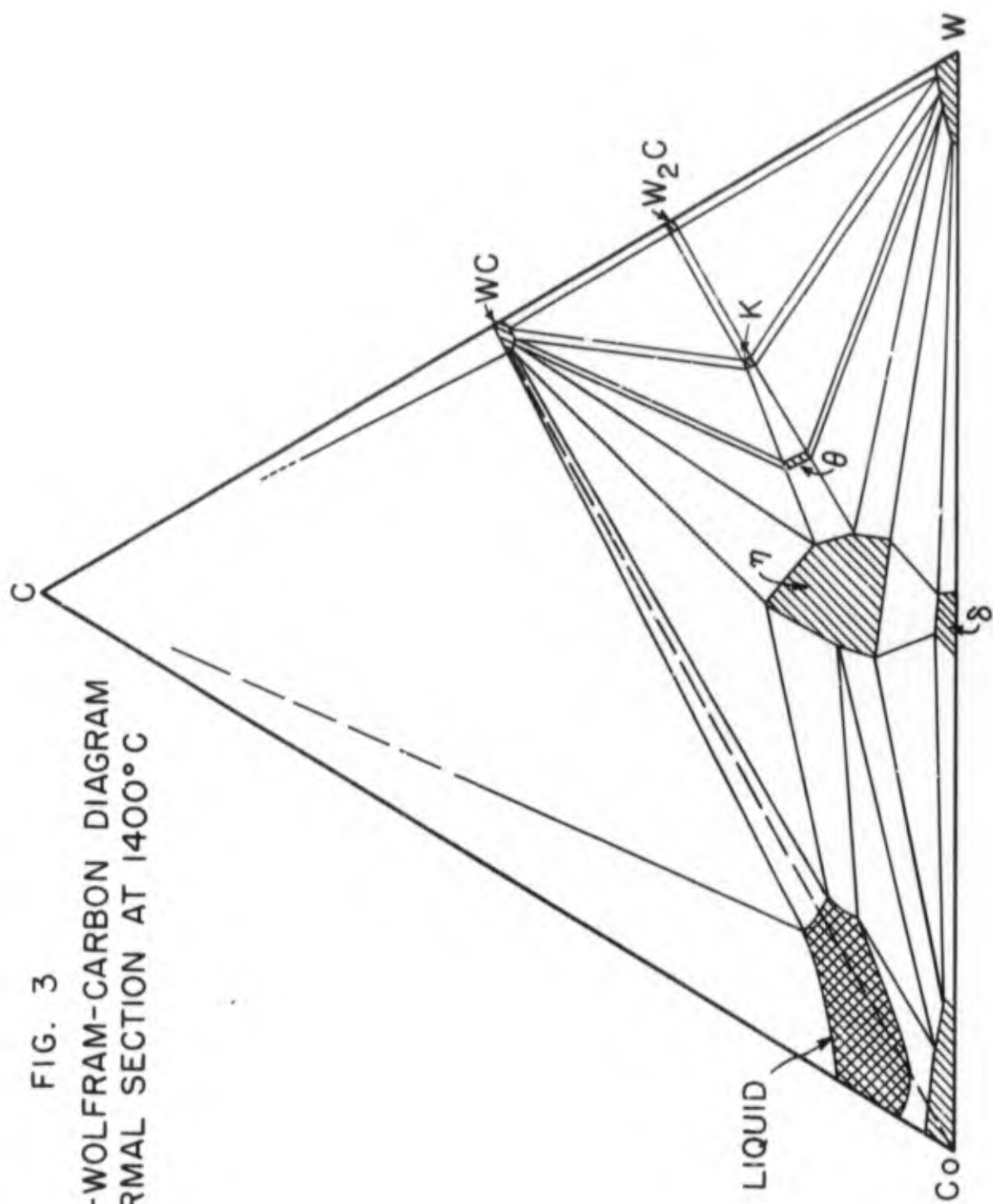


FIG. 3
 COBALT-WOLFRAM-CARBON DIAGRAM
 ISOTHERMAL SECTION AT 1400°C

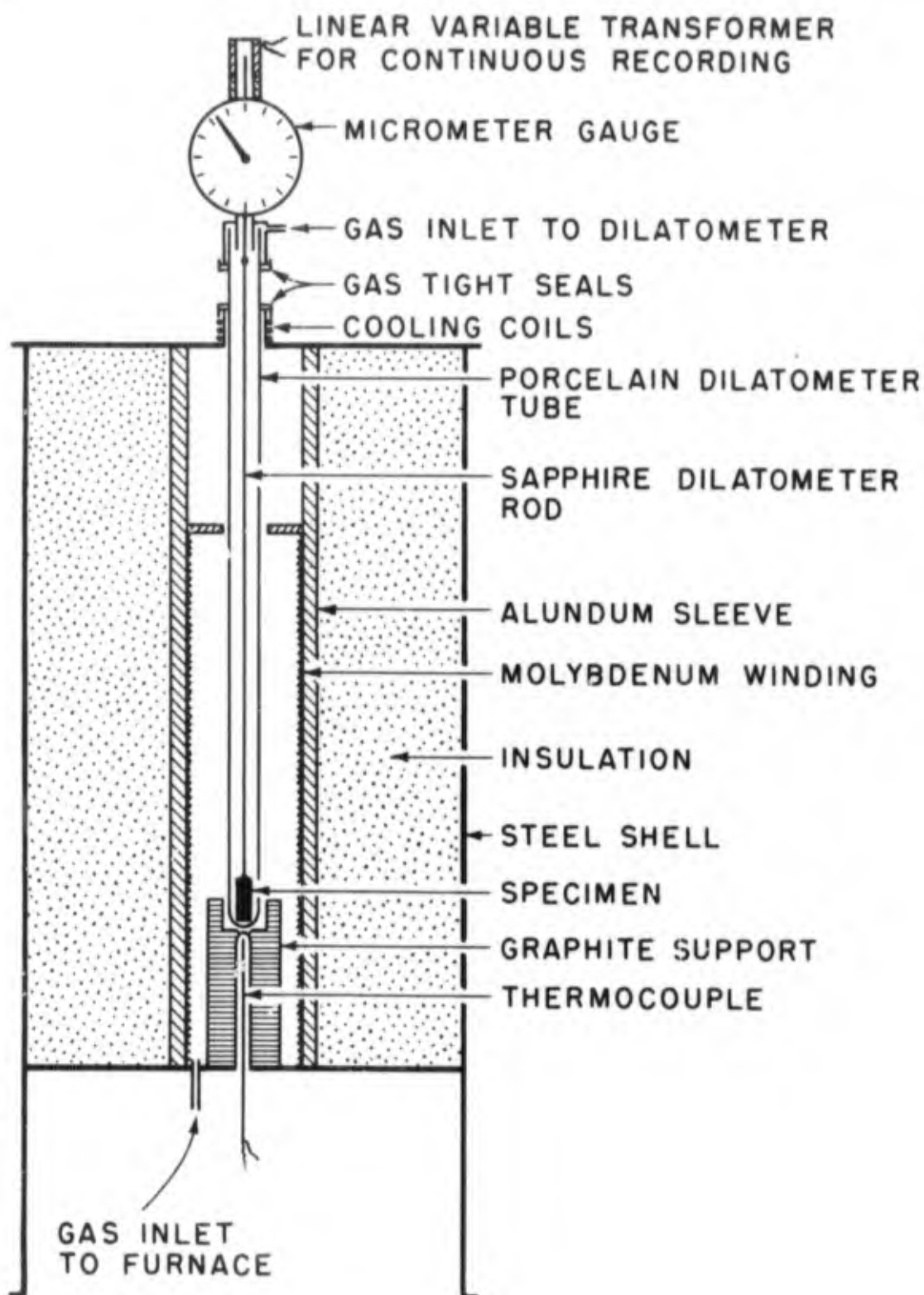


FIG. 4
 SINTERING DILATOMETER

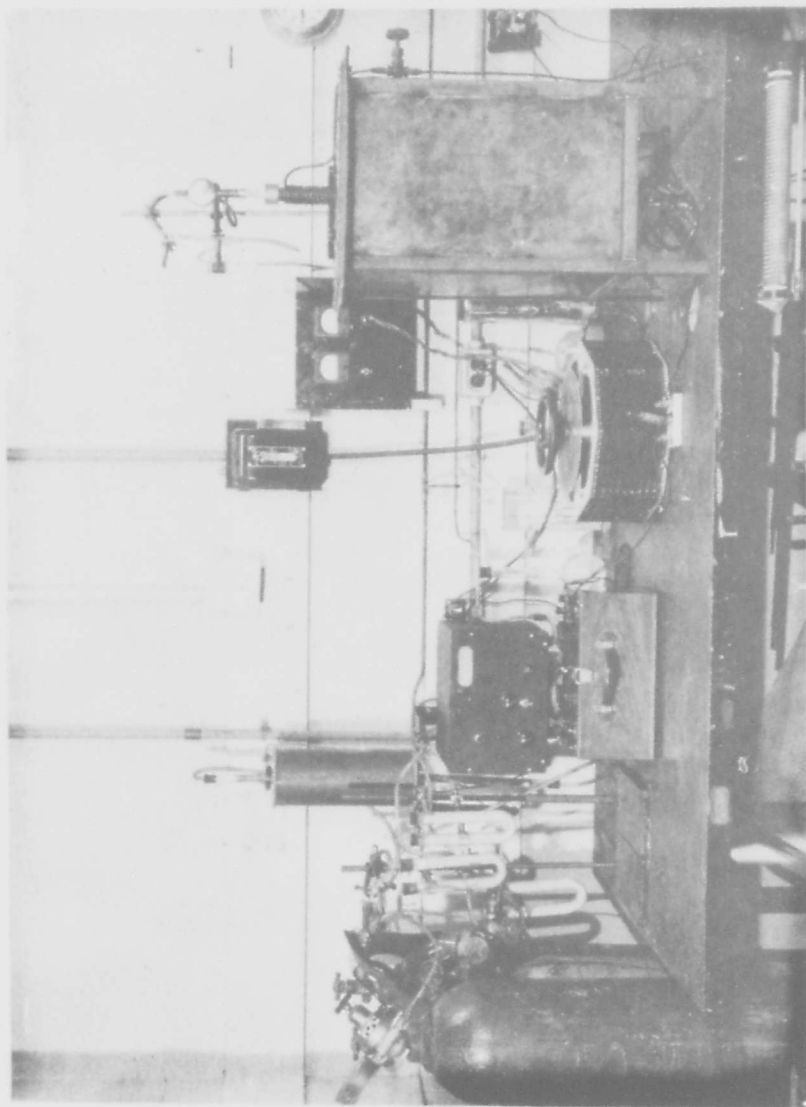
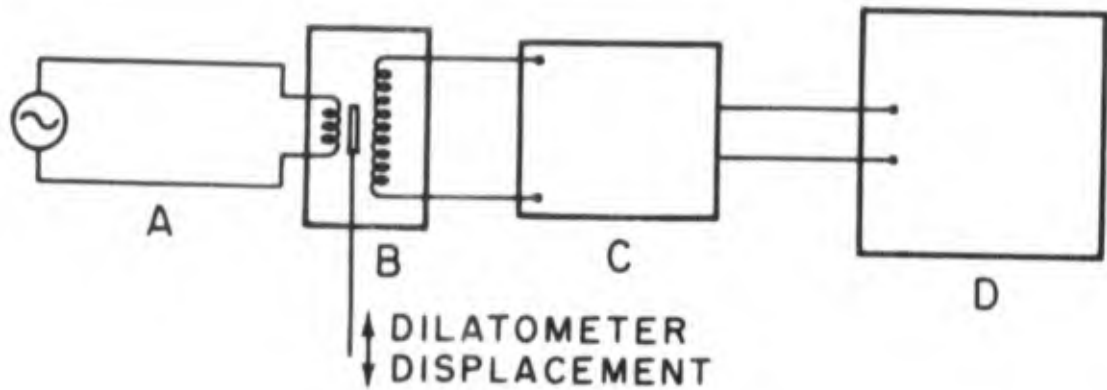


FIGURE 5

Sintering Dilatometer and Auxilliary Equipment

From Right to Left: Sintering Dilatometer, Variable Transformer, Potentiometer,
Temperature Controller, Gas Purification Train.



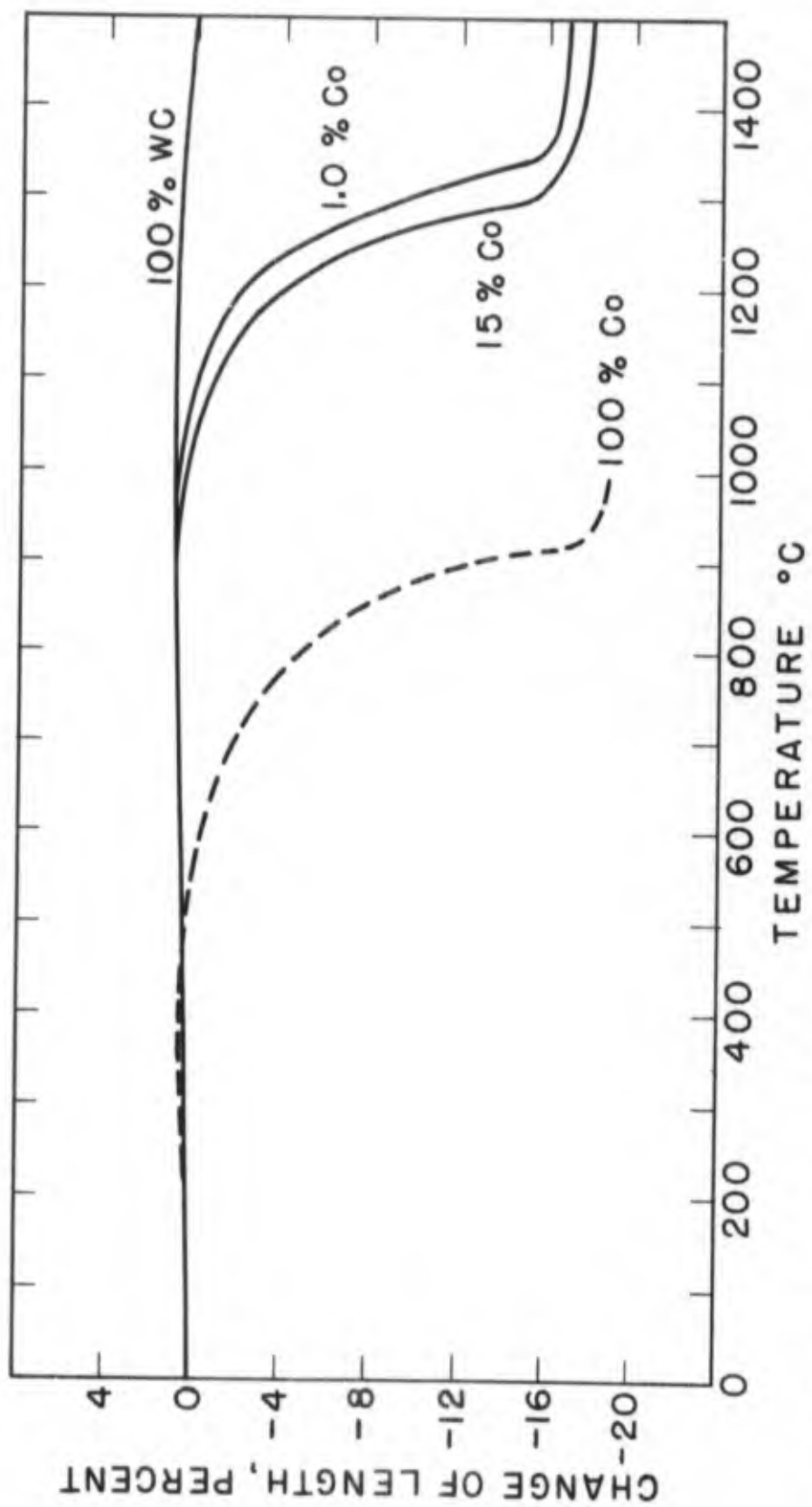
- A- 10V 60 CYCLES AC SOURCE
- B- LINEAR VARIABLE DIFFERENTIAL TRANSFORMER (SCHAEVITZ COIL)
- C- LINEAR AC AMPLIFIER - RECTIFIER
- D- BROWN POTENTIOMETER RECORDER

FIGURE 6 - COMPONENTS OF CONTINUOUS DILATOMETER RECORDER.

Table 1

Particle Size Distribution of Wolfram Carbide as
Determined at Watertown Arsenal

<u>Percent</u>	<u>Size</u>
100 percent smaller than	16 microns
100	14
99.3	12
97.6	10
95	8
91.7	6
76.4	4
20.6	2
3.25	1
1.15	0.7



SINTERING CURVES - CONSTANT RATE OF HEATING - CHANGE OF LENGTH VS TEMPERATURE

FIGURE 7

Table 2

Sintering Runs at Constant Heating Rate

Cobalt Content , percent	0.5	1	5	7.5	10	12.5	15
Linear Shrinkage, percent	1.6	17.1	16.9	16.8	17.6	18.0	19.3
Start of Noticeable Shrinkage, °C.	800	800	800	800	800	800	800
End of Rapid Shrinkage °C.	—	1350	1350	1350	1300	1300	1300
Density as Percent of Theoretical Density	60	86	93.5	92	95	97.3	98

Table 3

Isothermal Shrinkage

Sample No. 19

7.5 percent cobalt

Temperature °C.	Time Required for Maximum Shrinkage HRS	Maximum Shrinkage Percent	Total Time at Temperature HRS
1200	—	8.3	28.5
1250	—	13.4	144
1300	47	14.9	70
1350	5	16.7	8
1400	0.75	17.5	2

EFFECT OF TIME AND TEMPERATURE ON SHRINKAGE
SAMPLE NO. 19 7.5% Co

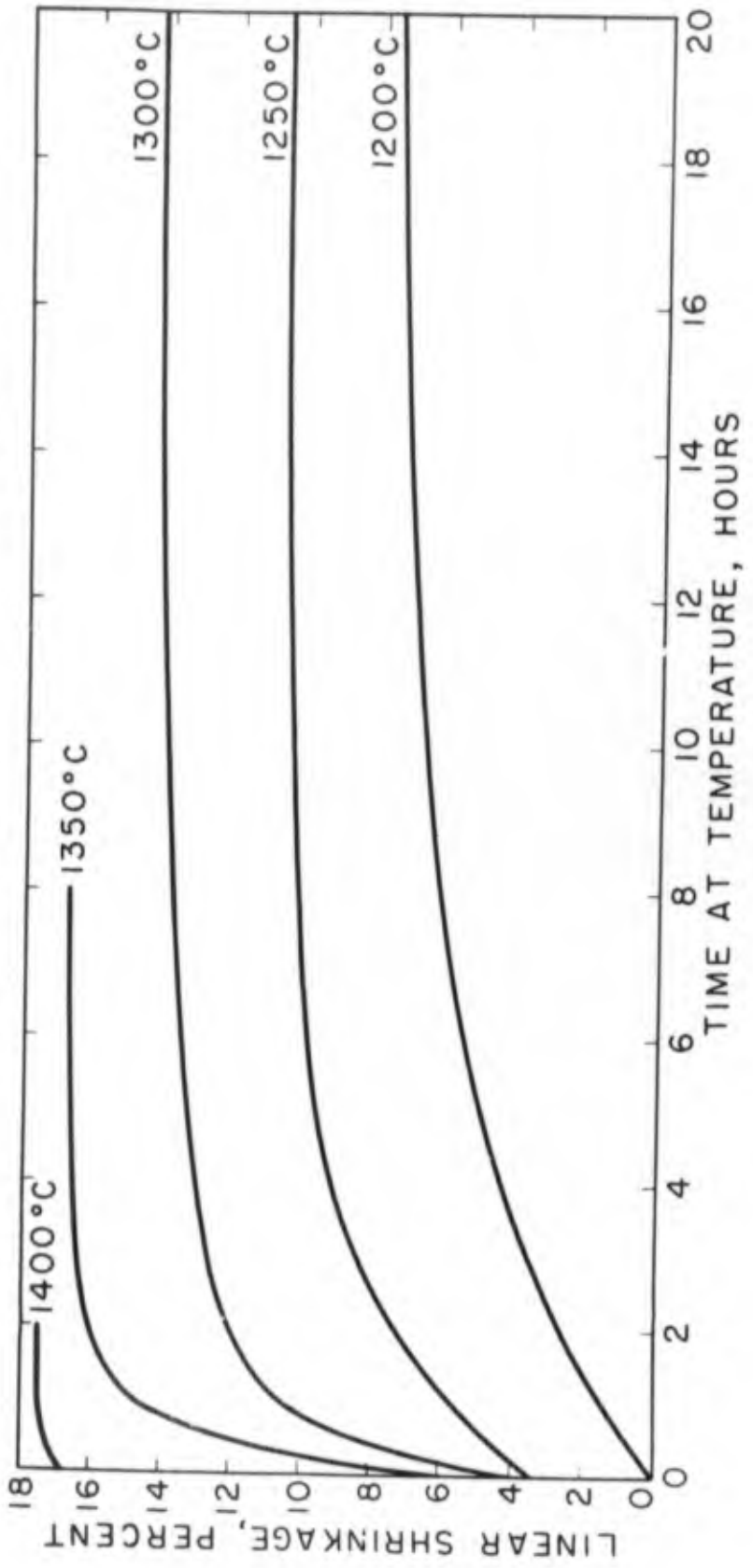
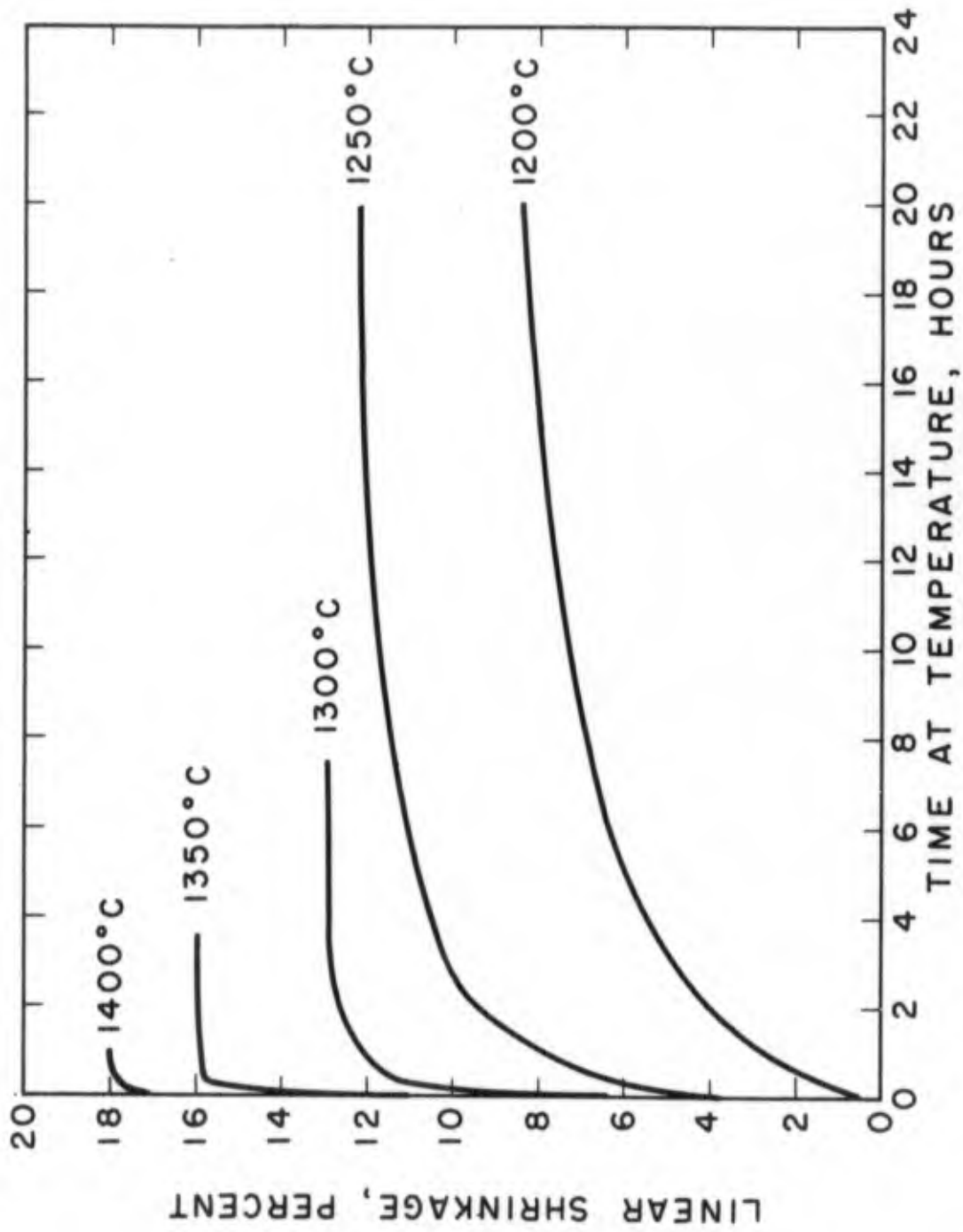


FIGURE 8



EFFECT OF TIME AND TEMPERATURE ON SHRINKAGE - SAMPLE No. 28 12.5% COBALT
 FIGURE 9

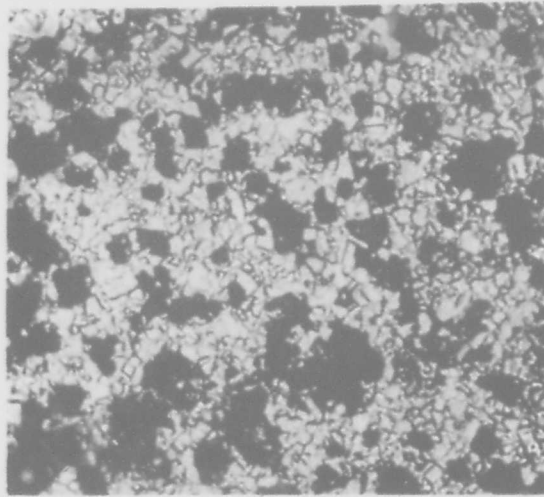


FIGURE 11

Sintered WC-Co alloy. 7.5% Cobalt. 3 hours at 1300°C. (1500X)

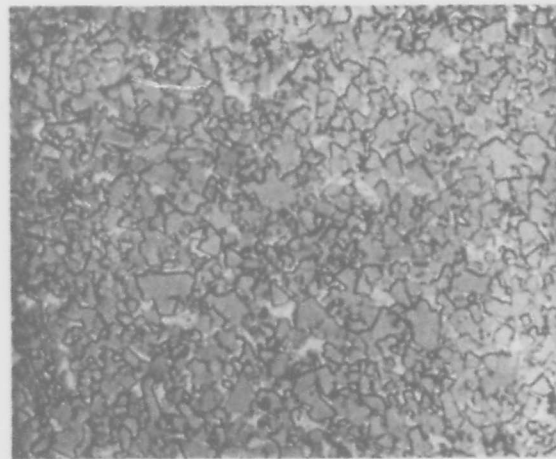


FIGURE 12

Sintered WC-Co Alloy. 7.5% Cobalt. 2 Hours at 1325°C. (1500X)

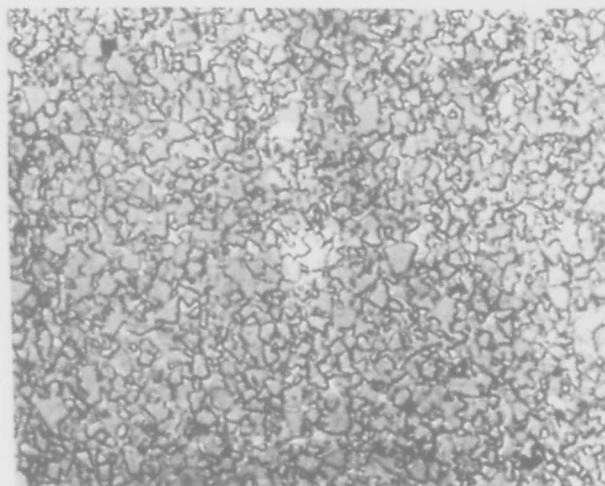


FIGURE 13

Sintered WC-Co alloy. 7.5% Cobalt. 3 hours at 1350°C (1500X)

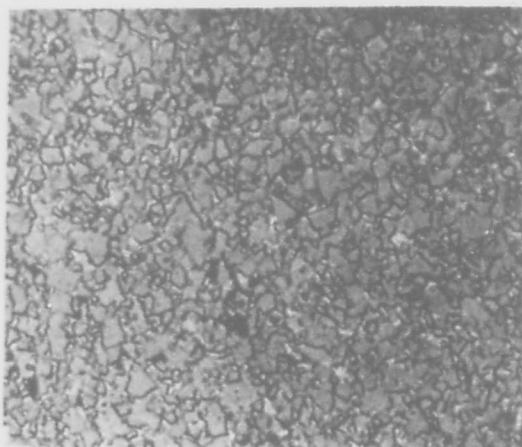
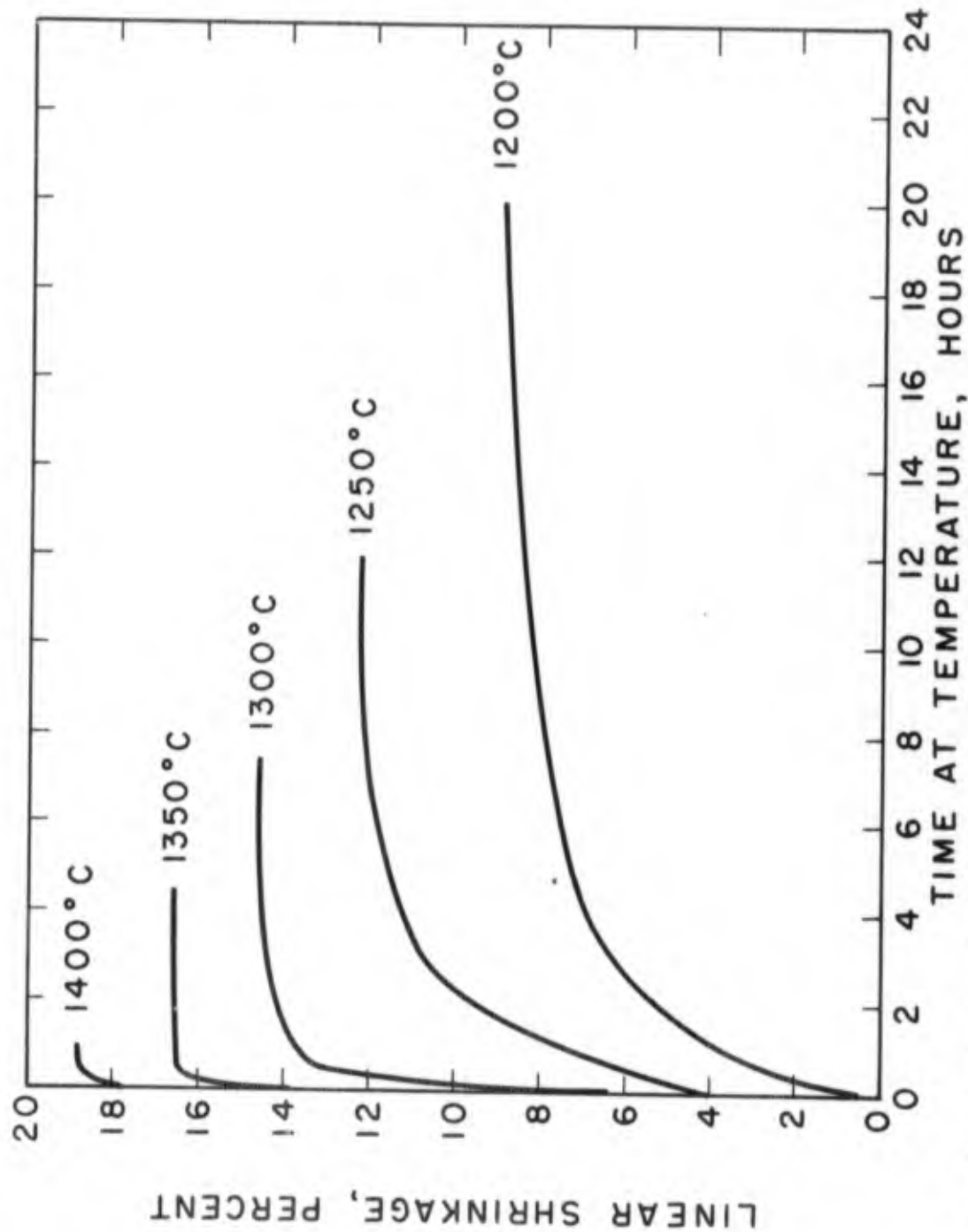
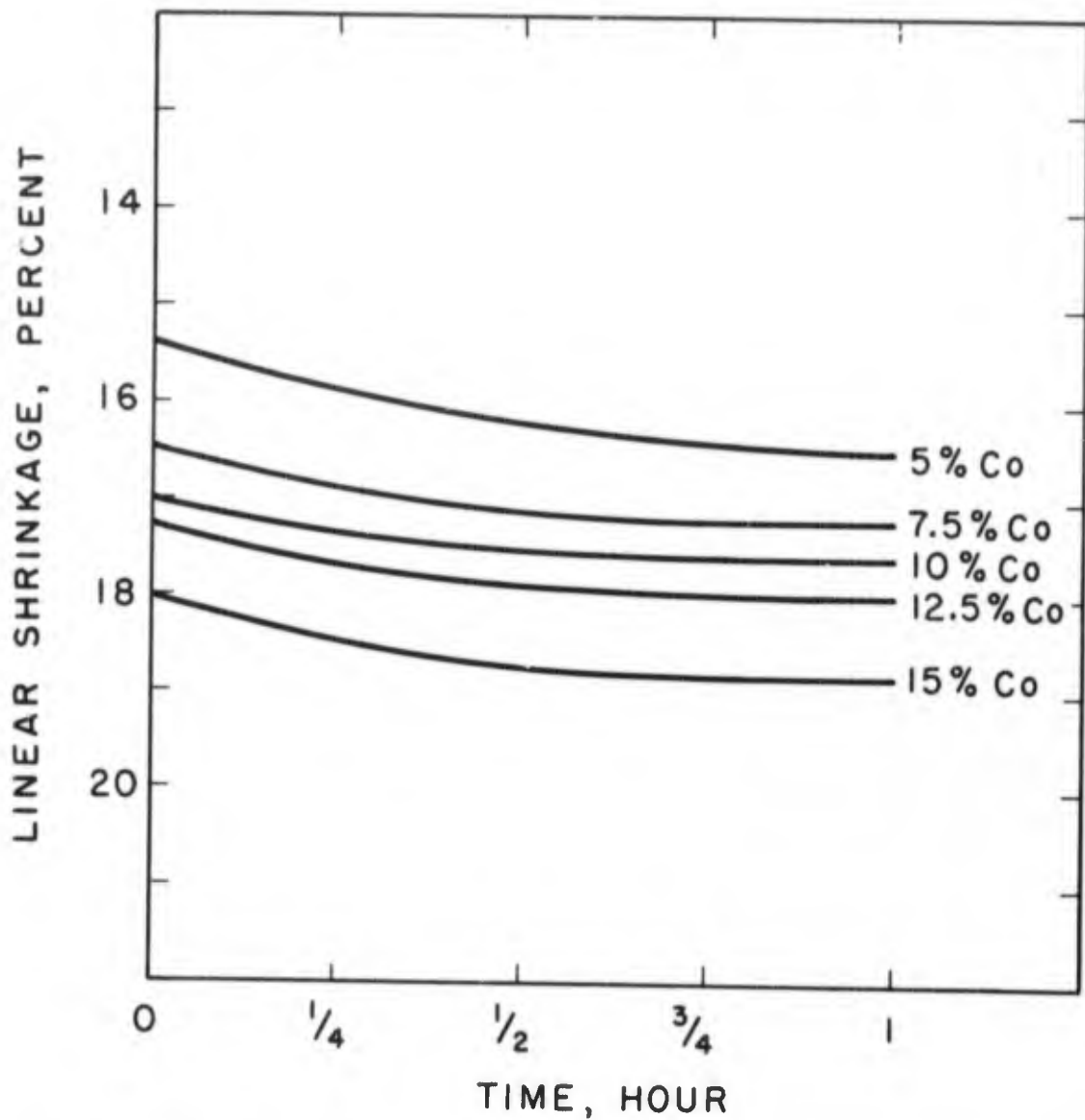


FIGURE 14

Sintered WC-Co Alloy. 7.5% Cobalt. 2 hours at 1400°C. (1500X)



EFFECT OF TIME AND TEMPERATURE ON SHRINKAGE - SAMPLE No. 27 15% COBALT
 FIGURE 10



SINTERED WC - Co ALLOYS - ISOTHERMAL
SINTERING CURVES AT 1400° C

FIGURE 15

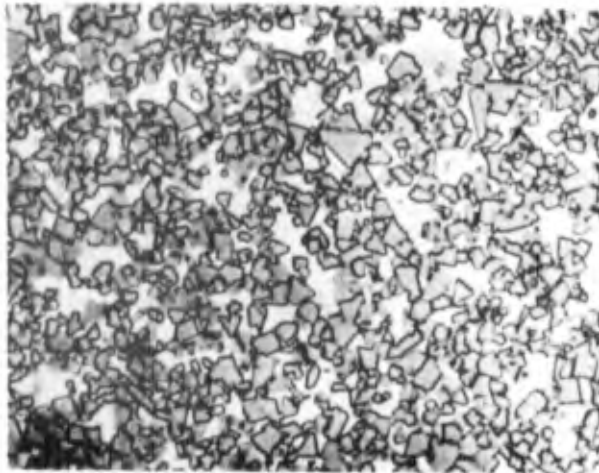


FIGURE 16

Sintered WC-Co Alloy. 15% Cobalt. $1\frac{1}{2}$ hours at 1350°C . (1500X)

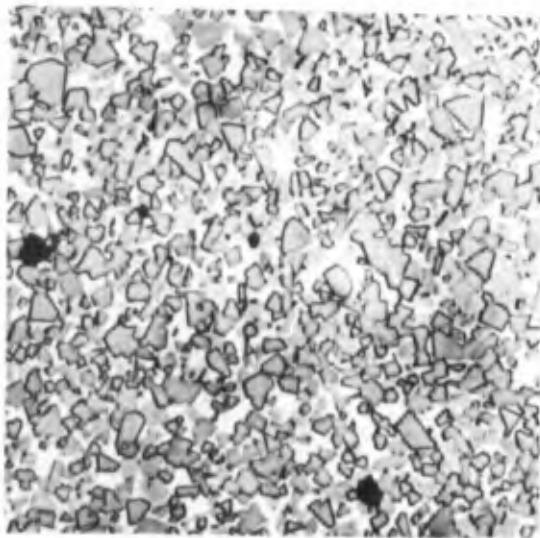
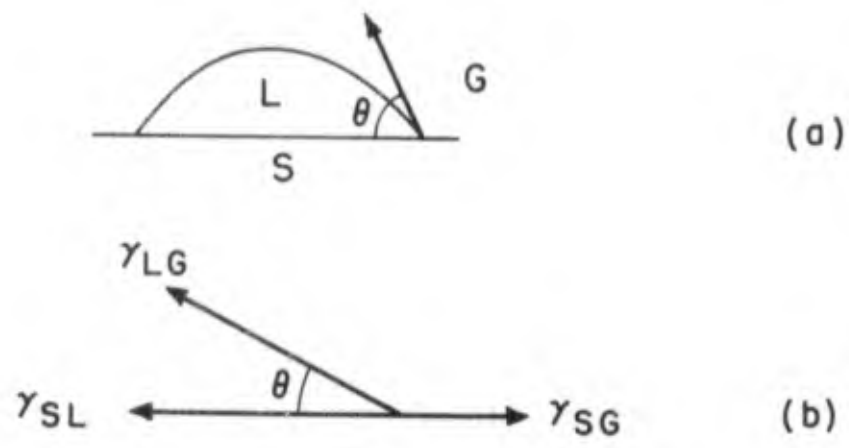


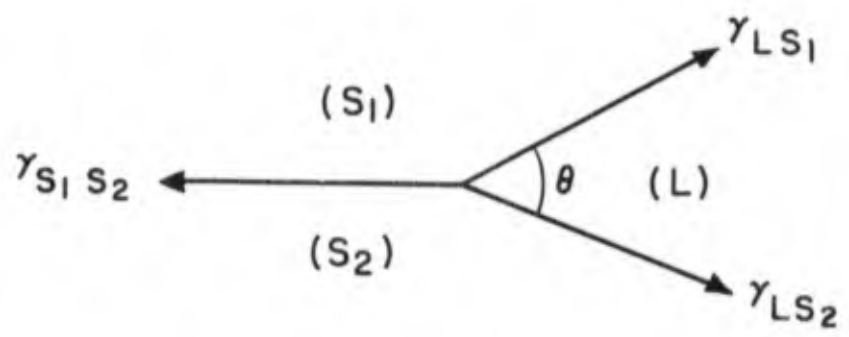
FIGURE 17

Sintered WC-Co Alloy. 15% Cobalt. $2\frac{3}{4}$ hours at 1350°C . (1500X)



INTERFACIAL TENSIONS AT THE INTERFACES OF A SOLID, LIQUID, AND GAS

FIGURE 18



INTERFACIAL TENSIONS OF LIQUID IN CONTACT WITH A SOLID GRAIN BOUNDARY

FIGURE 19

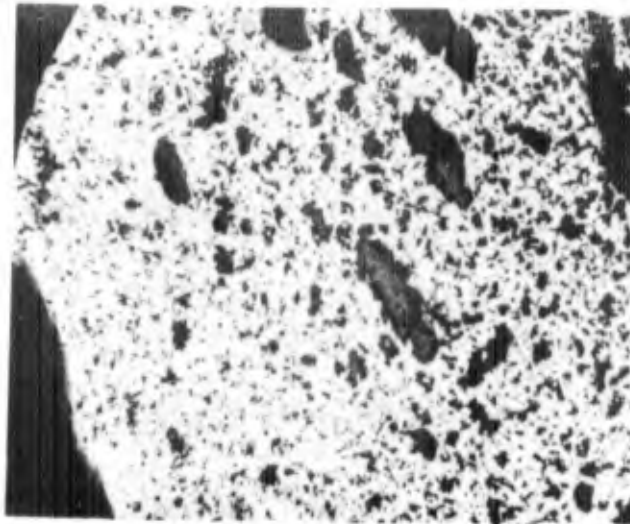


FIGURE 20

Cross section through cobalt infiltrated WC block
Original location of cobalt drop, at left of photograph (60X)

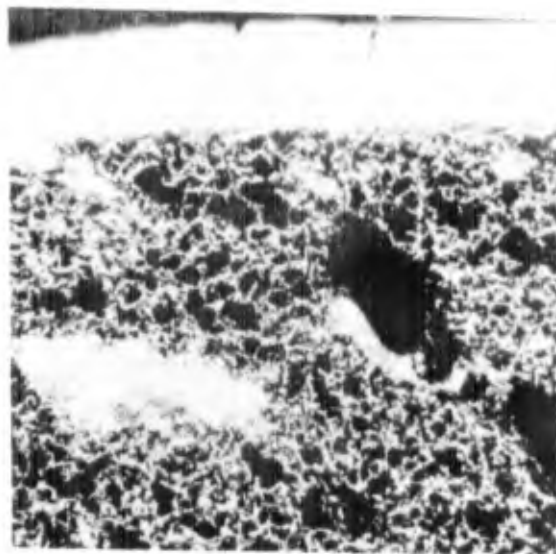


FIGURE 21

Cross section through copper infiltrated WC block
Part of original copper drop visible at top of photograph

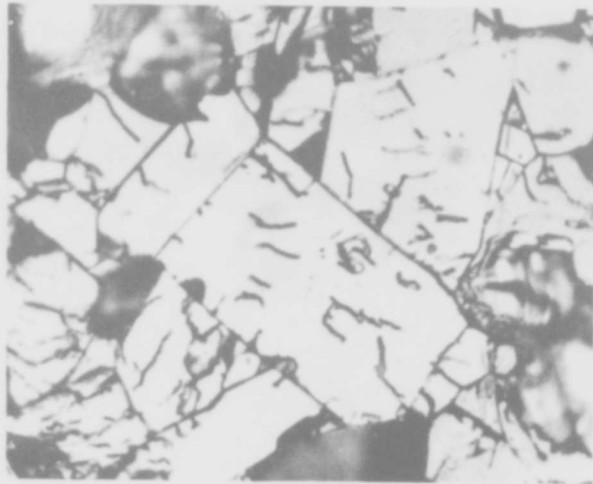


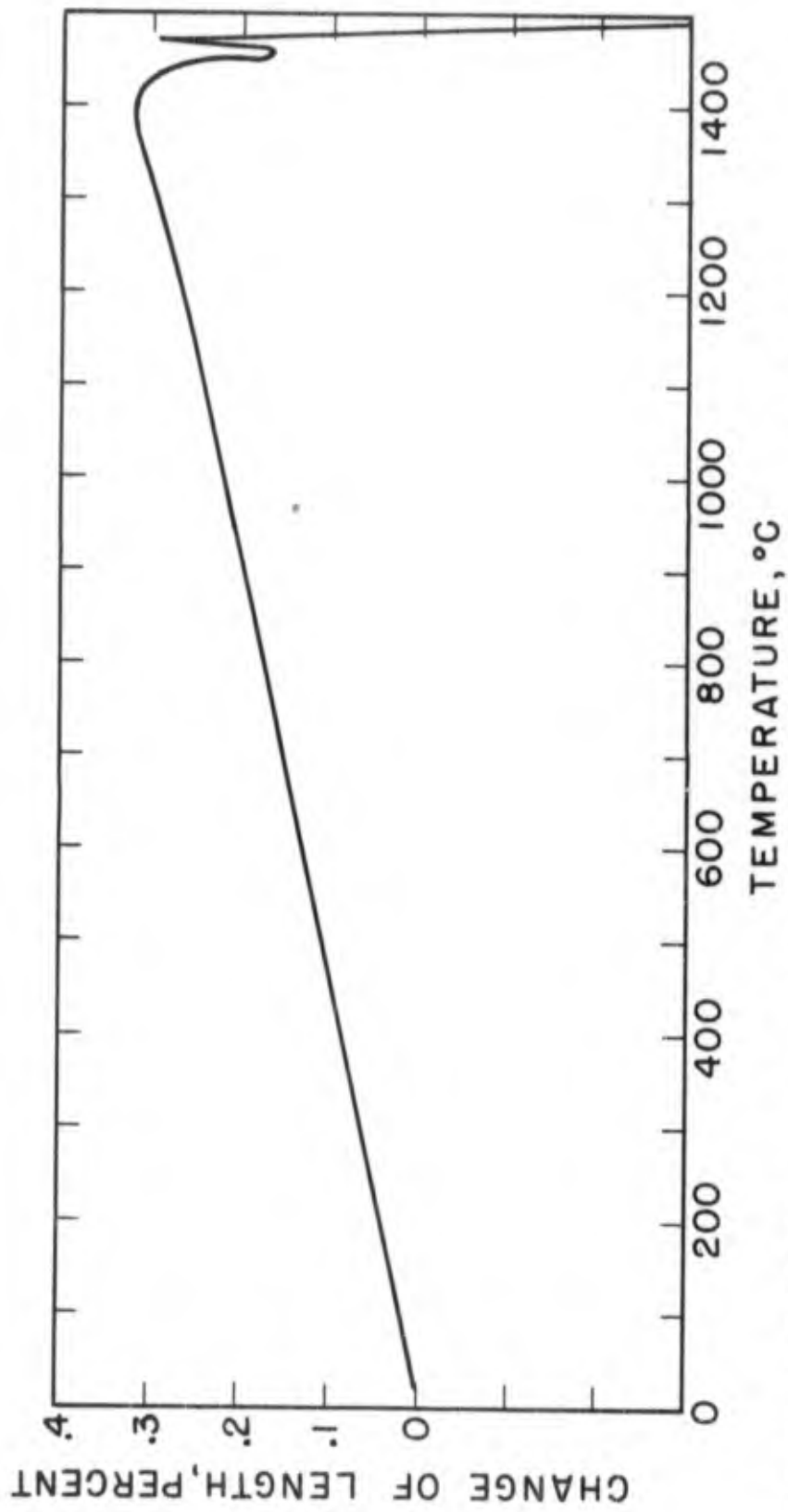
FIGURE 22

Microstructure of cobalt infiltrated WC block. (1500X)



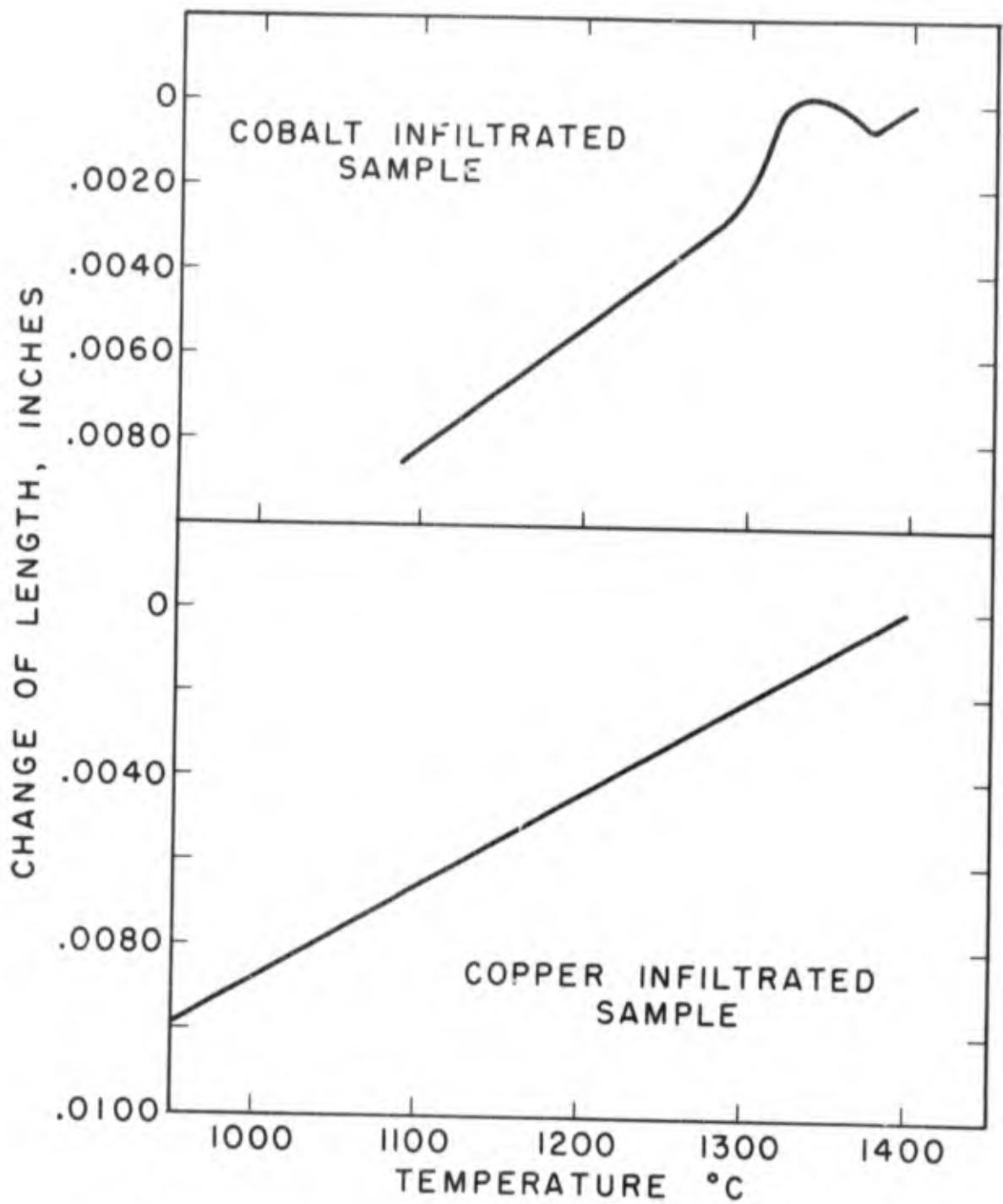
FIGURE 23

Microstructure of copper infiltrated WC block (1500X)



INFILTRATION WITH COBALT-DILATOMETRIC CURVE

FIGURE 24



DILATOMETRIC COOLING CURVES OF INFILTRATED WC COMPACTS

FIGURE 25

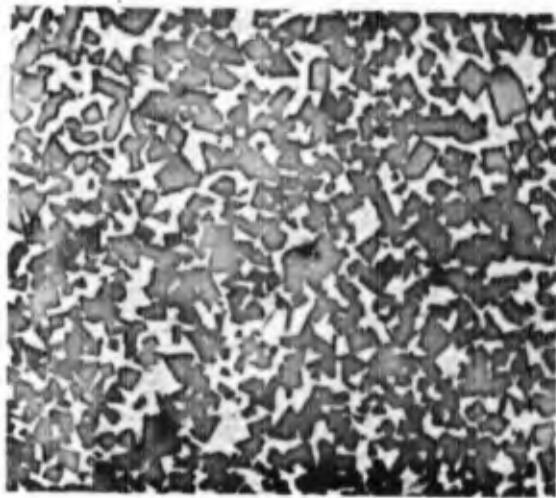


FIGURE 26

Microstructure of cobalt infiltrated WC compact (1500X)

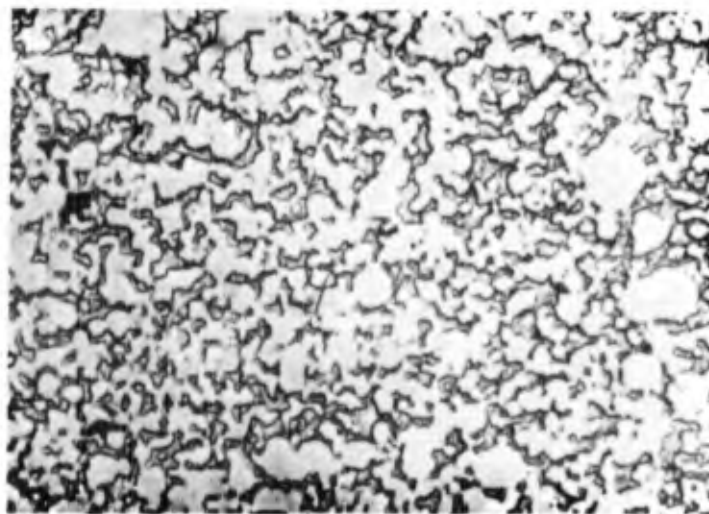


FIGURE 27

Microstructure of copper infiltrated WC compact (1500X)

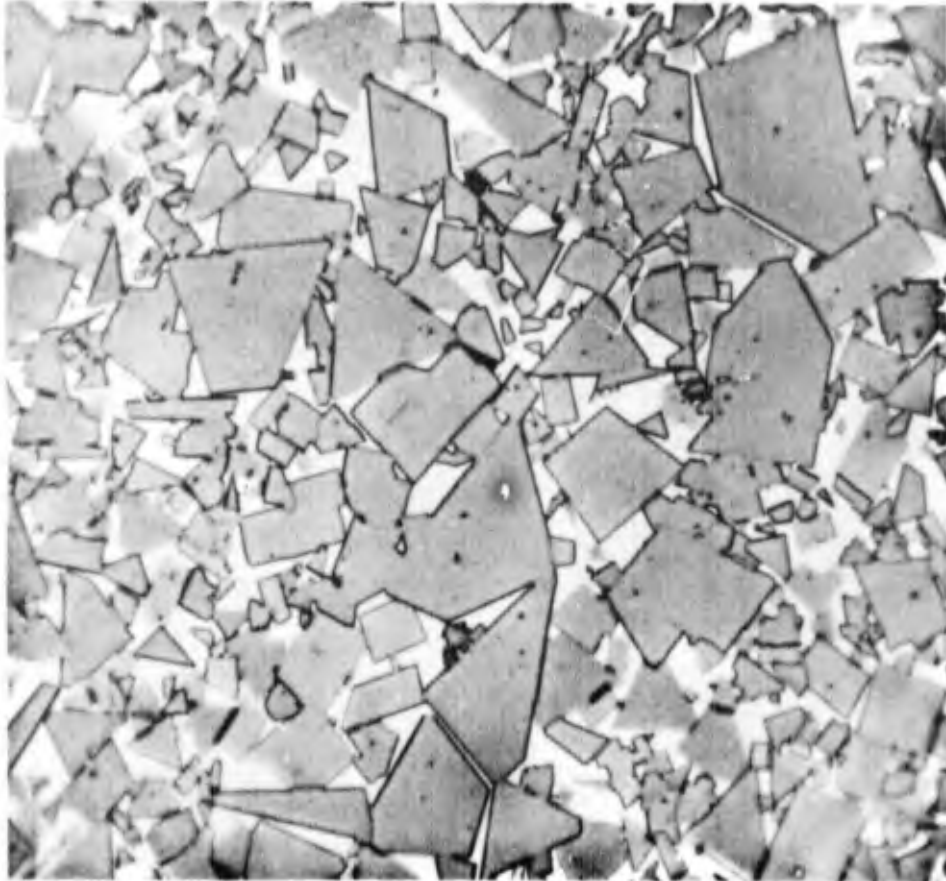


FIGURE 28

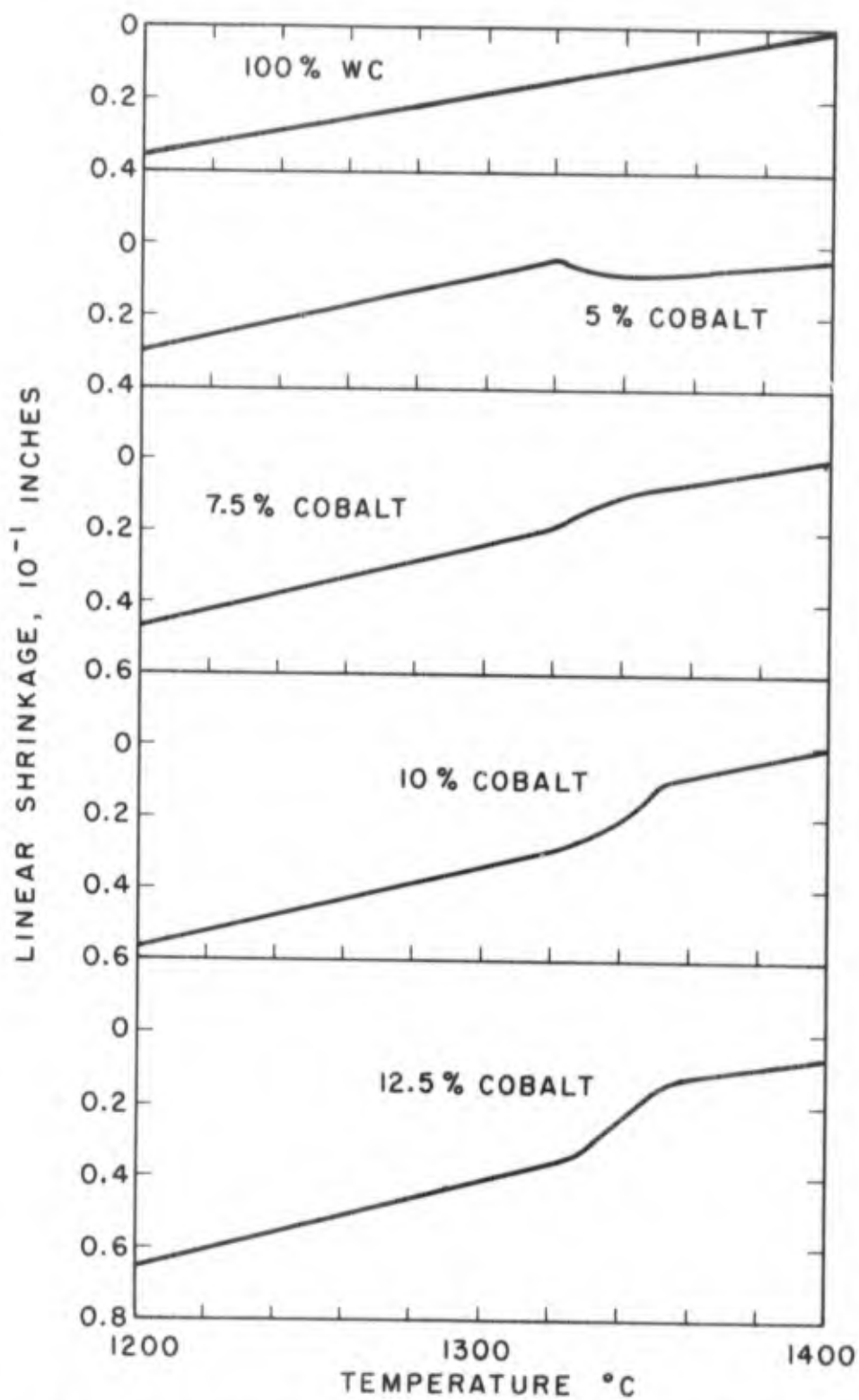
Microstructure of sintered WC-Co alloy. 12% Cobalt.
Abnormally large grains (1500X)

Courtesy of the Watertown Arsenal Laboratory

Table 4

Thermal Expansion of Pressed WC-Co Compacts (unsintered)
from 20°C. to 700°C.

<u>Composition</u>		<u>Measured Expansion</u>
<u>Cobalt</u>	<u>WC</u>	
0 percent	100 percent	0.0035 in/in
7.5	92.5	0.0040
12.5	87.5	0.0043
15	85	0.0050
25	75	0.0061

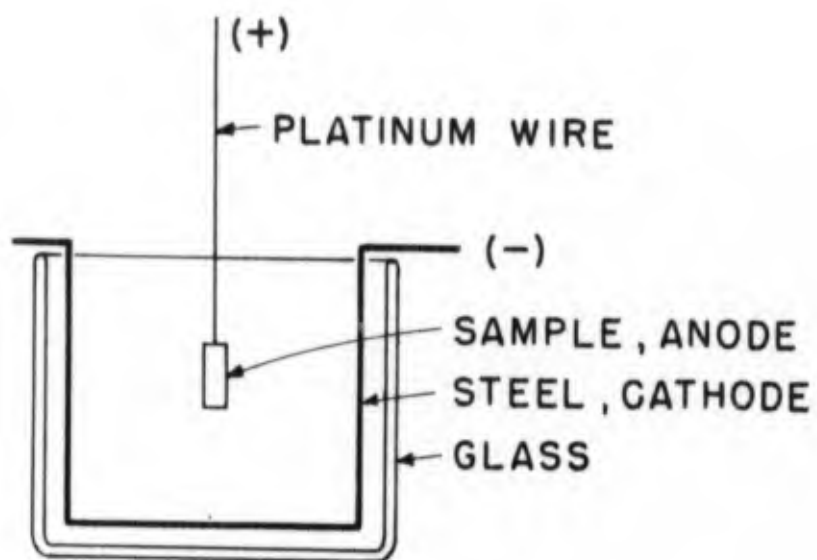


DISCONTINUOUS CHANGE OF LENGTH ON COOLING OF
SINTERED WC-Co ALLOYS OF DIFFERENT COMPOSITIONS
FIGURE 29

Table 5

Dimensional Changes at the Freezing Temperature of the Binder

<u>Cobalt Weight Percent</u>	<u>Cobalt Volume Percent</u>	<u>Measured Freezing Shrinkage (Linear, Percent)</u>	<u>Theoretical Freezing Shrinkage Linear, Percent)</u>
5	8.8	+ 0.05	- 0.09
7.5	11.6	- 0.06	- 0.12
10	16	- 0.17	- 0.16
12.5	20	- 0.21	- 0.20



ELECTROLYTIC LEACHING CELL

FIGURE 30



FIGURE 31

Sintered compacts after electrolytic leaching experiments.

From left to right: a) 100% WC, leached 56 hours;
b) 85% WC, 15% Co leached 24 hours; c) 90% WC, 10% Co
leached 24 hours; d) 92.5% WC, 7.5% Co leached 48 hours.

Length of samples: Approximately 1 inch.

Table 6

Results of Electrolytic Leaching Experiments

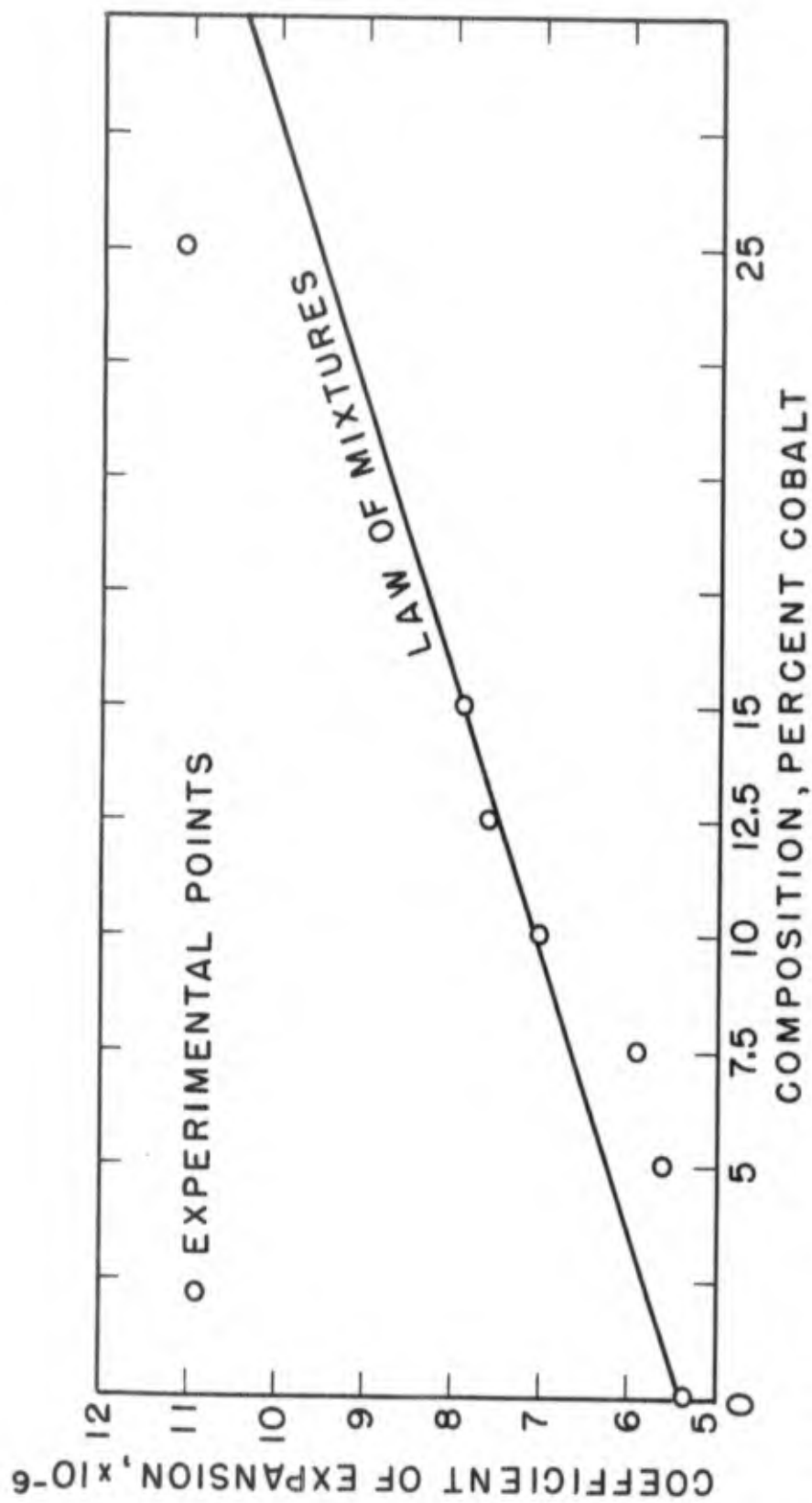
<u>Composition</u>		<u>Time Hours</u>	<u>Results</u>
<u>WC Percent</u>	<u>Co Percent</u>		
85	15	24	Strongly attacked
90	10	24	Strongly attacked
92.5	7.5	48	Strongly attacked
100	0	56	Intact

Table 7

Thermal Coefficients of Expansion ($\cdot 10^6$ in/in°C)

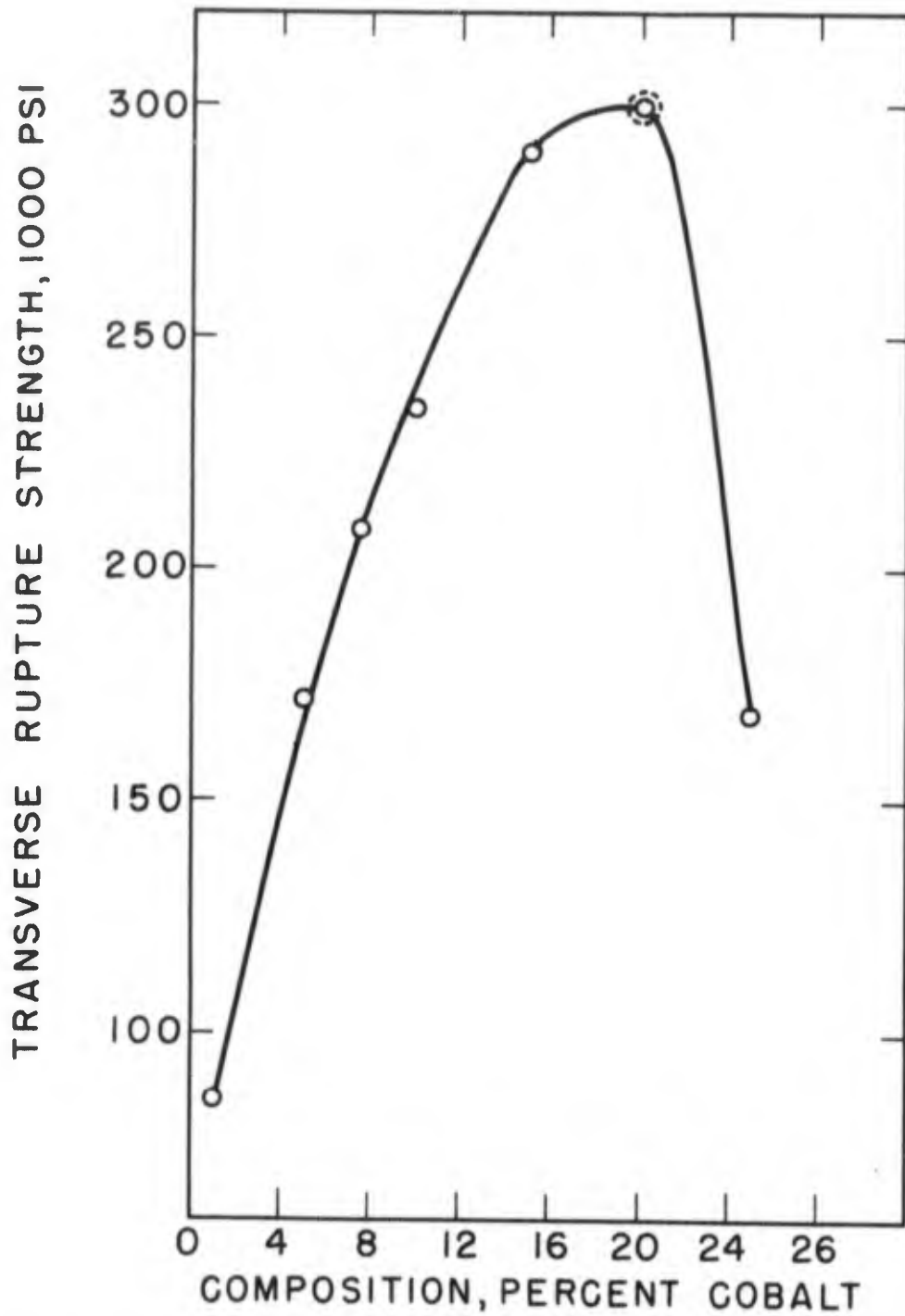
<u>Temperature Range</u>	<u>Composition</u>						
	100% WC	5% Co	7.5% Co	10% Co	12.5% Co	15% Co	25% Co
20 - 800°C.	5.4	5.6	5.9	7.0	7.6	7.9	11.1
800 - 1300°C.	9.2	10.4	10.5	12.4	12.7	13.0	*

* Specimen deforms at high temperatures



COEFFICIENT OF LINEAR THERMAL EXPANSION OF CEMENTED
WC-Co ALLOYS

FIGURE 32



SINTERED WC-Co ALLOYS - EFFECT OF COMPOSITION ON TRANSVERSE RUPTURE STRENGTH

FIGURE 33

Table 8

Strength of Cemented Wolfram Carbide (13% Co)

<u>Temperature</u>	<u>Transverse Rupture Strength</u>
20°C	248 000 psi
800	195 000
850	180 000
900	150 000

Table 9

Strength and Hardness of WC-Co Alloys Sintered at 1400°C.

<u>Composition</u>	<u>Strength</u>	<u>Hardness</u>
1 percent Co	96 000 psi	92 RA
5	172 000	90 - 92
10	234 000	89 - 90
15	289 000	88
25	169 000	80

Table 10

Effect of Time and Temperature on the Strength of WC-Co Alloys
7.5 percent Co

<u>Sintering Temperature</u>	<u>Time</u>	<u>Density</u>	<u>Bend Strength*</u>
1300°C	24 hours	14.56	209 000 psi
1350	1	13.35	132 000
1350	4	14.59	212 000
1350	8	14.63	202 000
1400	0.5	14.55	173 000
1400	1	14.70	179 000
1400	2	14.68	192 000

* Average of four measurements

Table 11

Effect of Time and Temperature on the Strength of
WC-Co Alloys 15 percent Co

<u>Sintering Temperature</u>	<u>Time</u>	<u>Density</u>	<u>Bend Strength*</u>
1300°C	24 hours	13.68	214 000 psi
1350	1	13.33	138 000
1350	4	13.71	213 000
1350	8	13.77	229 000
1400	0.5	13.89	183 000
1400	1	14.05	205 000
1400	2	13.94	237 000

* Average of four measurements

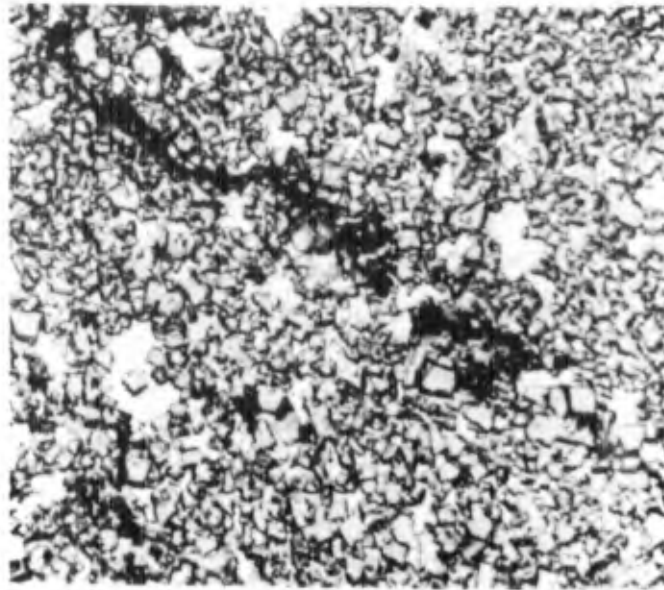


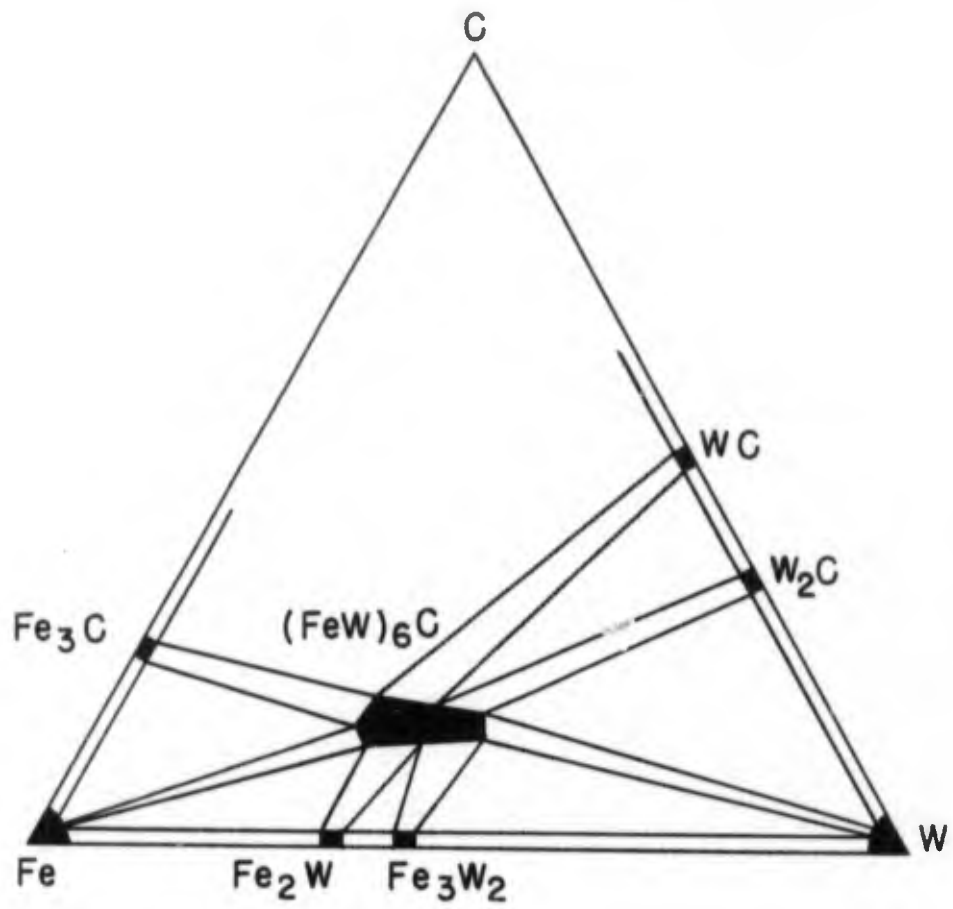
FIGURE 34

Sintered WC-Co alloy. Showing crack.
15% Cobalt (1500X)



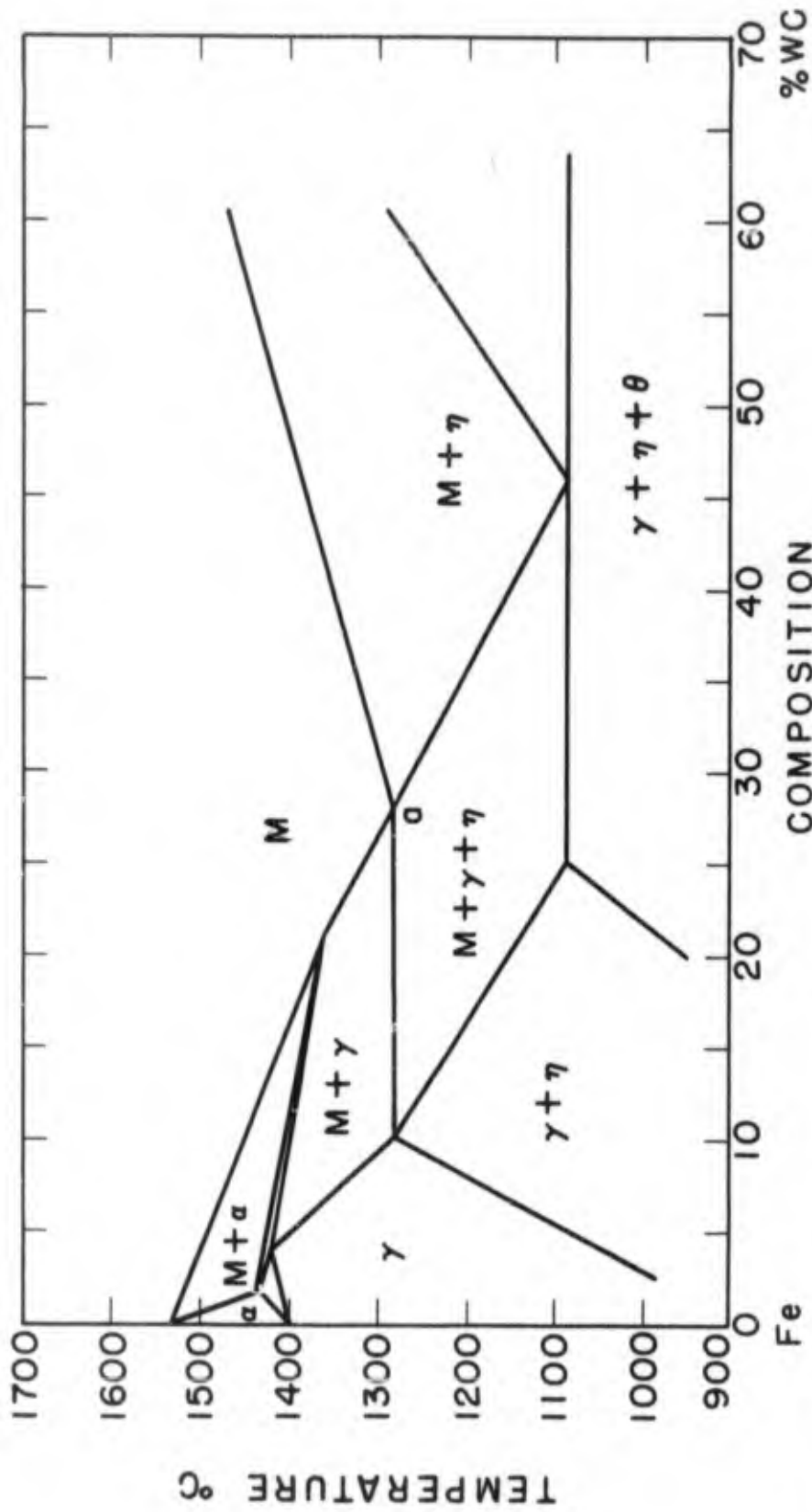
FIGURE 35

Sintered WC-Co alloy. Showing crack. Unknown composition.
Served as support in sintering furnace. (1500X)



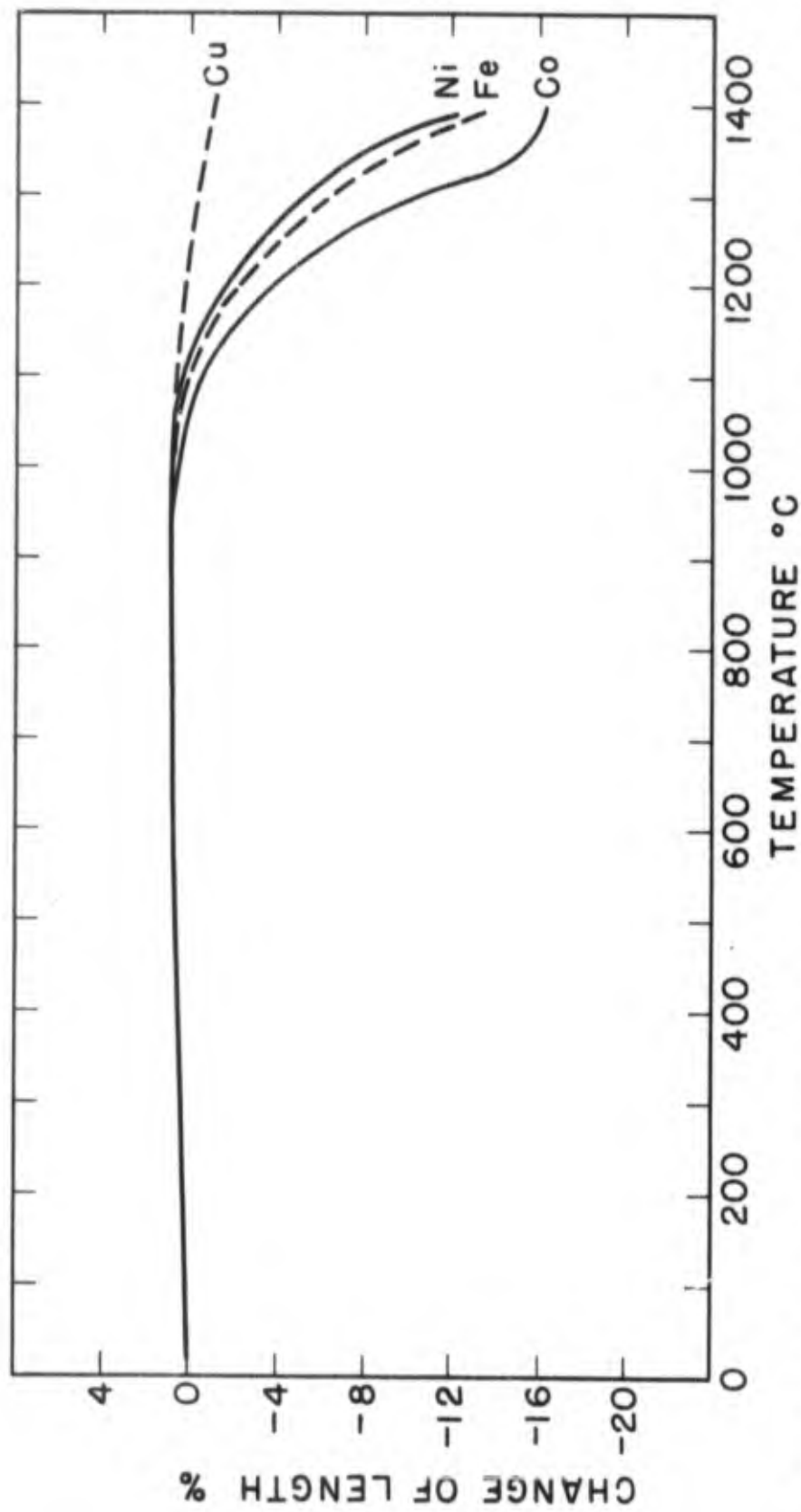
Fe - C - W TERNARY SYSTEM

FIGURE 36



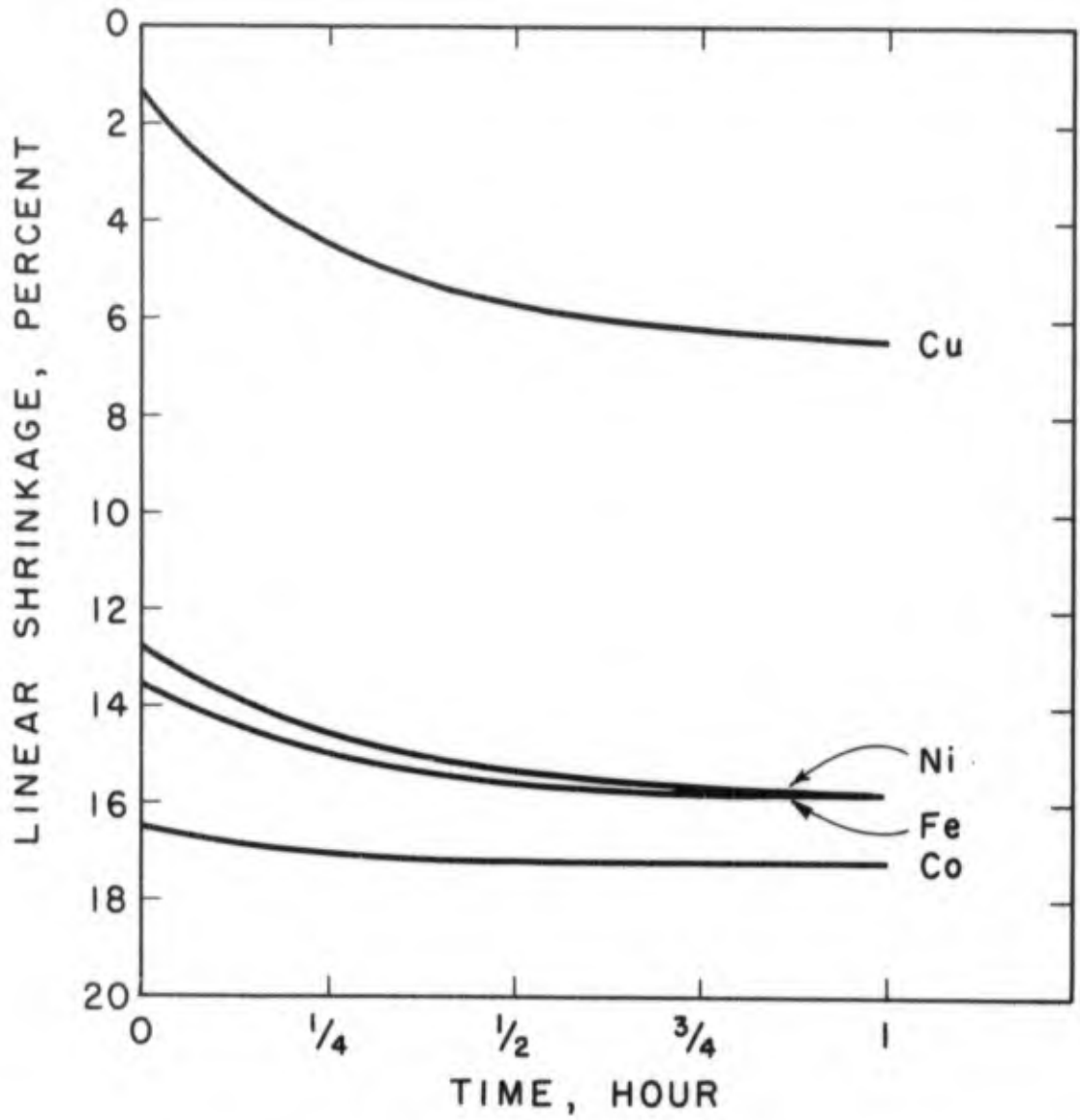
Fe-W-C TERNARY SYSTEM VERTICAL SECTION Fe-W-C

FIGURE 37



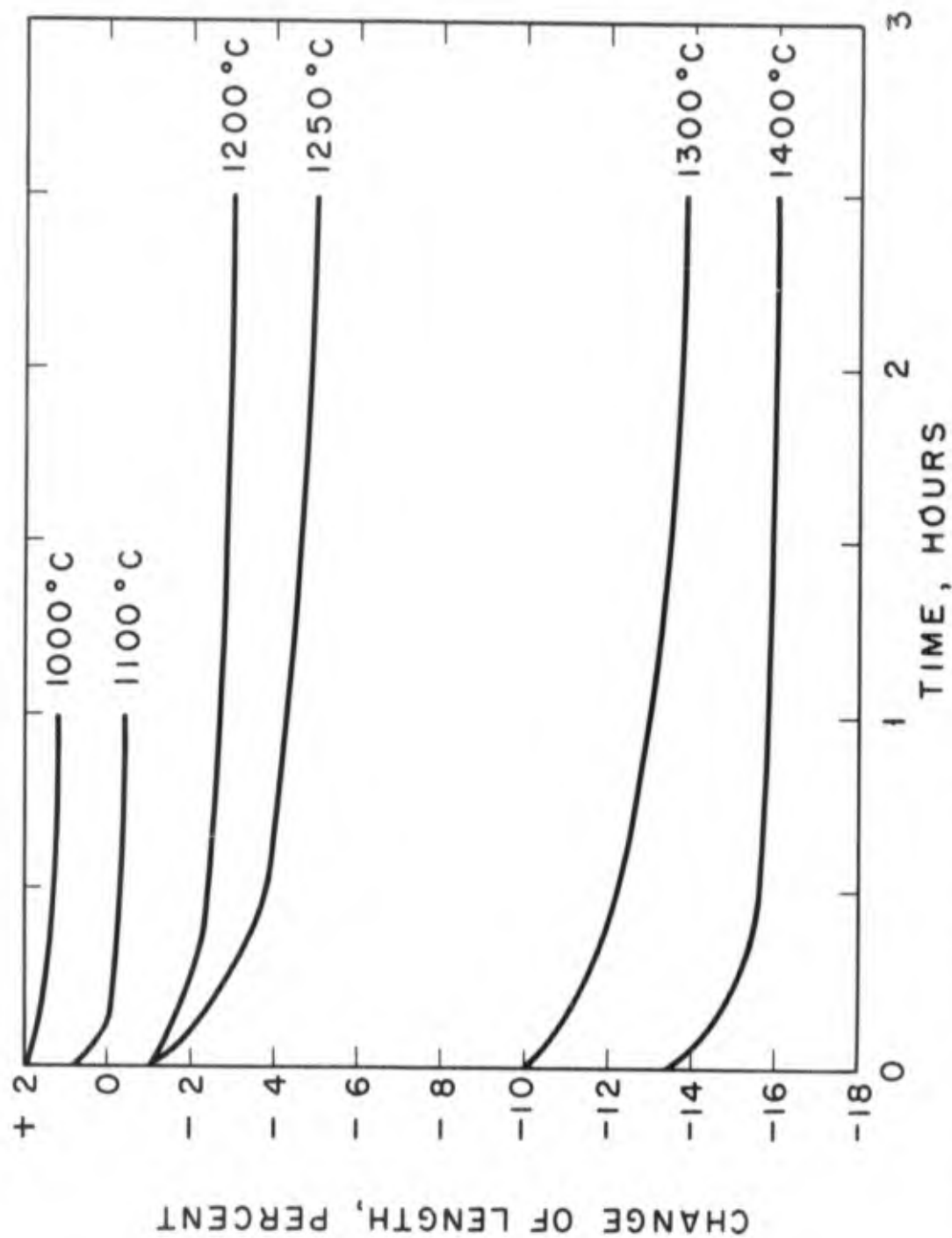
CEMENTED WC COMPACTS - VARIOUS BINDERS (7.5%)-SHRINKAGE CURVES
 CONSTANT RATE OF HEATING-CHANGE OF LENGTH VS TEMPERATURE

FIGURE 38



CEMENTED WC COMPACTS - VARIOUS BINDERS (7.5%) ISOTHERMAL SHRINKAGE AT 1400° C

FIGURE 39



SINTERING CURVES AT CONSTANT TEMPERATURE - 7.5% IRON BINDER
 FIGURE 40



FIGURE 41



FIGURE 42

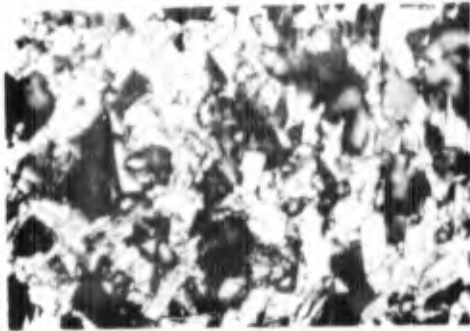


FIGURE 43



FIGURE 44

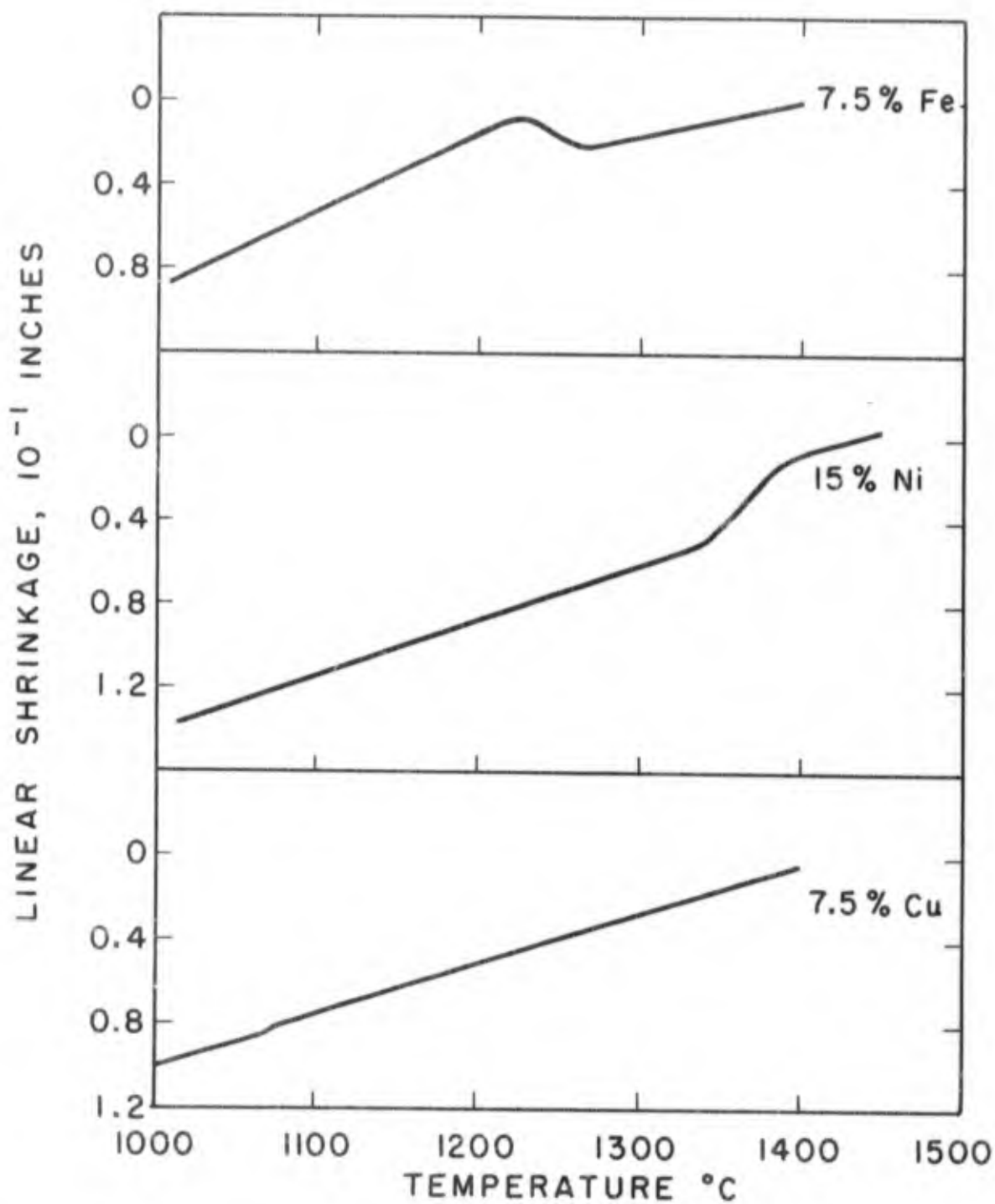
Microstructures of infiltrated WC blocks.

- Figure 41: Copper infiltrated (350X)
- Figure 42: Nickel infiltrated (350X)
- Figure 43: Iron infiltrated (350X)
- Figure 44: Cobalt infiltrated (350X)



FIGURE 45

Microstructure of nickel infiltrated wolfram carbide block,
showing eta phase. (1500X)



DISCONTINUOUS CHANGE OF LENGTH ON COOLING OF CEMENTED WOLFRAM CARBIDE COMPACTS WITH VARIOUS BINDERS

FIGURE 46

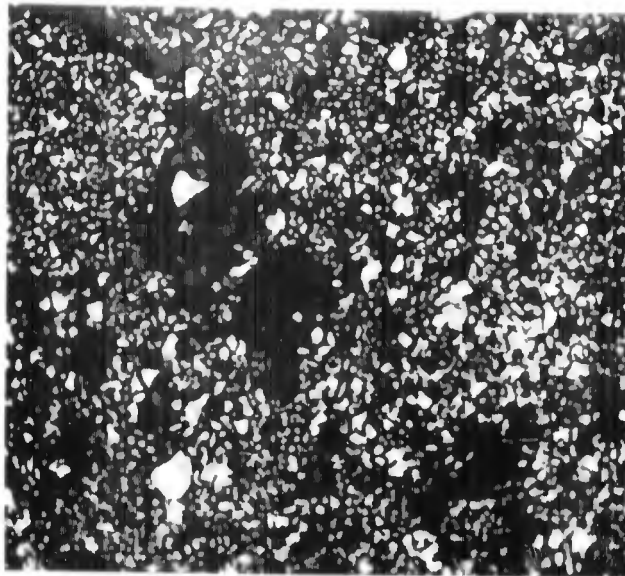


FIGURE 47

Cemented Wolfram Carbide. Iron Binder. 7.5% Iron
Sintered $2\frac{1}{2}$ hours at 1400°C . (1500X)

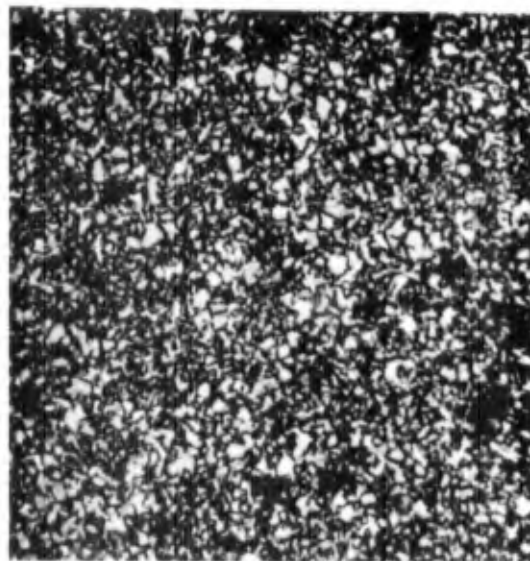


FIGURE 48

Cemented Wolfram Carbide. Nickel Binder. 7.5% Nickel.
Sintered $2\frac{1}{2}$ hours at 1400°C . (1500X)

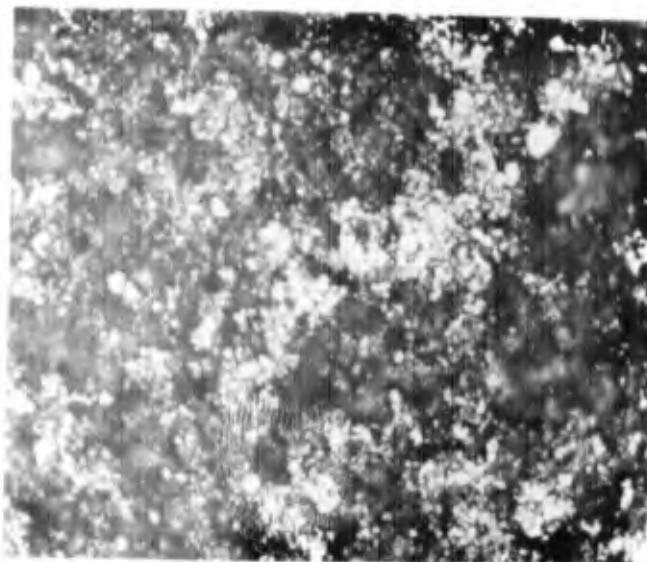


FIGURE 49

Cemented Wolfram Carbide. Copper Binder. 7.5% Copper.
Sintered 2 hours at 1400°C. (1500X)

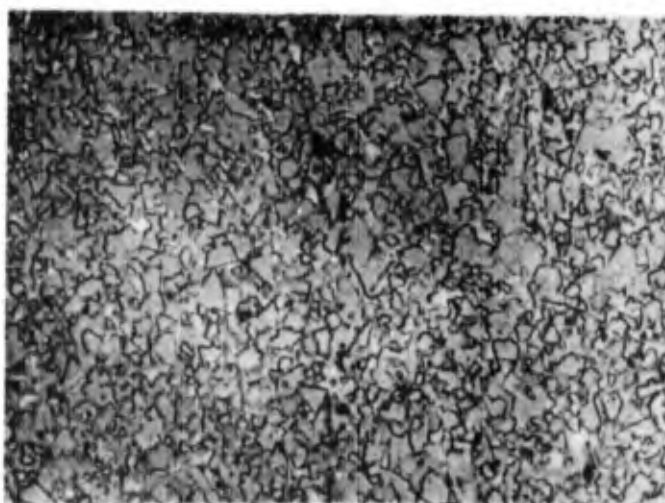


FIGURE 50

Cemented Wolfram Carbide. Cobalt Binder. 7.5% Cobalt.
Sintered 2 hours at 1400°C. (1500X)

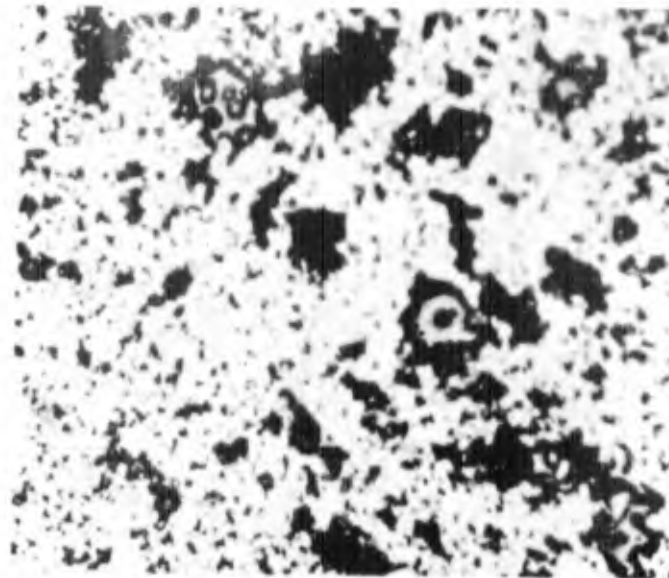


FIGURE 51

Eta phase in sintered WC-Fe alloy. (1500X)

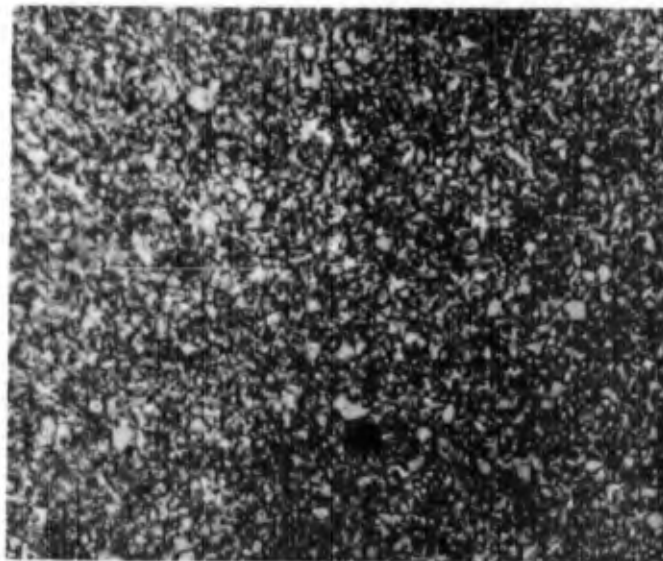


FIGURE 52

Cemented Wolfram Carbide. Nickel Binder. 15% Nickel.
Sintered 1 hour at 1500°C. (1500X)

Table 12

Physical Properties of Wolfram Carbide

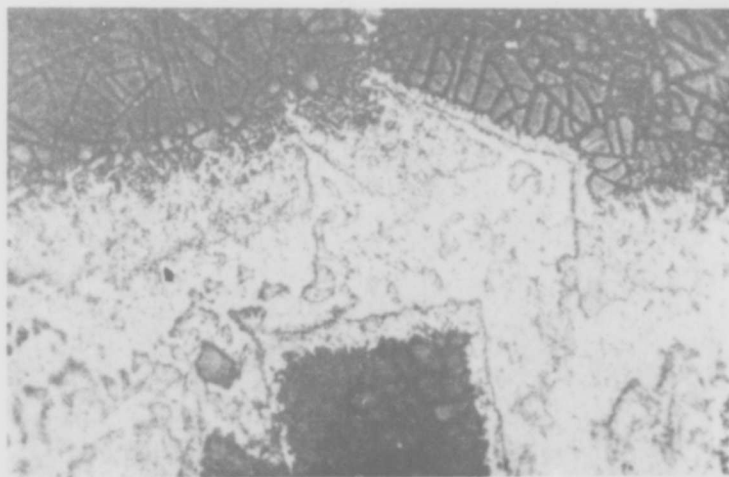
Cemented with Various Binders

<u>Binder</u>	<u>Amount of Binder</u>	<u>Sintering Treatment</u>	<u>Bend Strength</u>	<u>Hardness R_A</u>
Co	7.5%	1400°C 2½ hours	210 000 psi	87
Fe	7.5	1400°C 2½ hours	69 000	87
Ni	7.5	1400°C 2½ hours	85 000	87
Ni	15	1500°C 1 hour	172 000	85
Ni	15	1400°C 2½ hours	132 000	85

Table 13

Summary of Experimental Results

	Cu	Fe	Ni	Co
Extent of Shrinkage at 1400°C. 1 hour, 7.5% binder	6.5%	15.8%	15.8%	17.2%
Wettability, Angle of Contact with solid WC 1400°C.	20°	0°	0°	0°
Liquidus temperature as measured dilatometrically	1075°	1220°	1340°	1320°
Phases present in sintered compacts at room temperature	WC Cu	WC γ, Fe ₃ C	WC Ni	WC Co
Grain growth during sintering	None	Little	Little	Appreciable
Bend strength 7.5% binder sintered 1400°C. 1 hour	-	69 000 psi	85 000 psi	210 000 psi



No. 3. ~60%W, 2.0%C. Annealed at
1,000° for 2 hrs. ($K_3Fe(CN)_6$) $\times 200$

FIGURE 53

Shown by Takeda⁽⁴⁷⁾ to illustrate metastability of
the eta phase in the W-Fe-C system. Large grains
of eta transforming to WC at their peripheries.

Table 14

Results of Oxidation of Sintered WC-Co Compacts
Protected by Eta Phase on Surface

Sample	Time at 1450°C.		Surface Phases	Oxidation in Air			Increase of Dimension	Comments
	in Decarburizing Atmosphere			Temperature	Time			
1	-		WC, Co	1000°C.	1 hour	0.350 in.	Oxidized Badly	
2	5 hours		eta	1000°C.	-	-	Illustrates appearance	
3	5		eta	1000°C.	5 hours	0.002	Unattacked	
4	22		eta	1000°C.	24	0.002	Slight oxidation at edges	
5	1		eta	1000°C.	48	0.002	Slight oxidation at edges	
6	1		eta	1000°C.	96	0.003	Oxidation at edges	
					3	0.003	Unattacked	
					5	0.003	Unattacked	
					11½	0.004	Unattacked	
					6½	0.001	Unattacked	
					24	0.018	Badly Oxidized	

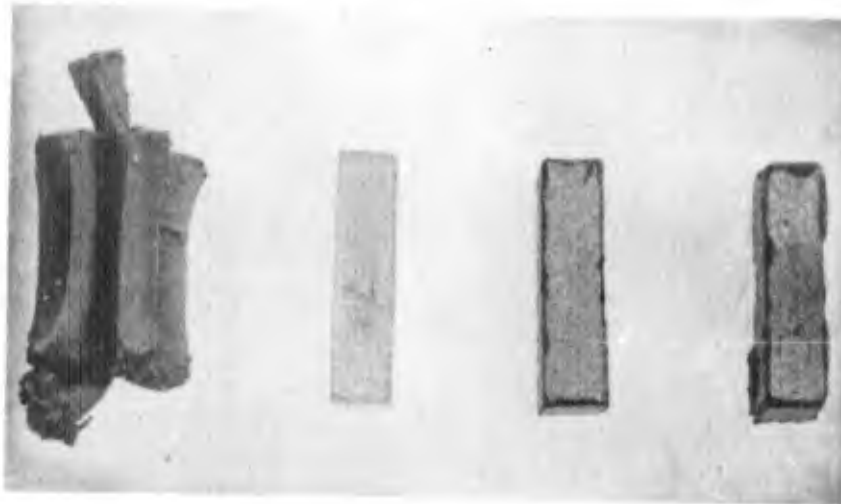


FIGURE 54

Photograph of Samples 1, 2, 3 and 4 (from left to right).
(See Appendix II, also Table 14)



FIGURE 55

Photograph of samples 5 and 6 (from left to right)
(See appendix II, also Table 14)

Table 15

Results of Oxidation of Sample of Eta Phase Composition

<u>Oxidation in Air</u>		<u>Increase of Dimension</u>	<u>Comments</u>
<u>Temperature</u>	<u>Time</u>		
1000°C.	4 hours	0.001 inch	Slight oxidation at edges
1000	20	0.005	Slight oxidation at edges
1000	34	0.008	Slight oxidation at edges
1000	66	(0.005)	Peeling of Surface
1000	96	(0.005)	Peeling of Surface

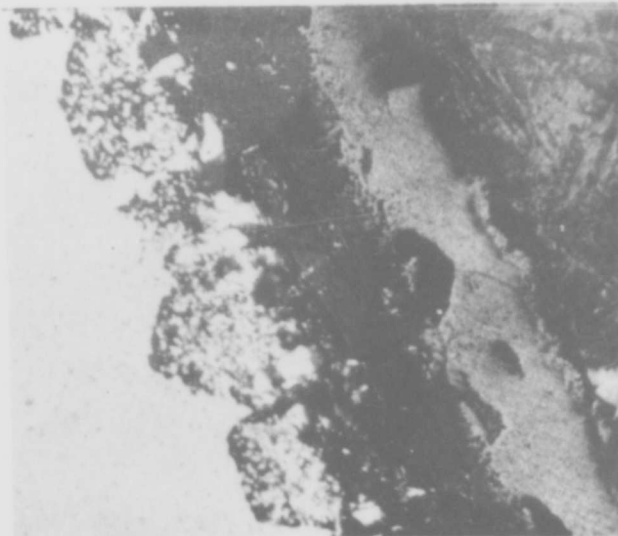
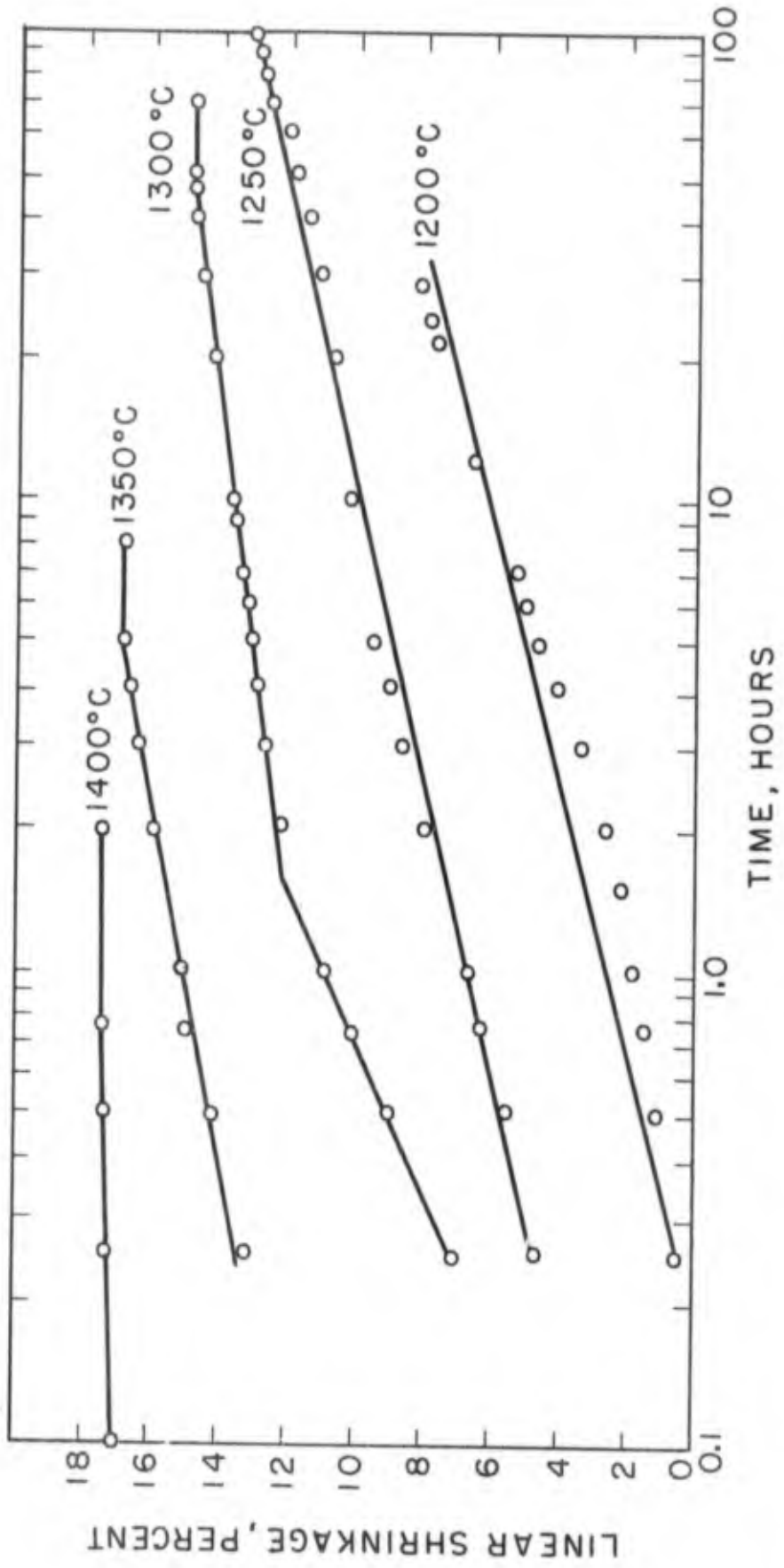


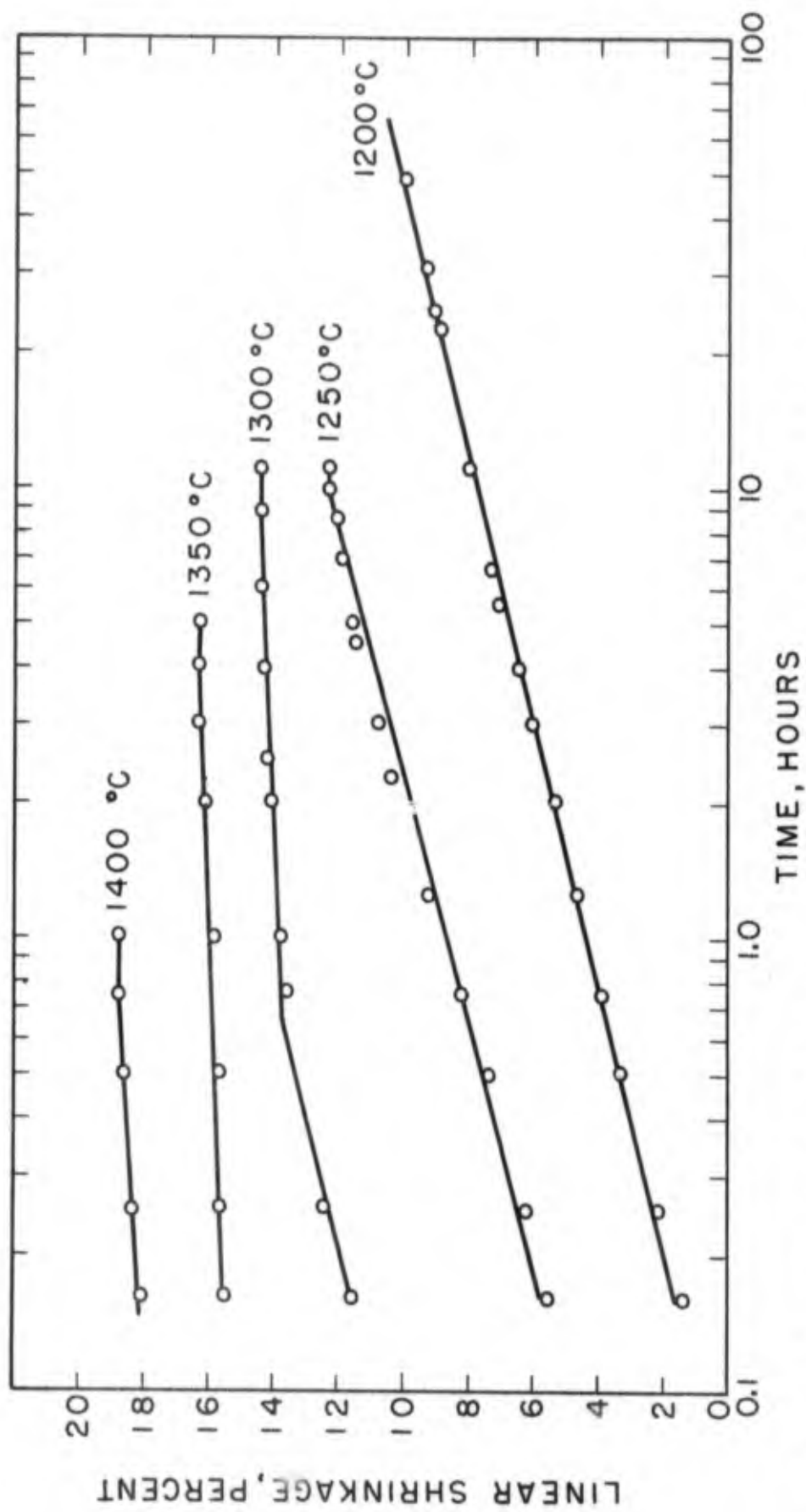
FIGURE 56

Microphotograph of surface layers of oxidized eta phase
on a sintered WC-Co alloy (250X)

From left to right: Sintered WC-Co core, eta phase,
blue layer, silver gray layer, bakelite



SINTERING CURVES - SHRINKAGE VS LOG TIME 7.5% COBALT
 FIGURE 57



SINTERING CURVES - SHRINKAGE VS LOG TIME 15% COBALT

FIGURE 58



1115°C.



1230°C.



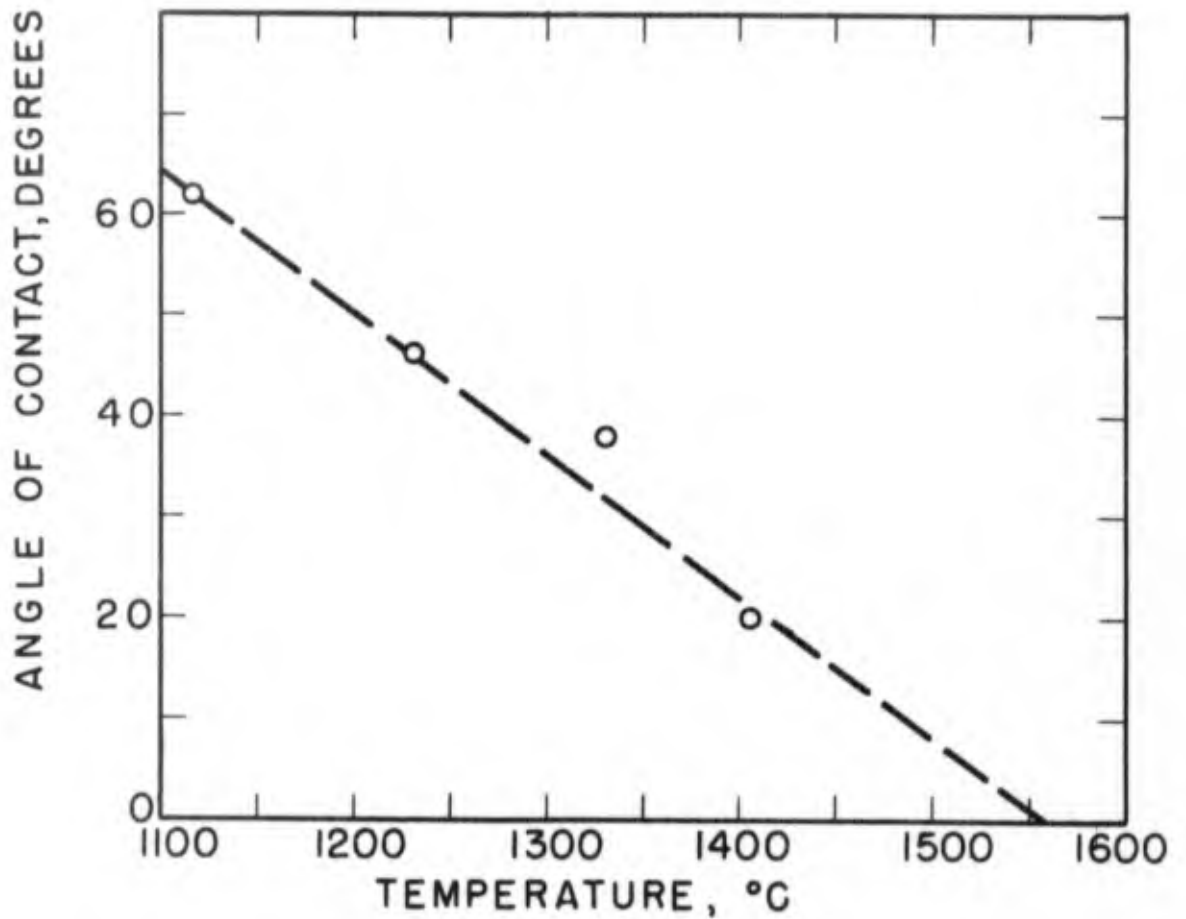
1330°C.



1405°C.

FIGURE 59

Profiles of drop of liquid copper on solid wolfram carbide.



VARIATION WITH TEMPERATURE OF THE ANGLE OF CONTACT OF LIQUID COPPER ON SOLID WOLFRAM CARBIDE

FIGURE 60

ATI- 113 035

Massachusetts Institute of Technology, Department of Metallurgy, Cambridge (Report No. WAL 671/99-18) BINDERS IN CEMENTED REFRACTORY ALLOYS - AND APPENDIXES I-IX - FINAL REPORT, by J.T. Norton; J. Gurland and P. Rautala. 15 June '51, 156 pp. Incl. photos, tables, diagrs, graphs.

UNCLASSIFIED

**A detailed study of the action of the binder phase in cemented wolfram carbide alloys, conducted with the objective of explaining the several factors which control the physical and mechanical properties of the sintered parts and of providing a basis for the proper
(over)**

DIVISION: Materials, Non-Metallic (8)

SECTION: Ceramics (1)

DISTRIBUTION: Copies obtainable from CADO.

- 1. Ceramics - Binders .**
- 2. Carbides**
- 3. Refractories**
 - I. Norton, J.T.**
 - II. Gurland, J.**
 - III. Rautala, P.**
 - IV. USA Contr. No. DA-19-020-ORD-10**

CENTRAL AIR DOCUMENTS OFFICE

selection of the best binder materials and sintering techniques for specific situations, is presented. The sintering behavior of wolfram carbide cobalt alloys is discussed in detail. On the basis of the experiments it can be shown that densification takes place by a rearrangement of the carbide particles under the influence of the surface tension forces of the binder. The resulting structure is essentially one of carbide particles embedded in a matrix of cobalt. The strength and brittleness of the sintered compacts depend on the mechanical properties of the binder.

ATI- 113 035